

Science and Technology Program Report No. 174

Investigation of Low-Pressure Membrane Performance, Cleaning, and Economics Using a Techno-Economic Modeling Approach



U.S. Department of the Interior
Bureau of Reclamation

September 2012

REPORT DOCUMENTATION PAGE

Form Approved
OMB No. 0704-0188

Public reporting burden for this collection of information is estimated to average 1 hour per response, including the time for reviewing instructions, searching existing data sources, gathering and maintaining the data needed, and completing and reviewing this collection of information. Send comments regarding this burden estimate or any other aspect of this collection of information, including suggestions for reducing this burden to Department of Defense, Washington Headquarters Services, Directorate for Information Operations and Reports (0704-0188), 1215 Jefferson Davis Highway, Suite 1204, Arlington, VA 22202-4302. Respondents should be aware that notwithstanding any other provision of law, no person shall be subject to any penalty for failing to comply with a collection of information if it does not display a currently valid OMB control number. **PLEASE DO NOT RETURN YOUR FORM TO THE ABOVE ADDRESS.**

1. REPORT DATE (DD-MM-YYYY) September 2012		2. REPORT TYPE Final		3. DATES COVERED (From - To)	
4. TITLE AND SUBTITLE Investigation of Low-Pressure Membrane Performance, Cleaning, and Economics Using a Techno-Economic Modeling Approach				5a. PROJECT NUMBER	
				5b. GRANT NUMBER	
				5c. PROGRAM ELEMENT NUMBER	
6. AUTHOR(S) Katie Guerra, Bureau of Reclamation John Pellegrino, University of Colorado				5d. PROJECT NUMBER	
				5e. TASK NUMBER	
				5f. WORK UNIT NUMBER	
7. PERFORMING ORGANIZATION NAME(S) AND ADDRESS(ES) U.S. Department of the Interior Bureau of Reclamation Denver Federal Center PO Box 25007 Denver CO 80225-0007				8. PERFORMING ORGANIZATION REPORT NUMBER	
9. SPONSORING / MONITORING AGENCY NAME(S) AND ADDRESS(ES) U.S. Department of the Interior Bureau of Reclamation, Denver Federal Center PO Box 25007, Denver CO 80225-0007				10. SPONSOR/MONITOR'S ACRONYM(S) Reclamation	
				11. SPONSOR/MONITOR'S REPORT NUMBER(S) S&T Report No. 174	
12. DISTRIBUTION / AVAILABILITY STATEMENT Available from the National Technical Information Service Operations Division, 5285 Port Royal Road, Springfield VA 22161					
13. SUPPLEMENTARY NOTES Report can be downloaded from Reclamation Web site: www.usbr.gov/pmts/water/publications/reports.html					
14. ABSTRACT (Maximum 200 words) This work uses experimental results with a data-driven model to evaluate the technical and economic factors that impact lifecycle costs for low-pressure (microfiltration and ultrafiltration) membranes. Laboratory experiments quantified differences in the fouling propensity for an alumina ceramic and a polyethersulfone (PES) polymeric ultrafiltration membrane. Comparing the rate of transmembrane pressure increase of different membranes as a function of Peclet number is a new method for comparing different types of membrane materials on an equivalent basis over a wide range of operating conditions.					
15. SUBJECT TERMS					
16. SECURITY CLASSIFICATION OF:			17. LIMITATION OF ABSTRACT SAR	18. NUMBER OF PAGES 127	19a. NAME OF RESPONSIBLE PERSON Katie Guerra
a. REPORT UL	b. ABSTRACT UL	c. THIS PAGE UL			19b. TELEPHONE NUMBER (include area code) 303-445-2013

Science and Technology Program Report No. 174

Investigation of Low-Pressure Membrane Performance, Cleaning, and Economics Using a Techno-Economic Modeling Approach

Prepared for Reclamation Under Agreement No. A10-1541-AW20-112-41-4-1

by

**Katie Guerra, Bureau of Reclamation
John Pellegrino, University of Colorado**



**U.S. Department of the Interior
Bureau of Reclamation
Technical Service Center
Water and Environmental Resources Division
Water Treatment Engineering Research Group
Denver, Colorado**

September 2012

MISSION STATEMENTS

The U.S. Department of the Interior protects America's natural resources and heritage, honors our cultures and tribal communities, and supplies the energy to power our future.

The mission of the Bureau of Reclamation is to manage, develop, and protect water and related resources in an environmentally and economically sound manner in the interest of the American public.

Disclaimer

The views, analysis, recommendations, and conclusions in this report are those of the authors and do not represent official or unofficial policies or opinions of the United States Government, and the United States takes no position with regard to any findings, conclusions, or recommendations made. As such, mention of trade names or commercial products does not constitute their endorsement by the United States Government.

Abstract

This work uses experimental results with a data-driven model to evaluate the technical and economic factors that impact lifecycle costs for low-pressure (microfiltration and ultrafiltration) membranes. Laboratory experiments quantified differences in the fouling propensity for an alumina ceramic and a polyethersulfone (PES) polymeric ultrafiltration membrane. Comparing the rate of transmembrane pressure increase of different membranes as a function of the Peclet (Pe) number is a new method for comparing different types of membrane materials on an equivalent basis over a wide range of operating conditions.

For a bentonite suspension, both the alumina and PES membranes exhibited negligible fouling at Pe less than 8.5. At Pe greater than 8.5, the alumina membrane exhibited significantly less fouling than the PES membrane. For a more complex colloidal mixture, both membranes exhibited similar, low rates of fouling at Pe less than 5.6. At Pe greater than 5.6, the alumina membrane exhibited significantly higher fouling rates than the PES membrane. These results illustrate that the feed water composition and the operating conditions determine which membrane exhibits better performance.

A new cleaning method, which combines hydraulic and chemical cleaning, and includes membrane permeance monitoring to assess the progress of cleaning, was developed and demonstrated. The new cleaning protocol reduced chemical cleaning times by up to 85 percent (%) over conventional cleaning protocols. The alumina membrane required 20% more time and 2.5 times larger volume of cleaning chemicals to completely regenerate the membrane than the PES membrane.

The data-driven cost model is a novel tool that can be used to identify the economic benefit of one material compared to another when the operating conditions and performance characteristics for the two materials are different, based on the time rate of change of the transmembrane pressure at a constant flux and apparent Pe, obtained from experiments.

For the analysis conducted, the alumina membrane is cost competitive with the PES membrane:

- When PES membrane life is less than 3 years.
- If the alumina membrane is operated with a fouling rate greater than 2.5 times that of the PES membrane.
- When the alumina membrane material cost is less than or equal to \$250 per square meter.

Acronyms

AFM	atomic force microscopy
Al ³⁺	aluminum
Al ₂ O ₃	alumina
ATZ	aminotetrazole
AWWA	American Water Works Association
CEPIC	Chemical Engineers Plant Cost Index
CFV	cross-flow velocity
DI	deionized
EDTA	ethylenediaminetetraacetic
EEM	excitation-emission matrix
FTE	full time employees
FWP	feed water permeance
g/mol	grams per mole
GW	ground water
kDa	kilodaltons
kg/m ³	kilogram per cubic meter
kg/mol	kilograms per mole
kPa	kilopascal
kWh	kilowatthours
L	liter
L/d	liters per day
L/h	liter per hour
L/m ²	liters per square meters
mA	milliampere
m ³ /m ² /s	cubic meter per square meter per second
m ³ /m ² /s/Pa	cubic meter per square meter per second per pascal
MF	microfiltration
mg	milligram
MGD	million gallons per day
mg/L	milligrams/liter

min/d	minutes per day
MPa	megapascal
m/s	meters per second
NaCl	sodium chloride
nm	nanometer
NOM	natural organic matter
NRC	National Research Council
NTU	Nephelometric Turbidity Units
O&M	operation and maintenance
PA	polyamide
PAN	polyacrylonitrile
PAN/PSF	polyacrylonitrile/polyethersulfone
Pe	Peclet
PES	polyethersulfone
PP	polypropylene
ppm	parts per million
PS	polysulfone
PTFE	polytetrafluoroethylene
PVC	polyvinyl chloride
PVDF	polyvinylidene fluoride
PVP	polyvinylpyrrolidone
PWP	pure water permeance
Re	Reynolds number
RSM	response surface methodology
SDS	sodium dodecyl sulfate
SiC	silicon carbide
SDWA	Safe Drinking Water Act
TCF	thin film composite
TiO ₂	titanium dioxide
TMP	transmembrane pressure
TOC	total organic carbon
TWPC	total water production cost
WW	waste water
UF	ultrafiltration

V/A	volume-to-area ratio
ZiO ₂	zirconia
ZrO ₂	zirconium dioxide
°C	degrees Celsius
\$	dollars
\$/kWh	dollars per kilowatthour
\$/person/y	dollars per person per year
μm	micrometer
%	percent
>	greater than
<	less than

Contents

	<i>Page</i>
Abstract	iii
Acronyms.....	v
1. Introduction	1
1.1 Research Objectives and Hypotheses	2
1.2 Significance of Research.....	3
1.3 Limitations of Research.....	5
1.4 Report Organization.....	6
2. Review of Literature.....	9
2.1 Factors Affecting Membrane Fouling.....	9
2.1.1 Membrane Material Properties	9
2.1.2 Membrane Module Configuration and Hydrodynamic Conditions	11
2.1.3 Feed Water Characteristics	15
2.2 Membrane Cleaning and Regeneration.....	16
2.2.1 Backwash.....	16
2.2.2 Chemical Cleaning.....	18
2.3 Assessment of Literature to Compare Ceramic and Polymeric Membranes	20
2.4 Summary	30
3. Data-Driven Model Development.....	31
3.1 Parameters.....	31
3.2 Variables	34
3.3 Engineering Design Equations.....	35
3.4 Membrane System Cost	36
3.4.1 Capital Costs	37
3.4.2 Operating and Maintenance Costs	38
4. Membrane Properties and Feed Water Quality	41
4.1 Membranes.....	41
4.2 Friction Factor.....	42
4.3 Molecular Mass Cutoff Determination	45
4.4 Feed Water	46
4.4.1 Clear Creek Surface Water	46
4.4.2 Bentonite Suspension.....	47
4.4.3 Complex Mixture.....	47
4.5 Experimental Equipment	49
5. Preliminary Ceramic Membrane Study.....	51
5.1 Identification of Operating Condition Ranges.....	51
5.2 Experimental Approach	52
5.2.1 Experimental Factors	53
5.2.2 Response Variables.....	53
5.2.3 Data Analysis	54

Contents (continued)

	<i>Page</i>
5.3 Results and Discussion	54
5.3.1 Filtration Experiments	54
5.3.2 Filtrate Water Quality	55
5.3.3 Response Surface Methodology	56
5.3.4 Production Cost Analysis.....	57
5.4 Summary	58
6. Comparison of Membrane Fouling Tendency	61
6.1 Membrane Conditioning	61
6.2 Fouling Conditions	61
6.3 Results.....	62
6.3.1 Bentonite Suspension.....	62
6.3.2 Complex Mixture.....	64
6.4 Discussion of Results for Bentonite Suspension	69
6.5 Discussion of Results for Complex Mixture.....	70
6.6 Effect of Surface Energy on Filtration Results	73
6.7 Integration of Performance Results into Cost Model	73
6.7.1 Calculating Average Operating Pressure.....	74
6.7.2 Calculating Operating Conditions for Full-Scale Membranes.....	74
6.8 Summary	75
7. Comparison of Membrane Cleaning Efficiency.....	77
7.1 Experimental Procedure.....	77
7.1.1 Fouling.....	77
7.1.2 Cleaning.....	77
7.2 Results.....	79
7.3 Integration of Cleaning Results into Cost Model	83
7.3.1 Chemical Cleaning Cost	84
7.3.2 Long-Term Irreversible Fouling	84
7.4 Summary	84
8. Cost Model Simulation Results.....	87
8.1 Cost Comparison for Operation Under Similar Hydrodynamic Conditions	87
8.2 Identification of Key Economic Leverage Points.....	93
8.3 Summary	98
9. Conclusions	101
10. Recommendations	105
10.1 Material Characterization.....	105
10.2 Fouling Studies with Other Water Types.....	105
10.3 Modeling Membrane Fouling of Ceramic and Polymeric Membranes.....	106
11. References Cited	107

Contents (continued)

	<i>Page</i>
Appendix A Data Acquisition and Experimental Protocol.....	115
Appendix B Hydrodynamic Conditions for Modules.....	121
Appendix C Inputs and Outputs.....	125

Tables

	<i>Page</i>
Table 2.1 Selection of commercially available ceramic membrane products.....	14
Table 2.2 Selection of commercially available pressure driven, inside-out polymeric membrane products.....	15
Table 2.3 Comparison of ceramic and polymeric membrane operating conditions ¹	15
Table 2.4 Ceramic membrane literature data.....	22
Table 2.5 Polymeric membrane literature data ¹	23
Table 3.1 Parameter names, descriptions, units, values, and reference for determining the values used.....	32
Table 3.2 Full size membrane specifications and characteristics based on manufacturer specifications and vendor quotes.....	33
Table 3.3 Summary of model variables.....	34
Table 3.4 Summary of calculated parameters for cost components and plant design results.....	36
Table 4.1 Membrane specifications.....	41
Table 4.2 Liquid solution properties at 20 °C.....	43
Table 4.3 Comparison of coefficient of friction values.....	45
Table 4.4 Clear Creek feed water characteristics.....	46
Table 4.5 Complex feed mixture characteristics.....	48
Table 5.1 Summary of experimental conditions, response variables, and TPC.....	55
Table 5.2 Membrane area and annualized cost for optimal operating conditions.....	57
Table 6.1 Linear expressions of revised Hermia model.....	70
Table 6.2 Results of regression analysis comparing Hermia model fits.....	72
Table 7.1 Experimental conditions for fouling and cleaning cycles.....	78
Table 7.2 Summary of cleaning time and chemical consumption for each membrane.....	83
Table 8.1 Summary of fouling rates for the alumina and PES membranes.....	87

Tables (continued)

	<i>Page</i>
Table 8.2	Cost model results for $Pe = 5.5$ 89
Table 8.3	Cost model results for $Pe = 9.1$ 91
Table 8.4	Cost model results for $Pe = 11.4$ 93
Table 8.5	Summary of results for the cost comparison 99

Figures

	<i>Page</i>
Figure 1.1	Tradeoffs between operating conditions and total water production cost 4
Figure 2.1	Schematic diagram of dead-end and cross-flow filtration 12
Figure 2.2	Effect of backwash pressure on backwash efficiency 18
Figure 2.3	Literature data – flux comparison 25
Figure 2.4	Literature data – permeance comparison 26
Figure 4.1	End view of alumina (left) and PES (right) modules 41
Figure 4.2	AFM of alumina (left) and PES (right) membranes 42
Figure 4.3	Friction factor plotted as a function of Re for alumina and PES membranes 44
Figure 4.4	Coefficient of friction for alumina and PES membranes 44
Figure 4.5	Dextran rejection for alumina and PES membranes 45
Figure 4.6	DLS results for bentonite feed solution 47
Figure 4.7	UV-Vis spectrum of complex mixture 48
Figure 4.8	EEM of complex mixture 49
Figure 4.9	Analysis of complex feed water composition 49
Figure 4.10	Schematic diagram of filtration equipment 50
Figure 5.1	Average flux versus volume filtered for select set of experiments 54
Figure 5.2	Response surface for J/J_0 56
Figure 5.3	Response surface for J_{avg} 56
Figure 5.4	Membrane material cost parametric analysis results 58
Figure 6.1	Alumina membrane permeance for bentonite suspension 62
Figure 6.2	PES membrane permeance for bentonite suspension 63
Figure 6.3	Alumina membrane permeance at different Pe 63
Figure 6.4	Polymeric membrane performance at different Pe 64
Figure 6.6	Alumina membrane permeance to complex mixture 65
Figure 6.5	Rate of pressure increase versus Pe for the alumina and PES membranes 65
Figure 6.8	Alumina membrane fouling rate for different values of Pe 66
Figure 6.7	PES membrane permeance to complex feed mixture 66

Figures (continued)

	<i>Page</i>
Figure 6.9	PES membrane fouling rate at different values of Pe 67
Figure 6.10	Comparison of alumina and PES membrane fouling as a function of Pe 67
Figure 6.11	Observed DOC rejection for alumina and PES membranes 68
Figure 6.12	Ceramic membrane filtrate 69
Figure 6.13	Polymeric membrane filtrate 69
Figure 6.14	Illustration of the four modes of fouling described by the Hermia model 70
Figure 6.15	Plots of linear expressions for the alumina membrane for a) cake formation, b) intermediate blocking, c) standard blocking, and d) pore plugging 71
Figure 6.16	Plots of linear expressions for the PES membrane for a) cake formation, b) standard blocking, c) intermediate blocking, and d) pore plugging 72
Figure 7.1	Color of the filtrate during caustic cleaning (pH 11, 400 ppm NaOCl); initial (left); after 4 minutes (middle); after 5 minutes (right) 78
Figure 7.2	Backwash effluent after 1 minute (left), 4 minutes (middle), and 5 minutes (right); color evolution indicates complete cleaning has been accomplished 79
Figure 7.3	PWP before and after fouling cycles for the alumina membrane 80
Figure 7.4	Initial and final PWP for multiple fouling and cleaning cycles for the PES membrane 80
Figure 7.5	Alumina membrane rejection for each fouling and cleaning cycle 81
Figure 7.6	PES membrane rejection over fouling and cleaning cycles 81
Figure 7.7	Alumina membrane cleaning duration for each cycle. 82
Figure 7.8	Cleaning time for the PES membrane 82
Figure 7.9	EEM of cleaning filtrate sample. 83
Figure 8.1	Economic comparison at $Pe = 5.5$ 88
Figure 8.2	TPC as a function of pressure increase between backwashes for the alumina membrane at a flux of 125 at a $Pe = 9.1$ 90
Figure 8.3	Economic comparison at $Pe = 9.1$ 91
Figure 8.4	Economic comparison for bentonite suspension at $Pe = 11.4$ 93
Figure 8.5	Comparison of capital cost components (not amortized) 94
Figure 8.6	Comparison of O&M cost components 94
Figure 8.7	Capital cost components for alumina membrane at $Pe = 11.4$ 96

Figures (continued)

	<i>Page</i>
Figure 8.8 Operating and maintenance costs for alumina membrane at $Pe = 11.4$	96
Figure 8.9 Effect of reducing the number of plant operators on TPC for hypothetical alumina membrane at $Pe = 11.4$	97
Figure 8.10 Effect of reducing polymeric membrane lifespan and reducing ceramic membrane material cost.....	98

1. Introduction

In many areas of the United States, fresh water resources are over-allocated, and there is a need to develop “new” water supplies to meet the increasing water demand due to population growth and the impacts of climate change on water quality and quantity. Water sources that are presently unused, such as municipal and industrial wastewater and brackish ground and surface water, have contaminant concentrations that typically exceed water quality standards and often require using water treatment processes to improve the water quality to useable standards. Low-pressure membrane separation processes, termed microfiltration (MF) and ultrafiltration (UF), are widely used for water and waste water treatment for removing total and dissolved organic carbon (DOC), suspended solids and particulates, heavy metals, oil and grease, and bacteria and viruses. Membrane processes commonly are employed because they are efficient, have a relatively small footprint, provide a physical barrier for pathogens, and can be used to remove multiple contaminants in a single process with lower chemical and energy requirements compared to other water treatment technologies.

Since the early 1990s, MF and UF have become increasingly popular alternatives to conventional water treatment technologies, such as coagulation/flocculation, sedimentation, and media filtration, for removing particulates, bacteria and viruses, and natural organic matter (Adham, Chiu et al. 2005) from surface water, wastewater, and industrial water supplies. MF and UF membranes can also be used as pretreatment technologies for desalination processes such as reverse osmosis membranes (Jacangelo, Trussel et al. 1997).

The most commonly used materials for MF and UF membranes are polymers, such as polyacrylonitrile (PAN), polyvinylidene fluoride (PVDF), polyethersulfone (PES), or polypropylene (PP); however, membranes also can be made from ceramic materials such as titanium dioxide (TiO_2), zirconium dioxide (ZrO_2) and alumina (Al_2O_3). For many years, ceramic membranes have been used extensively in the pharmaceutical, food and beverage, and industrial water treatment sectors, where their resistance to harsh operating and/or cleaning environments has added benefit; but they have not been major competitors to polymeric membranes for commodity applications such as drinking water and waste water treatment. The high material cost of ceramic membranes coupled with a lack of full-scale operational experience has limited their incorporation in the latter applications (Tan 2010).

Ceramic membranes offer many potential advantages over polymeric membranes for water treatment applications. Ceramic membranes have extremely high thermal, chemical, and mechanical stability and, therefore, can withstand strong cleaning chemicals, elevated temperatures, and are not susceptible to breakage. Ceramic membranes are resistant to oxidants, such as ozone and chlorine, which

cause degradation of some types of polymeric membranes. These characteristics have significant implications for membrane cleaning and operation under harsh environmental and operational conditions. Membrane materials used for MF and UF applications dictate the physicochemical interactions between the membrane and constituents in the feed water (related to the rate of membrane fouling), chemical cleaning requirements, energy demand, size and capacity of the process equipment, and membrane material cost for a membrane application. Therefore, selection of the appropriate material will result in a more sustainable and affordable water treatment system.

1.1 Research Objectives and Hypotheses

In the past few years, the municipal water treatment industry has been gaining interest in ceramic membranes. Currently, it is unclear whether the reported advantages of ceramic membranes, such as longer operational life, chemical stability, and thermal stability, will translate into a measurable cost savings compared to polymeric membranes.

The objectives of this research are two-fold:

1. To describe ceramic and polymeric membrane fouling propensity and cleaning (or regeneration) efficiency in such a way that observed differences are due to material property differences and not operational differences and,
2. To quantify the impact of performance and operational differences between ceramic and polymeric membranes in terms of process economics.

The overarching hypothesis driving this research is that ceramic membranes exhibit different fouling behavior and cleaning efficiency than polymeric membranes due to different material properties and hydrodynamic conditions resulting from differences in module configuration. The specific hypotheses of this research are as follows:

1. The high flux attributed to ceramic membranes results from being operated at a higher pressure.
2. Ceramic membranes will have a higher lifetime-sustained-flux than polymeric membranes due to more complete regeneration, measured as flux or pressure recovery, after chemical cleaning.
3. Ceramic membranes can operate at higher pressures and experience less fouling than polymeric membranes, leading to a cost savings because they require less membrane area (fewer membrane modules) to meet design production capacity.

4. Because ceramic membrane material cost is high, minimizing flux decline, which is accomplished by either operating at a higher crossflow velocity or a reduced pressure, does not necessarily reduce the plant life cycle cost.
5. Technical lever points, such as material cost and operating conditions, can be identified to determine the economic efficiency of any membrane, including both ceramic and polymeric ones.

1.2 Significance of Research

The previous studies conducted to compare ceramic and polymeric membrane flux behavior did not take into account the influence of membrane module geometry and operating conditions (which determine the hydrodynamic conditions within the membrane system) on membrane fouling. Without comparing ceramic and polymeric membranes on the same water type under the same apparent hydrodynamic conditions, it is difficult to draw generalized conclusions about which membrane is best suited for a given application. To increase the certainty that observed differences in flux behavior, rejection, and cleaning efficiency are a result of material property differences and not operational differences, experiments should be conducted so that the membranes are exposed to the same mass of foulant per unit area under the same hydrodynamic conditions.

This research addresses deficiencies in past work and builds upon the existing knowledge base of ceramic and polymeric membrane filtration to experimentally compare ceramic and polymeric membranes so that differences between the two types of membranes can be attributed to specific material properties or hydrodynamic differences. Furthermore, the cleaning efficiency of these ceramic and polymeric membranes, exposed to the same mass of foulant per unit area under the same hydrodynamic conditions, is quantified. This approach ensures that differences in cleaning efficiency can be attributed to differences in membrane physicochemical properties versus differences in the quantity and structure of the membrane foulant.

The results of the experimental analysis of performance and cleaning efficiency are used in a techno-economic model to describe the life cycle costs for a hypothetical membrane plant using these ceramic or polymeric membranes. This approach allows the integration of both performance and cost differences between the two types of membranes and is used to identify the technical and economic lever points that dictate which membrane system is more cost effective. Additionally, this model allows the comparison of different materials based on a number of other important factors, such as chemical usage, power consumption, and feed water recovery. The following graph illustrates the value of considering performance and operational factors in cost calculations.

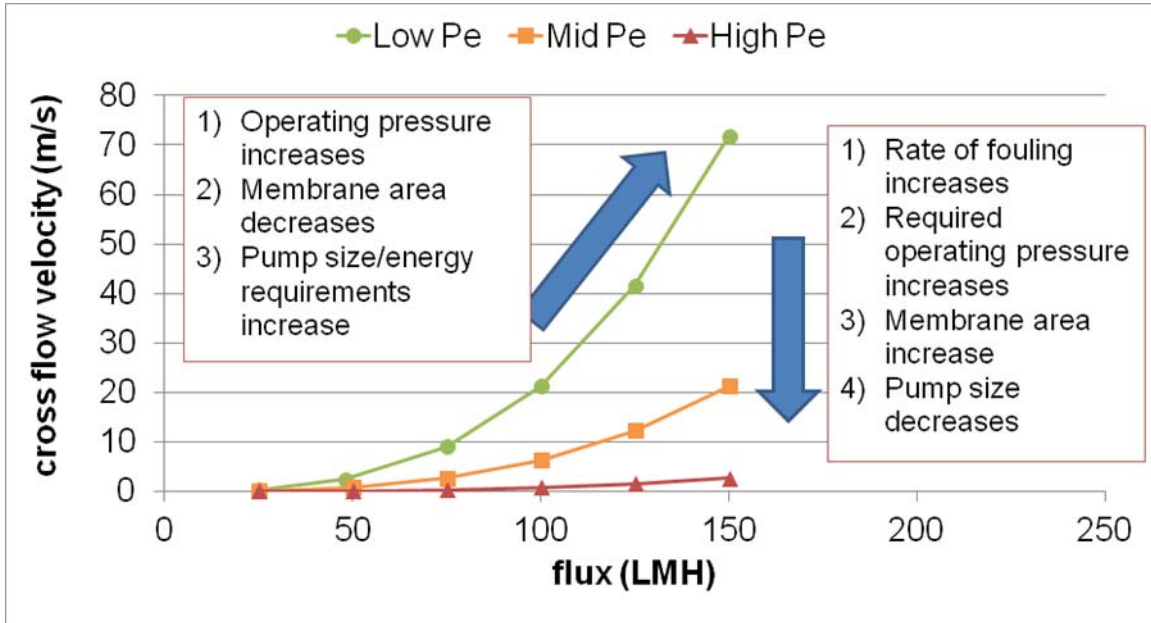


Figure 1.1 Tradeoffs between operating conditions and total water production cost.

While the quantitative results presented in this report are specific to the water types and membranes tested, the broad contributions of this work are the methods developed—namely, the membrane testing protocol and data-driven cost model. The testing protocol and data-driven model can be used to evaluate the performance and cost of other types of membranes for feed water types other than those evaluated in this work. When using these methods to evaluate other membranes and feed water types, the data required are the time rate of change of transmembrane pressure and the corresponding values of the apparent Pe.

Government research programs, such as Desalination and Water Purification Research, managed by the Bureau of Reclamation, and Future Naval Capabilities, managed by the Office of Naval Research, fund research to develop new membrane products. The techno-economic model developed in this project currently is being used to evaluate the performance benefits of novel membranes developed from these research programs so that they can be compared on an equivalent basis to existing, commercially available membrane products. Furthermore, this tool can be used to estimate the potential economic benefit (reduction in total water production cost) of incremental improvements in membrane material properties, improved cleaning and regeneration techniques, and improved process operating conditions. Therefore, a cost/benefit analysis can be conducted to determine the benefit of investing research dollars in the different areas of membrane science.

This research is directly in line with recommendations from the National Research Council (NRC) stating that, while membranes are an effective, robust technology, more research is needed to minimize the cost of [low-pressure membrane systems] by reducing membrane fouling and optimizing membrane

design and operation (NRC 2008). The techno-economic model developed in this work represents a decision analysis tool that will facilitate the selection of different membrane materials, based on performance specifications, and identify efficient operating conditions for microfiltration and ultrafiltration membrane plants. Selection of appropriate membrane materials and efficient plant operation will lead to a reduction in the cost of implementing these systems.

1.3 Limitations of Research

This research focused on broad aspects of membrane performance and operation in the context of process economics. While the laboratory results presented are specific to the feed water types and membranes tested, the methods developed are applicable to a wide range of applications. This work does not address broad material science issues, such as membrane surface modification to improve performance.

Membrane filtration processes are complex systems with numerous controlled and uncontrolled variables. Assumptions are made to use previously developed correlations, to simplify the analysis of the system, and to extrapolate data from the laboratory to predict observations at full-scale. Therefore, the following assumptions and limitations apply to this work:

- All experiments were conducted under laminar (and possibly transition) flow; therefore, correlations used in this work may not be appropriate for turbulent flow conditions.
- Membrane module configuration affects the hydrodynamic conditions at the membrane/water interface. The measurements made in this study use tubular, inside-out flow modules. Other configurations, such as flat sheet, spiral wound, or outside-in, have not been considered in this work; and the conclusions drawn from this research should not be applied directly to other module configurations without judicious modifications.
- Feed water composition generally was assumed to be uniform from one experiment to the next; however, large volumes of synthetic feed water were prepared for these experiments. Due to limitations in measurement accuracy, minor differences in feed water composition were observed. Corrections were made to account for the different mass per volume of filtrate generated, and the effects of concentration on the rate of fouling were assumed to be negligible.

The cost model developed in this task is subject to the following limitations:

- The cost of equipment, such as pumps, tanks, and piping, are modeled as continuous functions; however, this equipment is produced and sold in discrete sizes.
- The cost estimates presented in this work represent appraisal level cost estimates with uncertainties of approximately 25 percent (%). To conduct more accurate cost estimates, vendor quotes specific to an application must be obtained.

1.4 Report Organization

The research plan to address each of the hypotheses outlined in section 1.2 translates into the various chapters of this report.

A comprehensive literature review is presented in chapter 2. The review summarizes the results of past studies to compare ceramic and polymeric membranes and assesses how the broad material property difference between the two classes of membranes may contribute to performance differences. Also, an evaluation of the anecdotal claim that ceramic membranes exhibit higher flux than polymeric membranes is conducted through the assessment of previously published literature to validate hypothesis 1.

Chapter 3 describes in detail the cost model used in this work. This chapter identifies the components of the cost model that require additional data from laboratory experiments and membrane characterization and presents justification for the range of values chosen for parameters and variables.

Chapter 4 describes the materials and methods used in this work, including membrane and feed water quality characterization and a description of the experimental equipment used to conduct the filtration and cleaning experiments.

Chapter 5 summarizes a study conducted to evaluate the influence of different operating parameters on ceramic membranes. This study was used to gain experience with operation of ceramic membranes and identify economic lever points associated with ceramic membrane systems. This chapter addresses hypothesis 4. This chapter has been published in *Separation and Purification Technology* (Guerra, Pellegrino et al. 2012).

Chapter 6 presents the data comparing the filtration performance (rate of fouling and rejection) for the ceramic and polymeric membranes under the same apparent hydrodynamic conditions and provides the data necessary to evaluate hypothesis 5.

Chapter 7 presents the data comparing the cleaning efficiency of the two membranes and is used to assess the validity of hypothesis 2.

Chapter 8 details the cost model results for the two types of membranes and includes parametric analyses to evaluate how changes in the input parameters, such as membrane material cost, impact the lifecycle cost estimates. Results from this chapter are currently under review for publication in Separation Science and Technology. This chapter is used to address hypotheses 3 and 5.

Chapter 9 summarizes the conclusions drawn from this research study.

Chapter 10 outlines recommendations for future research regarding performance comparison of ceramic and polymeric membranes and low-pressure membrane cost modeling.

2. Review of Literature

Ceramic and polymeric membrane material properties differ in many regards, including porosity, surface energy, chemical and thermal stability, and pore size distribution, which affect fouling potential, solute rejection, and cleaning efficiency. Differences in material properties and module configuration between ceramic and polymeric membranes will affect the solute/membrane interactions and the hydrodynamics during filtration—thus, impacting the fouling behavior, solute rejection, and cleaning efficiency (Belfort, Davis et al. 1994; Bacchin, Aimar et al. 2006). To identify or quantify the benefits provided by using ceramic membranes, it is necessary to understand how these characteristics contribute to fouling, solute rejection, and cleaning efficiency.

The major factors that contribute to flux decline and membrane cleaning and regeneration are considered in this chapter, as well as a summary of past work to compare ceramic and polymeric membranes. This review describes the current state of knowledge regarding performance factors, namely membrane productivity, fouling tendency, and cleaning efficiency, that determine the total water production cost for these two types of membranes. This review also is used to identify relevant ranges for module geometry, operating variables, and backwash and cleaning parameters for the two types of membranes.

2.1 Factors Affecting Membrane Fouling

Fouling, due to adhesion and deposition of particles and colloids onto membrane surfaces and into membrane pores, is the biggest challenge associated with the operation of low-pressure membrane processes. Fouling increases the pressure required to generate the desired volume of product water and requires expensive chemical cleaning for removal. Irreversible fouling, which cannot be removed with chemical cleaning, reduces the performance of the membranes over time and eventually necessitates membrane replacement. Membrane material properties, module hydrodynamic conditions, and feed water characteristics dictate the degree to which a membrane will foul.

2.1.1 Membrane Material Properties

The degree of fouling by a given solute is not only a function of the solute properties but also of the membrane material properties and the resulting interaction between the solute and the membrane surface. Material properties that influence membrane fouling and water productivity are pore size/molecular weight cutoff, surface and bulk porosity, membrane thickness, surface hydrophobicity, surface charge, and surface roughness.

2.1.1.1 Pore Size Distribution

Pore size distribution is an important factor governing the separation capability and the resistance of the membrane to the flow of solvent for low-pressure membranes. Both ceramic and polymeric membranes are commercially available in a range of pore sizes completely spanning the definition of MF and UF; pore sizes range from 0.45–0.005 micrometer (μm). Membrane manufacturers provide a nominal pore size for their products. However, literature has shown that there is a significant difference between the nominal and reported pore sizes for membranes; therefore, to accurately predict membrane performance, accurate pore size distribution measurement is necessary.

2.1.1.2 Membrane Permeance

Pure water permeance is the normalized productivity of membranes, is calculated as the pressure normalized flux of deionized water through the membrane, and is commonly used to describe low-pressure membranes. Permeance is influenced by the material structure (porosity, tortuosity, thickness, etc.). Thinner membranes with lower tortuosity offer less resistance to fluid flow and, therefore, exhibit higher permeances. Higher porosity membranes also offer less resistance to flow.

2.1.1.3 Surface Energy and Surface Charge

Membrane surface energy influences the degree to which solutes adsorb onto the membrane surface. High energy surfaces are less favorable to adsorption than low energy surfaces. Contact angle is the most widely used method for characterizing the surface energy (also known as hydrophilic or hydrophobic nature) of membranes and has been used widely by many researchers (Gekas, Persson et al. 1992; Gourley, Britten et al. 1994; Nabe, Staude et al. 1997; Susanto and Ulbricht 2005; Lozier, Cappucci et al. 2008). Lower water contact angles indicate that a surface is more hydrophilic. Alpha-alumina membranes are naturally hydrophilic due to the high energy chemical bonds that make up the material, while many polymeric membranes (i.e., polypropylene, polysulfone, polytetrafluoroethylene, etc.) are considered lower energy surfaces. Modifications can be made to polymeric materials to increase surface energy; however, the surface energy of most polymeric materials is significantly lower than for ceramic materials (Huang, Young et al. 2009).

Membranes that are more hydrophilic are believed to exhibit higher flux and reduced fouling compared to hydrophobic membranes, because many common membrane foulants are hydrophobic (Hofs, Ogier et al. 2011). However, correlation between hydrophobicity and fouling potential is difficult to assess (Maximous, Nakhla et al. 2009).

Although MF and UF are mainly size-based sieving processes, charge interactions are also significant, since they can affect the accumulation of solute on the membrane surface due to electrostatic interactions between the surface and the

solutes. Membranes acquire a charge, when in the presence of an aqueous solution, that is dependent on the pH of the solution. Therefore, the pH of the feed water and the types of solutes in suspension greatly influence the role of membrane surface charge on fouling. The surface charge of membranes often is characterized by measurements of zeta potential.

2.1.1.4 Surface Roughness

Surface roughness is believed to affect membrane fouling; however, a direct correlation between roughness and membrane fouling generally is not accepted. The role of membrane roughness on fouling also may be influenced by the surface energy of the membrane. Weis and Bird found that a rougher, hydrophilic membrane fouled less than a smoother, hydrophobic membrane. For membranes of similar hydrophobicity but different roughness, fouling was found to be less severe for a smoother membrane (Weis, Bird et al. 2005). However, others have reported that membrane roughness results in a larger membrane surface area for adhesion of foulants; and, therefore, increased roughness results in more severe fouling (Elimelech, Xiaohua et al. 1997; Du, Peldszus et al. 2009).

2.1.2 Membrane Module Configuration and Hydrodynamic Conditions

The hydrodynamics of low-pressure membrane systems are largely defined by the mode of operation (dead-end or cross-flow) and then by the module configuration (channel or hollow fiber inner diameter, length of the channel, etc.) and the operating conditions (permeate flux and the cross-flow velocity of the feed water in the channel or fiber).

There are two modes of operation in which low-pressure membranes, both ceramic and polymeric, can be used; cross-flow and dead-end, figure 2.1. In dead-end filtration mode, all of the water that is fed to the membrane passes through the membrane as filtrate, or product water. In cross-flow mode, some of the feed water continues through the module unfiltered. Cross-flow mode can minimize membrane fouling by facilitating transport of solute away from the membrane surface but also requires a recirculation loop to recycle the reject water back the feed stream to maximize product water recovery. Dead-end filtration usually requires more frequent backwashes and may cause more irreversible fouling of the membrane—that is, fouling that cannot be removed by backwash or cleaning.

During cross-flow membrane filtration, solvent passes through the membrane to the permeate, leaving a solute rich solution in the retentate stream resulting in an accumulation of dissolved or suspended solutes near the membrane surface (termed concentration polarization); see figure 2.1b.

Concentration polarization inhibits solvent flux through the membrane by increasing the osmotic pressure at the membrane surface (Belfort, Davis et al.

1994) and, thereby, lowering the net transmembrane pressure driving force for permeation. The concentration boundary layer exists between the lower, bulk solute concentration in the feed stream and the region of higher solute concentration near the membrane surface.

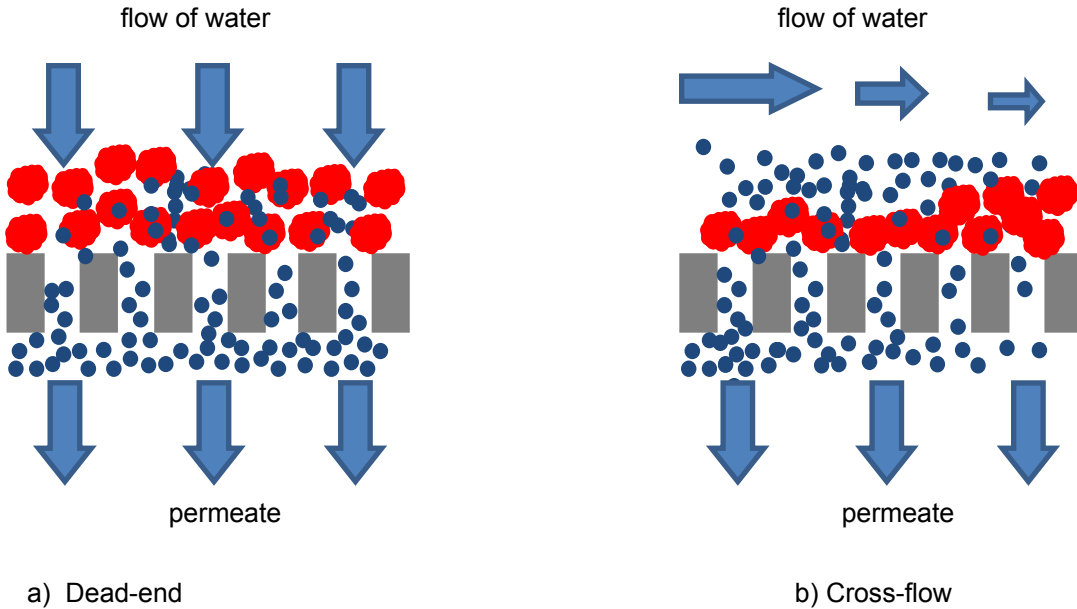


Figure 2.1 Schematic diagram of dead-end and cross-flow filtration.

The thickness of the concentration boundary layer is determined by the forced convection delivering solute to the membrane surface and the diffusive back-transport of solute away from the concentration boundary layer. The film theory model is commonly used to describe the solution flux under these circumstances (Cheryan 1998).

A mass balance across the concentration polarization layer, results in the following equation describing the solvent flux through the membrane:

$$J_v = k \cdot \ln \left(\frac{C_m - C_p}{C_b - C_p} \right) \quad (\text{Equation 2.1})$$

Where k is the mass transfer coefficient, C_m is the solute concentration at the membrane surface (C_m cannot be directly measured); C_b is the bulk solute concentration, and C_p is the permeate's solute concentration. Simply stated, the rate of solute transfer back to the bulk fluid from the membrane interface is proportional to the concentration difference, wherein k describes the proportionality.

Mass transfer correlations have been developed for commonly encountered fluid-solid interfacial geometries, flow regimes, and solution/suspension characteristics. Mass transfer correlations are typically reported as correlations of dimensionless

numbers, primarily the Sherwood, Schmidt, and Reynolds number. Typically, an accuracy of $\pm 10\%$ is observed for mass transfer correlations for solid-liquid interfaces (Cussler 2009).

The following correlation, having a strong theoretical and experimental basis, is used for laminar flow through a circular tube:

$$\frac{k \cdot d}{D} = 1.62 \left(\frac{d^2 \cdot v}{L \cdot D} \right)^{1/3} \quad (\text{Equation 2.2})$$

Where, d is the hydraulic diameter of the tube, v is the cross-flow velocity, L is the length of the tube, and D is the diffusion coefficient.

There are many different expressions used to estimate the diffusion coefficient of solutes. The Stokes-Einstein equation, used for spherical particles under laminar flow, is most generally used, equation 2.3.

$$D = \frac{k_B T}{6\pi\eta r} \quad (\text{Equation 2.3})$$

Where, k_B = Boltzman's constant, 1.38×10^{-23} , T = temperature, η = viscosity, and r = radius of spherical particle. Estimation of more accurate values of the diffusion coefficient, using the Stokes-Einstein equation, requires the actual viscosity at the membrane surface, which is difficult, if not impossible, to determine. Where possible, measured values always should be used.

The Peclet (Pe) number is used to characterize the ratio of the convective transport toward the membrane surface (flux) and the diffusive back-transport away from the membrane surface, k . Larger mass transfer coefficients will result from advantageous channel hydrodynamics (higher cross-flow velocity, larger diameter channel, and shorter channel length) and will tend to reduce fouling potential due to the cake formation and concentration polarization. To compare our ceramic and polymeric membranes on an equivalent hydraulic basis, the same nominal Pe^1 or J/k ratio is used.

In principle, for $Pe = 1$, there is no net momentum acting on the solutes because, by definition, the solute mass transfer to the membrane surface from water permeation is equal to the solute mass transfer away from the membrane surface. For typical MF and UF applications, Pe greater than ($>$) 1; therefore, solutes accumulate on the membrane surface, resulting in concentration polarization and fouling, observed as a pressure increase during operation at constant flux (Bacchin and Aimar 2005; Bacchin, Aimar et al. 2006).

The calculated values of Pe are nominal (or apparent) values since the mass transfer coefficients are correlations based on many idealized assumptions, including the flow channel geometry, and rely on values that cannot be directly

¹ The nominal Pe is what we calculate using correlations and estimates.

measured (diffusion coefficient of solute and solute velocity at the membrane surface) but are approximated using measurements of the bulk fluid properties.

2.1.2.1 Ceramic Membrane Module Configuration and Operational Experience

Typically, ceramic membranes are operated in an inside-out flow configuration. The number and dimensions of the tubular flow channels vary significantly between the commercially available products; see table 2.1. The channel shape and diameter affect the hydrodynamics of the channel.

Table 2.1 Selection of commercially available ceramic membrane products¹

	Product Line(s)	Filtration Range	Support Materials	Membrane Materials	Channel Configuration
Pall	Membralox® Schumasiv®	5 nm to 0.2 µm	Al ₂ O ₃	Al ₂ O ₃ (MF) ZrO ₂ and TiO ₂ (UF)	Hexagonal and round
Corning	CerCor®	5 nm to 0.2 µm	Mullite (3 Al ₂ O ₃ •2 SiO ₂)	ZrO ₂ (MF) TiO ₂ (UF)	Square and round
TAMI	Ceram Inside®	0.02–1.4 µm	ATZ	ZrO ₂ (MF) TiO ₂ (UF)	Flower shaped
Atech	Atech	0.01–1.2 µm	Al ₂ O ₃	Al ₂ O ₃ (MF) ZrO ₂ and TiO ₂ (UF)	Single or multiple round
Orelis	Kerasep™	5 kDa to 0.8 µm	Al ₂ O ₃	ZrO ₂ and TiO ₂	Single or multiple round

¹ nm = nanometer; ATZ = aminotetrazole; kDa = kilodaltons.

2.1.2.2 Polymeric Membrane Configuration and Operational Experience

Polymeric ultrafiltration membranes for full-scale applications are typically hollow fiber in configuration with fiber diameters ranging from 1–2 millimeters (mm) in diameter. For some industrial applications, spiral-wound modules may be used. MF/UF plants typically are delivered as a package plant and are designed and constructed by the manufacturer. Table 2.2 presents a summary of some of the commercially available polymeric membranes from package systems.

The following table, table 2.3, summarizes the main operating parameters for ceramic and polymeric membranes. The values for ceramic membrane operating parameters were obtained from literature, while the polymeric membrane parameters are based on full-scale plant information (Adham, Chiu et al. 2005).

Table 2.2 Selection of commercially available pressure driven, inside-out polymeric membrane products¹

	Product Line(s)	Filtration Range/MWCO	Membrane Materials	Configuration/ Fiber ID (mm)
Pall	Microza®	MF and UF, 1 µm to 80,000 Da	PVDF	Inside-out/0.7 or 0.8
USFilter	M10C®	MF 0.1 and 0.2 µm	PP, PVDF	Outside-in
Koch Membrane Systems	PMPW®	100,000 Da	Polysulfone	Inside-out/0.9
Hydranautics	HYDRACap	UF – 150,000 Da	Hydrophilic modified PES	Inside-out/0.8 or 1.2
Norit	X-Flow – Horizontal	UF – 0.025 µm		Inside-out/0.8
Aquasource		UF – 0.01 µm	CA and PS	Inside-out/0.93

¹ ID = inside diameter; Da = dalton; MWCO = molecular mass cutoffs; CA = cellulose acetate; PS = polysulfone.

Table 2.3 Comparison of ceramic and polymeric membrane operating conditions¹

	Ceramic	Polymeric
Filtration mode	Dead-end or cross-flow	Dead-end or cross-flow
Cross-flow velocity (m/s)	0–4	0.1–1 (limited data available)
Feed water recovery (%)	90–100	70–100
Flux (L/m ² /h)	NA	40–110
Lifespan (y)	15–20	4–8

¹ m/s = meter per second; L/m²/h = liter per square meter per hour; NA = information not available; y = year.

2.1.3 Feed Water Characteristics

The primary constituents that contribute to low-pressure membrane fouling are microorganisms, natural organic matter (NOM), colloids, and particulates (Lozier 2005). Many different parameters are used to qualitatively describe the membrane-solute and solute-solute interactions that affect membrane performance. The composition of the feed water can be characterized using the following measurements: turbidity, alkalinity, temperature, pH, total and dissolved organic carbon, ionic strength, specific ion concentrations, ultraviolet (UV) absorbance, and zeta-potential.

2.2 Membrane Cleaning and Regeneration

Membrane fouling, resulting in a loss of productivity, is unavoidable in nearly all filtration applications. Some membrane fouling is reversible and can be removed from the membrane through hydraulic and/or chemical cleaning, but irreversible fouling cannot be removed and ultimately necessitates membrane replacement. Both types of fouling will decrease membrane performance. Reversing, removing, and/or mitigating membrane fouling will lead to increased economic efficiency for membrane applications through a reduction in the required transmembrane pressure or an increased membrane lifespan.

2.2.1 Backwash

Backwash is accomplished by flowing permeate water through the membrane from the permeate side to the feed side to remove foulants from the membrane surface. Backwash is used to maintain high flux in membrane systems between chemical cleanings and is used to minimize the use of chemicals and waste generation by reducing chemical cleaning frequency. Backwash strategies for ceramic membranes can take advantage of the improved mechanical strength and chemical and thermal resistance of ceramic materials to employ backwash regimes that could damage polymeric membranes. Alternative backwash strategies include chemically-enhanced backwash at high or low pH and high temperature backwash.

Hofs et al. has conducted a study primarily focused on backwashing the two types of membranes after fouling due to filtration of surface water containing natural organic matter (Hofs, Ogier et al. 2011). Four types of ceramic membranes, ZrO_2 , Al_2O_3 , TiO_2 , silicon carbide (SiC), and two polymeric membranes, PES and polyvinylpyrrolidone (PVP), were evaluated. The membranes were operated at a constant flux of $150 \text{ L m}^{-2} \text{ h}^{-1}$. Two different backwashes were considered: constant pressure and constant flux. Backwashes were executed for 1 minute after every 20 minutes of filtration. Reversible fouling was defined as the difference in pressure before and after backwash averaged over multiple cycles. The transmembrane pressure (TMP) at time t (TMP_t) minus the TMP at $t = 0$ (TMP_0) was plotted versus the permeate volume. Irreversible fouling was defined as the slope of a linear fit to the TMP values immediately following each of the backwashes. The authors found that polymeric, Al_2O_3 , and zirconia (ZrO_2) membranes had similar levels of reversible fouling; however, the polymeric membranes experienced more irreversible fouling than the ceramic membranes. The authors concluded that the more hydrophilic membranes exhibited less irreversible fouling.

Other backwash studies, not specific to comparing the two types of membranes, were surveyed to identify the appropriate range of conditions to be considered in experimental work. Results from these studies also are presented here to provide a justification for experiments presented in subsequent chapters.

The backwash frequency reported in the literature for ceramic and polymeric membranes ranges from 3–90 minutes (Sondhi and Bhawe 2001; Gilbert 2010). Lerch et al. used a backwash frequency of 30 min and backwash duration of 30 s (Lerch, Panglisch et al. 2005). Backwash frequency for polymeric membranes typically ranges from 15–75 minutes. Reducing the frequency of backwash will result in an increase in pressure during the filtration cycles, which results in an increase in the energy consumption; however, more frequent backwashes means that the overall plant size needs to be larger to account for the filtrate water consumed during backwash and to produce additional filtrate because the plant is not producing filtrate during backwashing.

Some research claims that high backwash flux, accomplished using high backwash pressure, results in more complete productivity recovery (Hofs, Ogier et al. 2011). However, findings from Katsoufidou et al. are contradictory. They studied the effect of backwash pressure on backwash efficiency for NOM and sodium alginate fouling of PES UF membranes with MWCO of 150 kilograms per mole (kg/mol) and found that low backwash pressure resulted in a higher flux recovery because a high backwash pressure compacted the foulant that accumulated within the membrane pores and increased the resistance of the foulant layer (Katsoufidou, Sioutopoulos et al.; Katsoufidou, Yiantisios et al. 2005; Katsoufidou, Yiantisios et al. 2007; Katsoufidou, Yiantisios et al. 2008).

The findings reported by Katsoufidou, et al. are partially supported by preliminary experiments conducted for this research study. Backwash was conducted at pressures of 15, 40, and 80 pounds per square inch (psi), respectively, for an alumina composite ceramic membrane; see figure 2.2. The filtration conditions in between backwashes were identical, and the same membrane was used for each of the experiments. The 40-psi backwash resulted in the least amount of flux decline over the course of the filtration experiment, whereas the 80-psi backwash exhibited the largest amount of flux decline. The 15-psi backwash produced slightly better results than the 80-psi backwash but was not as efficient as the 40-psi backwash. This is likely because the 15 psi was insufficient to remove foulant from the membrane, suggesting that there is an optimum backwash pressure, between 15–40 psi for this particular membrane, to maximize flux recovery.

Backwash effectiveness was also found to be dependent upon the location of foulant within the membrane module and the pore size of the membrane. Kumar et al. found that backwash was most effective at removing solute accumulated on the membrane surface, but could not effectively remove foulant adsorbed within the membrane pore structure (Kumar, Madhu et al. 2007). They also showed that backwash was more effective for a membrane with a larger channel diameter.

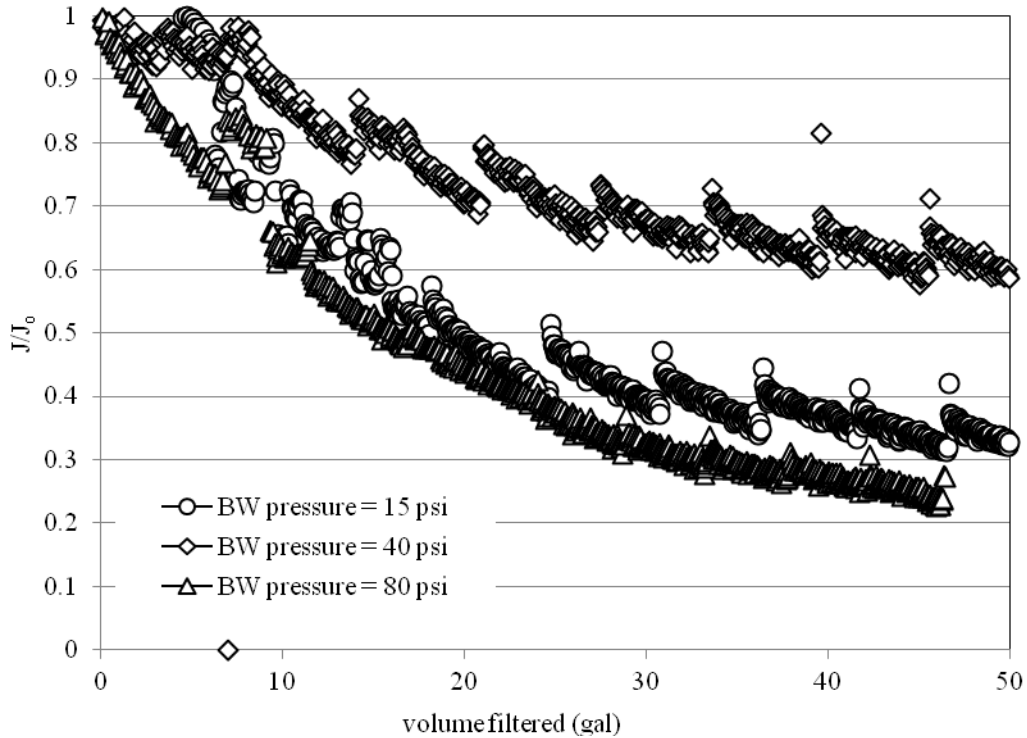


Figure 2.2 Effect of backwash pressure on backwash efficiency.

2.2.2 Chemical Cleaning

Chemical cleaning is used to recover fouling not removed through clean water flushing and backwash. Cleaning agents typically are flushed over the membrane surface and allowed to soak within the membrane system for minutes to hours to enhance cleaning efficiency. Chemical cleaning typically is followed by feed water flushes to remove cleaning chemicals from the membrane system prior to filtration. Because chemical cleaning requires plant downtime and generates a waste for disposal, cleaning frequency should be minimized.

In 2010, a comprehensive review of the literature on membrane cleaning was published (Porcelli and Judd 2010). Porcelli and Judd explain that membrane cleaning consists of the following processes, independent of the membrane material to be cleaned: transport of cleaning agent through foulant layers to membrane surface, solubilization and detachment of foulant from the membrane surface, and transport of detached foulant to the bulk solution. The efficiency of the processes outlined above depends upon proper selection of cleaning chemicals and cleaning conditions.

2.2.2.1 Types of Cleaning Chemicals

The following categories of cleaning chemicals have been identified in the literature for use on both ceramic and polymeric membranes: caustics, oxidants,

acids, and detergents (Bartlett, Bird et al. 1995; Gan, Howell et al. 1999; Koyuncu, Lüttge et al. 2008). For caustic cleaning, sodium hydroxide is most commonly used at pH levels of 11–12 (less if membrane resistance is an issue, e.g., PVDF). Hydroxide reacts with weakly acidic organic matter, carboxylic and phenolic functional groups, and promotes cleavage of polysaccharides and proteins into small sugars and amides (Porcelli and Judd 2010).

Oxidants, such as hydrogen peroxide and sodium hypochlorite can be used for cleaning applications; however, some polymeric membranes are not tolerant to chlorine, and the use of sodium hypochlorite generates chlorinated organic compounds, which can have adverse health and environmental effects. However, oxidants are useful for membrane cleaning because they degrade NOM functional groups and make them more susceptible to hydrolysis at high pH; therefore, oxidant use in combination with alkaline cleaning agents is effective for reversing NOM fouling (Liu, Caothien et al. 2001; Zondervan and Roffel 2007; Porcelli and Judd 2010). Gan et al. also showed that combined cleaning chemicals (caustic and oxidant) provide fast, effective cleaning for ceramic membranes fouled with complex feed solution (Gan, Howell et al. 1999).

Acids primarily are used in membrane cleaning for removing inorganic scale and metal oxides. Additionally, some organic compounds, such as polysaccharides and proteins, also hydrolyze in the presences of acids (Porcelli and Judd 2010). Hydrochloric, sulfuric, nitric, and citric are commonly used acids in membrane cleaning.

Detergents and cleaning additives, such as ethylenediaminetetraacetic acid (EDTA), sodium dodecyl sulfate (SDS), and proprietary cleaning agents, are effective at removing a wide variety of foulants; however, their use is limited for water treatment applications by both cost and regulatory issues with disposal and residual agent carryover into the product water (Porcelli and Judd 2010). Combined chemical cleaning solutions consisting of detergents and caustics have been shown to be effective for protein cleaning (Almecija, Martinez-Ferez et al. 2009).

Sequential cleaning steps, consisting of different types of cleaning agents, have been shown to be most effective for nearly all types of fouling. More efficient cleaning is observed for NOM fouling using sequential cleaning steps of separate alkaline and acidic cleaning steps (Bird and Bartlett 2002; Blanpain-Avet, Migdal et al. 2004).

2.2.2.2 Regimes

Cleaning solutions typically are recirculated through the membrane system. Most often, the filtrate ports are closed; and the cleaning solution is in contact with the feed side portion of the membrane. In some studies, static cleaning has been

conducted in which the membrane is left to soak in the chemical solution for prescribed amounts of time. Often, sequential steps of recirculation and soaking are used.

Recirculation of the cleaning chemicals at a high cross-flow velocity and a low TMP have been proven to be effective at increasing cleaning efficiency (Gan, Howell et al. 1999). It has been shown that some permeation of cleaning solution through the membranes is beneficial for removing pore fouling (Mercadé-Prieto and Chen 2005).

2.2.2.3 Duration

Most frequently, cleaning times in the literature are on the order of hours. Gan et al. used cleaning times of 200–300 minutes (Gan, Howell et al. 1999); and Lee et al. conducted cleanings for 1–5 hours (Lee, Amy et al. 2001). Often with cleaning studies, it is difficult to monitor the progress of cleaning; and, therefore, optimal times may be difficult to establish.

In some studies, particularly relating to cleaning of protein fouled membranes, it has been observed that the majority of cleaning efficiency is realized within the first 5 minutes of cleaning; and cleaning beyond 20 minutes promotes re-deposition of foulants (Blanpain-Avet, Migdal et al. 2004; Popović, Tekić et al. 2009).

2.2.2.4 Temperature

Cleaning with chemical solutions at elevated temperature has been shown to improve cleaning efficiency. Numerous authors have shown that cleaning at a temperature near 50 degrees Celsius (°C) produces efficient cleaning and may be close to an optimal cleaning temperature (Bird and Bartlett 2002; Chen, Kim et al. 2003; Mercadé-Prieto and Chen 2005; Almecija, Martinez-Ferez et al. 2009).

2.3 Assessment of Literature to Compare Ceramic and Polymeric Membranes

Reported benefits of ceramic membranes compared to polymeric membranes include higher flux (possibly due to a higher porosity), less flux decline (possibly due to higher hydrophilicity), and higher cleaning efficiency (possibly due to greater chemical stability) (American Water Works Association [AWWA] 1996; Gaulinger 2007; Cornelissen, Hofs et al. 2009; Booker 2010). In most drinking water applications, water is treated as a commodity product; and the treatment costs must be low. Therefore, if ceramic membranes are to be a competitor to polymeric membranes for municipal water treatment applications, the reported benefits must translate into a costs savings over polymeric membranes.

This section focuses on validating the claim that ceramic membranes have a higher flux than polymeric membranes (AWWA 1996; Gaulinger 2007;

Cornelissen, Hofs et al. 2009; Booker 2010). The claim that ceramic membranes have higher flux is largely anecdotal, and data from the literature is not widely available to support the claim. In fact, observations from the literature are conflicting with respect to which membrane has a higher flux. For example, citations can be found that suggest ceramic membranes exhibit better performance (i.e., higher flux, higher permeance, and/or less fouling) than polymeric membranes (Mueller, Cen et al. 1997; Lee and Cho 2004; Mueller, Schaefer et al. 2008), while other studies reported that polymeric membranes exhibited better performance characteristics (Bodzek and Konieczny 1998; Kabsch-Korbutowicz and Urbanowska 2010).

Data were collected from the peer-reviewed and open literature for ceramic and polymeric UF and MF studies to identify whether previously published studies support the notion that ceramic membranes are operated at a higher flux. These data then were used to determine whether differences in reported fluxes correspond to differences in operating conditions (i.e., operating pressure) or to an intrinsic difference in permeance between the two materials.

To evaluate the data from different studies, the feed water permeance and feed water flux are compared for the two membrane types versus the pure water permeance of the membrane. The pure water permeance is an intrinsic property of the membrane (as manufactured) and is a function of the membrane structure (that is, pore size distribution, porosity, thickness, asymmetry, etc.) and, perhaps, also its degree of hydrophilicity. Permeance is, therefore, used as the normalizing basis for comparing membranes with different separations capability. Pore size and molecular mass cutoff are not as useful a basis for comparison for several reasons, including that these values can vary based on the measurement method used and typically are best represented as a distribution (Mulder 2003).

Only studies that reported the data necessary to compute the following figures of merit were included in this analysis:

1. Pure water permeance (pressure normalized flux of deionized (DI) water)
2. Operating pressure during the filtration experiment
3. Steady state operating filtrate flux or flux at the end of experiment

The majority of the data used in the analysis were from the peer reviewed literature for small-scale, short-term research studies; however, data also were included for pilot and large-scale operations. The total number of data points considered in the analysis is 209. These data are summarized in tabular form by membrane type in tables 2.4 and 2.5.

Table 2.4 Ceramic membrane literature data¹

Membrane Material	MWCO or Pore Size	Pressure (kPa)	PWP x 1010 (m ³ /m ² /s/Pa)	Flux x 105 (m ³ /m ² /s)	FWP x 1010 (m ³ /m ² /s/Pa)	Feed Water Type	Reference
αAl ₂ O ₃	0.8 μm	69; 138	64.5	0.7–1.4	0.8–2.0	oil/water	Mueller 1997
αAl ₂ O ₃	0.2 μm	69; 138	24.2	0.6–1.2	0.4–1.7	oil/water	Mueller 1997
Kaolin composite	0.285 μm	69–276	19.4	0.5–1.5	0.5–0.8	oil/water	Nandi 2010
Kaolin composite	0.4 μm	41–165	19.4	1.0–2.1	1.3–2.4	oil/water	Nandi 2009
ZiO ₂	0.1 μm	80,000	11.1	3.5	4.3	oil/water	Koltuniewicz 1995
ZrO ₂ /TiO ₂	50,000 g/mol	350,000	1.4	4.7	1.3	oil/water	Lobo 2006
ZrO ₂ /TiO ₂	300,000 g/mol	350,000	3.3	8.6	2.5	oil/water	Lobo 2006
ZiO ₂	0.1 μm	300,000	30.7	13.9	4.6	oil/water	Srijaroonrat 1999
TiO ₂ /Al ₂ O ₃ /ZrO ₂	15,000 g/mol	200,000	2.4	2.1	1.1	well water	Bodzek 1998
TiO ₂ /Al ₂ O ₃ /ZrO ₂	300,000 g/mol	200,000	2.5	2.6	1.3	well water	Bodzek 1998
TiO ₂ /Al ₂ O ₃ /ZrO ₂	0.1 μm	200,000	2.5	3.4	1.7	well water	Bodzek 1998
TiO ₂ /Al ₂ O ₃ /ZrO ₂	0.2 μm	200,000	2.9	3.4	1.7	well water	Bodzek 1998
TiO ₂ /Al ₂ O ₃ /ZrO ₂	0.1 μm	100,000	2.6	2.5	2.5	well water	Konieczny 2006
TiO ₂ /Al ₂ O ₃ /ZrO ₂	0.2 μm	100,000	7.3	7.3	7.3	well water	Konieczny 2006
ZiO ₂	15,000 g/mol	100–400	1.6	0.9–2.9	0.3–1.6	PEG - 35,000 g/mol	Vincent Vela 2009
α-Al ₂ O ₃ /ZiO ₂	100,000 g/mol	140,000	16.9	10.8	7.7	seawater	Xu 2010
α-Al ₂ O ₃	0.01 μm	57–204	3.9	3.8–5.0	2.5–6.6	bentonite	Guerra 2010
αAl ₂ O ₃	0.2 μm	42	35.0	1.7–2.6	4.0–6.2	silica	Elzo 1998
αAl ₂ O ₃	0.2 μm	42	65.4	2.1	5.0	Silica	Huisman 1998
αAl ₂ O ₃	0.2 μm	100	43.1	2.0	2.0	oil/water	Li 2006
coal fly ash	NP	100	13.2	2.5	2.5	dying effluent	Jedidi 2011
αAl ₂ O ₃ /TiO ₂	20,000 g/mol	20–100	7.2	0.7–1.4	0.7–6.1	anaerobic digester effluent	Waeger 2010
αAl ₂ O ₃ /TiO ₂	0.05 μm	20–100	12.1	0.7–1.4	1.6–6.8	anaerobic digester effluent	Waeger 2010
αAl ₂ O ₃ /TiO ₂	0.2 μm	20–100	19.3	0.5–1.0	0.6–4.8	anaerobic digester effluent	Waeger 2010
Al ₂ O ₃ /ZrO ₂ /TiO ₂	1,000 g/mol	200–800	0.5	1.0–1.8	0.2–0.5	iron (III)	Bernat 2009
Al ₂ O ₃ /ZrO ₂ /TiO ₂	15,000 g/mol	200–800	1.6	2.3–2.7	0.3–1.2	iron (III)	Bernat 2009
Al ₂ O ₃ /ZrO ₂ /TiO ₂	50,000 g/mol	200–800	2.0	2.2–2.7	0.3–1.1	iron (III)	Bernat 2009

Table 2.4 Ceramic membrane literature data¹ (continued)

Membrane Material	MWCO or Pore Size	Pressure (kPa)	PWP x 1,010 (m ³ /m ² /s/Pa)	Flux x 105 (m ³ /m ² /s)	FWP x 1,010 (m ³ /m ² /s/Pa)	Feed Water Type	Reference
TiO ₂	5,000 g/mol	200–800	1.5	1.8–2.2	0.3–0.9	iron (III)	Bernat 2009
TiO ₂	10,000 g/mol	200–800	2.1	1.7–2.1	0.3–0.8	iron (III)	Bernat 2009
αAl ₂ O ₃ /TiO ₂	5,000 g/mol	200–800	1.7	1.2–1.3	0.2–0.7	iron (III)	Bernat 2009
NA	2,500 g/mol	100–400	4.5	0.5–1.1	0.3–0.5	palm oil mill effluent	Ahmad 2006
SiC		200	27.1	20.8	10.4	surface water	Mueller 2002
SiC		200	23.3	14.4	7.2	surface water	Mueller 2002
Al ₂ O ₃		200	29.5	29.3	14.7	surface water	Mueller 2002
		290	6.86	6.7	2.31	oil/water	Reed 1997

¹ kPa = kilopascal; PWP = pure water permeance; m³/m²/s/Pa = cubic meter per square meter per second per pascal; m³/m²/s = cubic meter per square meter per second; FWP = feed water permeance; NA = information not provided in original article; g/mol = grams per mole.

Table 2.5 Polymeric membrane literature data¹

Membrane Material	MWCO or Pore Size	PWP x 10 ¹⁰ (m ³ /m ² /s/Pa)	Pressure (Pa)	Flux x 10 ⁵ (m ³ /m ² /s)	FWP x 10 ¹⁰ (m ³ /m ² /s/Pa)	Feed Water Type	Reference
PS	0.007 μm	5.9	103	2.1–6.2	2.1 to 6.0	oil/water	Chakrabarty 2010
PS	0.006 μm	1.2	103	0.7–1.8	0.7 to 1.7	oil/water	Chakrabarty 2010
PS	0.007 μm	43.1	103	0.5–0.8	0.5 to 0.8	oil/water	Chakrabarty 2010
PS	0.007 μm	8.3	103	1.8–4.6	1.7 to 4.4	oil/water	Chakrabarty 2010
PS	0.007 μm	5.9	172	2.8–9.2	1.6 to 5.3	oil/water	Chakrabarty 2010
PS	0.006 μm	1.2	172	1.2–2.5	0.7 to 1.5	oil/water	Chakrabarty 2010
PS	0.006 μm	43.1	172	0.6–1.4	0.4 to 0.8	oil/water	Chakrabarty 2010
PS	0.007 μm	8.3	172	3.0–8.1	1.7 to 4.7	oil/water	Chakrabarty 2010
PVDF	0.45 μm	73.9	80, 120	1.7, 4.2	2.1, 3.5	oil/water	Koltuniewicz 1995
PS	0.1 μm	104.2	120,000	1.1	0.9	oil/water	Koltuniewicz 1995
PTFE	0.2 μm	72.1	30,000	0.4	1.3	oil/water	Hu 2007
PVDF	0.2 μm	43.3	30,000	0.3	1.0	oil/water	Hu 2007
PVDF	0.2 μm	48.7	30,000	0.3	1.0	oil/water	Hu 2007
PTFE	0.2 μm	42.2	30,000	0.3	0.9	oil/water	Hu 2007
Nitro-cellulose	0.2 μm	29.0	30,000	0.2	0.5	oil/water	Hu 2007
PAN	0.1 μm	8.9	69 to 138	0.2 to 6.3	0.3 to 9.1	oil/water	Mueller 1997
PAN/PS	0.2 μm	6.1	100	5.0	5.0	well water	Bodzek 1998
PAN/PS	NA	3.5	100	3.1	3.1	well water	Bodzek 1998
PAN/PS	NA	3.0	100	2.2	2.2	well water	Bodzek 1998
PAN/PS	NA	6.3	100	4.8	4.8	well water	Bodzek 1998

Table 2.5 PolymERIC membrane literature data¹ (continued)

Membrane Material	MWCO or Pore Size	PWP x 10 ¹⁰ (m ³ /m ² /s/Pa)	Pressure (Pa)	Flux x 10 ⁵ (m ³ /m ² /s)	FWP x 10 ¹⁰ (m ³ /m ² /s/Pa)	Feed Water Type	Reference
PES/PVP	0.2 µm	23.9	200	0.8	0.4	organic matter	Van de Ven 2008
PP/ regenerated cellulose	10,000 g/mol	0.6	300	1.4	0.5	natural organic matter	Aostin 2001
PP/ regenerated cellulose	100,000 g/mol	36.7	100	1.7	1.7	natural organic matter	Aostin 2001
PVC	0.05 µm	4.4	68, 100	1.7, 2.8	2.5, 2.8	surface water	Guo 2009
PES	100,000 g/mol	33.3	6.5	0.2, 0.3	3.8, 4.7	surface water	Peter-Varbanets 2011
PVDF	0.65 µm	23.9	45–230	2.9–7.0	2.1–6.5	WW	Benitez 2006
PVDF	0.1 µm	6.9	45–230	2.7–6.0	2.0–6.0	WW	Benitez 2006
PES	300,000 g/mol	21.4	35–180	3.2–8.0	2.7–9.1	WW	Benitez 2006
PA – TFC	8,000 g/mol	0.4	517	1.0	0.2	bovine serum albumin	Wang 2011
PA – TFC	8,000 g/mol	0.9	345	2.4	0.7	natural organic matter	Cho 2000
PP	0.2 µm	8.3	70	2.4	3.5	GW	Pianta 1998
Cellulose	100,000 g/mol	6.7	90	2.0	2.2	GW	Pianta 1998
PES	30,000 g/mol	3.2	50–300	1.0–3.5	1.2–2.0	silica	Bowen 2001
Cellulosic	0.01 µm	8.4	100	3.9	3.9	groundwater	Wetterau 1996
NA	0.01 µm	4.2	150	0.5, 1.0	0.3, 0.7	bentonite	Gourgues 1992
PES	10,000 g/mol	1.9	75, 159	1.0, 1.4	0.9, 1.3	bentonite	Guerra 2010
PES	100,000 g/mol	2.5	187	3.1	1.6	indegodying WW	Uzal 2009
PES	50,000 g/mol	2.3	187	2.9	1.5	indegodying WW	Uzal 2009
PES	20,000 g/mol	1.0	187	1.7	0.9	indegodying WW	Uzal 2009
PES	2,000 g/mol	0.1	307	0.2	0.1	indegodying WW	Uzal 2009
PES Composite-fluoro	1,000 g/mol	0.8	307	2.0	0.7	indegodying WW	Uzal 2009
PS	100,000 g/mol	20.2	50	2.1	4.2	WW 2 nd effluent	Bourgeois 2001

¹ NA = information not provided in original publication; PTFE = polytetrafluoroethylene; PA = polyamide; TFC = thin film composite; PVC = polyvinyl chloride; GW = ground water; WW = waste water.

Figure 2.3 presents the membrane flux versus the pure water permeance for each membrane. The closed and open symbols represent ceramic and polymeric membrane data, respectively. The ratio of the flux to the pure water permeance was used as the test statistic to compare the ceramic and polymeric membrane data sets using a two-sample t-test. The p-value, which represents the confidence

level related to the hypothesis that the two sample sets are equal (versus not equal), is 0.62. Statistically, there is no difference between fluxes for the two data sets, meaning that the blanket statement that ceramic membranes are operated at higher flux is not true when considering the available published literature.

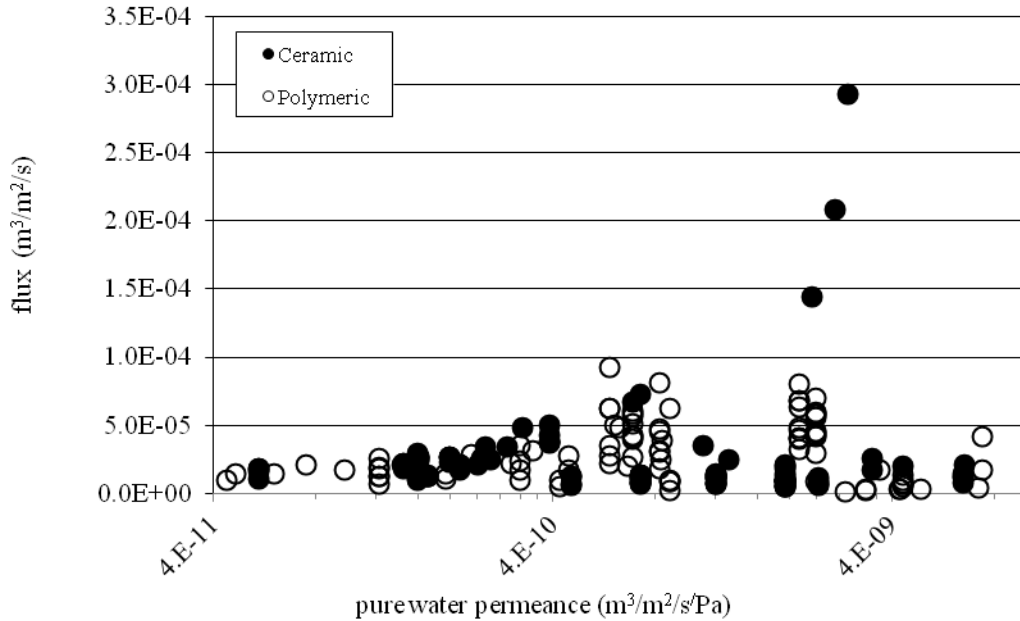


Figure 2.3 Literature data – flux comparison.

Figure 2.4 compares the feed water permeance of the two materials in terms of the pure water permeance. Simply stated, if there is a difference in the slope between the data for ceramic and polymeric materials, that would imply the ability to resist flux decline was greater in the materials with the higher slopes. The ratio of the feed water permeance to the pure water permeance was used as the test statistic to compare the feed water permeance values. The p-value for the hypothesis that the two sets are equal versus not equal is 0.27. Though there is lower confidence for accepting the null hypothesis, it is still much higher than the typical value of 0.05 used for statistical analysis. Thus, there is only 73% confidence that the literature suggests that ceramic membranes, as a whole, exhibit higher flux than polymeric membranes.

This analysis suggests that ceramic membranes are not intrinsically more permeable than polymeric membranes nor have they been tested at significantly higher fluxes. Therefore, other factors such as the rate of fouling and cleaning efficiency must be included, along with total plant cost, when comparing ceramic and polymeric membranes for commodity water treatment applications.

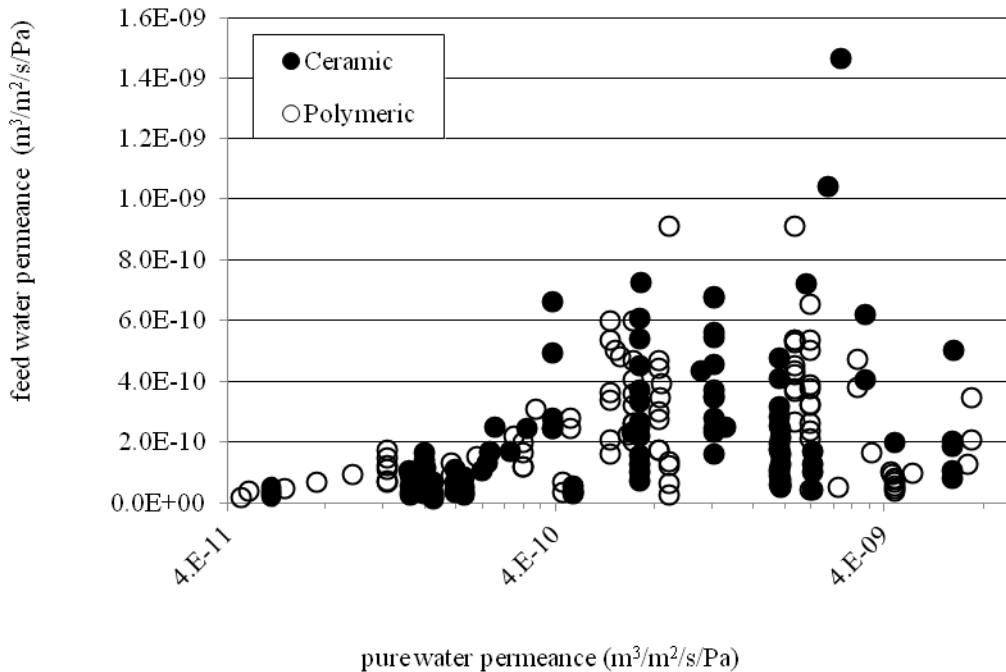


Figure 2.4 Literature data – permeance comparison.

Previously, researchers have conducted investigations to compare the flux behavior and rejection of ceramic and polymeric membranes. Generally, these studies attribute the differences in performance to material property differences and discount the operating conditions under which the membranes were compared; thus, the results are specific to the feed water tested, membrane module configuration used, and the hydrodynamic conditions under which the experiments were conducted (Mueller, Cen et al. 1997; Bodzek and Konieczny 1998; Bodzek and Konieczny 1998; Kabsch-Korbutowicz and Urbanowska 2010).

A recently published a study compared flux behavior and natural organic matter rejection of flat sheet regenerated cellulose and polyethersulfone polymeric membranes and a tubular titanium dioxide ceramic membranes (Kabsch-Korbutowicz and Urbanowska 2010). Three pore sizes or molecular mass cutoffs (MWCO) were evaluated for each material type: 5, 10, and 30 kg/mol for the regenerated cellulose and PES membranes, and 15, 50, and 300 kg/mol for the TiO₂ membrane. The feed solutions used for the study were Odra River water and a simplified model solution containing dechlorinated tap water and humic acid. All experiments were conducted at a constant pressure of 0.2 megapascal (MPa). The polymeric membranes were operated in dead-end filtration mode, and the ceramic membranes were operated in cross-flow mode.

The authors calculated the intrinsic membrane resistance (using pure water permeance data) and the initial resistance to flow for the Odra River water and the model solution. Based on the data presented in the paper, the regenerated

cellulose and PES membranes exhibited lower intrinsic membrane resistance and lower resistance to both the river water and the model solution than the ceramic membranes.

The authors also examined the influence of feed water pH on the degree of flux decline observed for the three different types of membranes. The regenerated cellulose showed negligible differences in flux declines for pH between 5–10. However, both the TiO₂ and PES membranes showed a dramatic increase in flux decline as the pH increased from 5 to 10. The authors claim that, since anions are less hydrated than cations, there is more adsorption of anions into the membrane pores, which reduces the pore size and inhibits flux at higher pH values. While this may be true, the authors fail to acknowledge that this difference may be attributed to the difference in surface charge of the materials.

Membrane rejection was characterized by reduction in UV₂₅₄² absorbance and color. The authors observed that the NOM rejection increased as the pH increased from 5 to 10. This trend was explained as that as pH increases, dissociation of phenolic and carboxylic groups occurs, and the macromolecule expands, making it more easily rejected. The authors did not comment on the fact that the rejection was similar for the ceramic and polymeric membranes at all pH values, except pH 5, which would suggest that surface charge may be responsible for this observation. Other studies have shown that ceramic membranes have an isoelectric point at pH values near 5 (Lee and Cho 2004).

The authors observed a decrease in rejection as MWCO increased for the PES and cellulose membranes. However, the opposite was found for the ceramic membrane. The 300-kg/mol membrane showed a greater reduction in absorbance and color than that of the 15- and 50-kg/mol membranes. For all three types of membranes tested, an increase in solution pH (5 to 10) resulted in an increase in rejection.

The authors conclude that the polymeric membranes have a higher hydraulic permeance compared to ceramic membranes and are less prone to fouling. They also concluded that the rejection of ceramic and polymeric membranes is comparable and that rejection and fouling tendency increased with increasing pH for both membrane types.

The authors attributed all of the observed differences in organic solute rejection and flux behavior to material property differences between ceramic and polymeric membranes; however, since they operated the two membrane systems in drastically different modes, it is impossible to determine how much of the observed difference was actually due to hydrodynamic and configurational differences. The authors did not present the data on an area-normalized basis. The 300-kg/mol membrane had a much lower flux decline than the 15- and 50-kg/mol ceramic membranes. While this is expected because of the larger

² The absorbance of ultraviolet light with a wavelength of 254 nanometers.

MWCO, the 300-kg/mol membrane area was four times larger than that of all of the other membranes tested; therefore, it may have been exposed to less mass of foulant per unit area. Furthermore, the authors fail to consider the hydraulic differences between testing in dead-end filtration mode and cross-flow filtration mode. Dead-end filtration will produce a thicker, more dense foulant layer. This foulant layer can increase the rejection of organic substances and also can increase the observed flux decline.

Bodzek and Konieczny also conducted a comparison study of a 0.2- μm polypropylene capillary membrane (1.8-mm diameter, 190 tubes, 0.48- m^2 area) and a 0.2- μm tubular ceramic membrane (2-mm channel diameter, seven channels, 0.037- m^2 area) (Bodzek and Konieczny 1998). The feed water for the study was surface water from a lake in Poland containing bacteria and inorganic constituents. The objective of the study was to compare the efficiency of ceramic and polymeric membranes. Efficiency was defined in terms of the volumetric flux versus time and bacteria content in the filtrate water for the study.

Experiments were conducted on the ceramic at 0.2 MPa at 4.0 m s^{-1} cross-flow velocity for a total of 10 hours. The 0.2- μm ceramic membrane flux declined from $5.2 \times 10^{-5} \text{ m}^3/\text{m}^2/\text{d}$ to $4 \times 10^{-5} \text{ m}^3/\text{m}^2/\text{d}$ over the 10-hour-long filtration experiment. The PP membrane was operated at 0.1 MPa and a cross-flow velocity of 1.31 m/s for 40 hours. The initial flux of the PP membrane was $3.2 \times 10^{-5} \text{ m}^3/\text{m}^2/\text{d}$ and decreased to $2.0 \times 10^{-5} \text{ m}^3/\text{m}^2/\text{d}$ over the 40-hour filtration period.

The filtrate water quality from each of the ceramic membranes and the capillary membrane met drinking water standards for bacteria removal; and in both cases, > 99% removal was observed. The authors did note that the bacterial load varied seasonally but failed to quantify this difference in terms of mass loading during the experiments. Based on the data presented, the ceramic membranes were exposed to a total organic carbon (TOC) concentration of 38.5 milligrams per liter (mg/L) while the polymeric membranes were exposed to 22.8 mg/L of TOC. When the mass of carbon per area is computed for each membrane experiment, the polymeric membrane was exposed to four times higher TOC concentration than the ceramic membrane.

The authors did not describe how the experimental conditions were determined; but based on the information presented, the hydrodynamic conditions were calculated to be $Pe = 5.7$ for the 0.2- μm ceramic membrane and $Pe = 7.0$ for the 0.2- μm polymeric membrane. Not only were the two membrane types not operated under the same hydrodynamic conditions, but the feed water quality was drastically different. Therefore, within this study, it is not possible to differentiate between hydrodynamic effects, material property effects, and feed water quality effects on membrane flux and rejection.

Bodzek and Konieczny also published another study evaluating the efficiency and the rejection of a flat sheet polyacrylonitrile/polyethersulfone (PAN/PSF)

membrane, tubular ceramic membranes, and a capillary polypropylene membrane. The membranes were operated at the following conditions specified by the manufacturers: 1.5 meters per second (m/s) for flat sheet, 0.28 m/s for capillary, and 4 m/s for ceramic which correspond to Pe values of 20.6, 5.7, and 11.6, respectively. All experiments were conducted for 5 hours.

As with the previous study by Bodzek and Konieczny, the water quality varied dramatically for each membrane type tested; however, the product water from each membrane tested met the water quality standards set forth by the drinking water regulations.

The authors conclude that the capillary membrane offers the “most favorable solution for the treatment of well waters.” The authors fail to explain how or why they arrived at this conclusion and do not acknowledge the dependence of their results on the different mass loading per area for the membrane types tested. Furthermore, the experiments were not conducted under the same hydrodynamic conditions.

Lee and Cho conducted a comparison of ceramic and polymeric membranes for NOM removal (Lee and Cho 2004). They tested polymeric and ceramic membranes of 8 kg/mol nominal MWCO and confirmed the nominal MWCO with their own characterization measurements. The polyamide thin film composite membrane had a measured MWCO of 7.83 kg/mol, and the CeRAM28 TiO₂ membrane had a measured MWCO of 7.66 kg/mol; the clean water permeance was 6.8 and 9.4 (L/m²/d/kPa),³ for the two membranes, respectively. They also conducted NOM and disinfection byproduct rejection studies with these membranes. The rejection studies were carefully conducted to ensure that the same hydrodynamic conditions were used for both the ceramic and polymeric membranes. The ceramic membrane was found to be more permeable than the polymeric membrane and showed a more complete rejection of disinfection byproduct precursors and similar NOM rejection to polymeric membranes. Flux behavior and cleaning efficiency were not considered in this study.

Muthukumar et al. evaluated a tubular ceramic membrane and a spiral wound polymeric membrane for treatment of secondary effluent for water reuse applications (Muthukumar, Nguyen et al. 2011). They found that the polymeric membrane experienced less fouling; however, it is unclear whether this was due to material properties or due to that the polymeric membrane had 25 times higher MWCO than the ceramic. The polymeric also showed significantly lower rejection (based on measurements of chemical oxygen demand), absorbance, and color (all indicators of smaller organic compounds). It is likely that increased rate of fouling for ceramic membrane is due to concentration polarization and retention of solutes on and in membrane structure.

³ Liters per square meter per day per kilopascal.

While a significant number of studies exist to compare the flux performance of ceramic and polymeric membranes, because of the way the tests were conducted, the applicability of the results is limited to the specific operating conditions used in the studies.

2.4 Summary

Membrane/solute interactions are complex because they depend on many different membrane material and solute properties; therefore, the fouling potential of membrane/solute systems is difficult to predict, and drawing generalized conclusions about the effects of these properties on fouling is not possible. Thus, there is an ongoing need for better predictive tools and continued experimentation.

The previously published literature on both ceramic and polymeric membranes provides a good basis for understanding the methods used to characterize membrane material properties, filtrate water quality, and the most efficient fouling and cleaning strategies for efficient membrane operation. These data will be used to define the range of operating parameters and solute types to be tested and will provide the basis for the development of fouling mitigation and cleaning strategies. Additionally, these data will be used to identify relevant experimental conditions under which to conduct a comparable comparison between ceramic and polymeric membranes.

The previous studies conducted to compare ceramic and polymeric membrane flux behavior did not consider the effect of hydrodynamics on flux behavior and rejection. Without comparing ceramic and polymeric membranes on the same water type under the same conditions, it is difficult to draw generalized conclusions about which membrane is best suited for a given application. To ensure that observed differences in flux behavior, rejection, and cleaning efficiency are a result of material property differences and not operational differences, experiments must be conducted so that the membranes are exposed to the same mass per area of foulant under the same hydrodynamic conditions.

In lieu of quantitative relationships describing the impacts of these factors on membrane fouling and economics, controlled experiments need to be conducted on specific membrane/solute systems to identify the best membrane material to use for a given application determined by the technical and economic drivers impacting the total water production cost for ceramic and polymeric membranes.

3. Data-Driven Model Development

Cost estimation of membrane equipment is commonly conducted to compare the cost of membrane treatment with other treatment alternatives and to secure financing or government bonds to pay for the capital expense required to build the proposed treatment system. Cost models also can be used to evaluate different design options and the impact of differences in operation to improve the unit cost of water produced.

Membrane treatment cost estimates are computed as the sum of the amortized cost of capital equipment and annual operating costs that include membrane replacement, power requirement, labor, maintenance, and chemicals (for cleaning and, if applicable, coagulation), represented as a cost per volume of water produced.

Membrane performance, which is characterized by the rate of transmembrane pressure increase required to maintain production of the plant's design flow rate, is based on experimental data and is used to quantify long-term and short-term fouling. The rate of membrane fouling, for each type of membrane, is dependent on the operating conditions including the transmembrane pressure, cross-flow velocity, and chemical cleaning frequency and efficacy. Engineering design equations govern the size and quantity of the treatment plant components based on the average required transmembrane pressure, recirculated water volume, frequency of chemical cleaning, volume of permeate water and chemicals consumed during cleaning, daily plant downtime, total membrane area, and actual plant feed flow rate.

Established correlations are used to generate the capital cost estimates for feed pumps, recirculation pumps, instrumentation and controls for process automation and monitoring, and valves and piping (Owen, Bandi et al. 1995; Sethi 1997).

This chapter presents an Excel[®]-based model that can be used to evaluate the relative impacts of membrane performance and operational parameters on the total water production cost. The following sections describe the parameters, variables, and equations used in the model. Parameters are used to define a case for which costs are calculated. The operating condition values are defined as variables within the range of values that are feasible based on equipment limitations and typical practice. Engineering design equations are used to size equipment and calculate the individual cost components.

3.1 Parameters

The parameter values and ranges used in the cost model are listed in table 3.1. These values were obtained from vendor quotes and typical water treatment

practice. The design plant production capacity is 18,925,000 liters per day (L/d) or 5 million gallons per day (MGD), which is reported to be the average hydraulic capacity for newly installed pressurized systems (Adham, Chiu et al. 2005). Smaller, de-centralized treatment plants are becoming more common to minimize water conveyance costs, minimize capital investment, and tailor plants to local water quality needs (Slaughter 2010). A 40-year plant lifespan was chosen for this work. The current prime interest (January 2012) rate is 3.25%, so 4% is a fairly competitive market interest rate.

Table 3.1 Parameter names, descriptions, units, values, and reference for determining the values used¹

Name	Description	Units	Value(s)	Reference
Q _d	Design plant flow rate (product delivered)	L/d	18,925,000	Typical practice
n	Plant lifespan	y	40	Typical practice
i	Annual interest rate	%	0.04	United States prime rate
d	Membrane channel diameter	m	Range of values, see table 3.2	Manufacturer
L	Membrane channel length/length of module	m	Range of values, see table 3.2.	Manufacturer
A _m	Membrane area per module	m ²	Range of values, see table 3.2.	Manufacturer
f*Re	Membrane friction constant		13 to 24	Results from chapter4
C _m	Membrane material cost	\$	50 to 500	Manufacturer
L _m	Membrane lifespan	y	5 to 20	Typical practice
C _h	Cost per vessel	\$	2000	Manufacturer
C _i	Pump cost index ratio		3.32	Sethi and Weisner
f ₁	Pump material adjustment factor		1.5	Sethi and Weisner
f ₂	Pump suction pressure range adjustment factor		1.0	Sethi and Weisner
L	Factor to account for labor cost		1.4	Typical practice
η	Pump efficiency		0.8	Manufacturer
F _i	Integrity test frequency	1/d	1	Typical practice
D _i	Integrity test duration	min	20	Typical practice
T _v	Time require for valve movement	min	1	Typical practice
O _m	Offline time – routine maintenance	min/d	10	Typical practice
C _e	Electricity cost	\$/kWh	0.1	Current rates
S _p	Personnel salary	\$/person/y	150,000	Typical practice
N _p	Number of personnel		1	Typical practice

¹ \$ = dollars; min/d = minutes per day; \$/kWh = dollars per kilowatthour; \$/person/y = dollars per person per year.

Table 3.2 describes the geometry of the commercially available, full-scale membrane modules that are made of materials similar to the ones used in the experimental portion of this study. Two sizes of each were chosen to illustrate the effect of differences in channel geometry on membrane plant costs.

Table 3.2 Full size membrane specifications and characteristics based on manufacturer specifications and vendor quotes

	Ceramic		Polymeric	
	alumina		polyethersulfone	
Channel diameter, d (m)	0.002	0.005	0.0009	0.0015
Module length, L (m)	0.864	0.864	1.486	1.486
Module area, A (m ²)	10.7	5.0	60	40
Material cost, C _m (\$/m ³)	400		50	
Vessel cost, C _v (\$/vessel)	2,000		0	
Maximum TMP, P _{max} (kPa)	1,034		138	

A membrane lifespan of 5 years was used for the polymeric membrane. In 2005, AWWA published a compendium of surveys of membrane plants; the 50 percentile membrane warranty life is 5 years (AWWA 2005). The current warranty offered by a ceramic membrane manufacturer is 20 years (Veolia presentation for the Water Treatment Engineering Research Group, Reclamation, in 2010). The most common reasons for membrane module replacement are a failed integrity test and loss of productivity due to irreversible fouling. Integrity loss usually necessitates replacing one membrane at a time, whereas loss of productivity typically is related to replacing large numbers (or all) of the membranes.

The friction constant is defined as the product of the Reynolds number and the friction factor. This parameter value was derived through experimentation, as discussed in chapter 4. The friction constants for the ceramic and polymeric membranes were determined to be 24 and 8.9, respectively.

Pump cost index ratio, I, is used to update the cost to the current year. The value of the factor is obtained by dividing the current index value, 896.7 (Chemical Engineers Plant Cost Index [CEPIC] for pumps and compressors from May 2009) by the corresponding value from January 1979, 269.9, to obtain a pump index cost ratio of 3.32. Pump material adjustment factor, f₁, was assumed for 316 stainless steel; the corresponding pump material adjustment factor is 1.5 (Perry and Chilton 1991). Pump suction pressure range adjustment factor, f₂, for low-pressure membrane systems, is 1.0 (Perry and Chilton 1991). The pump efficiency, η , is assumed to be 80%.

The labor factor, L, accounts for labor cost associated with the installation of the pumps. Commonly, labor costs for installation are assumed to be 40% of the total capital cost; therefore, the labor factor value is 1.4.

The integrity test frequency, F_i , is once per day per regulatory requirements. The integrity test duration, D_i , is assumed to be 20 minutes. The time required for valve movement, T_v , which accounts for the time required to change the valve position and stop the feed pump to switch from normal filtration mode to backwash mode and back to normal filtration mode, is assumed to be 60 seconds based on experience with automated valve movement from laboratory experiments. The offline time, T_m , accounts for daily offline time due to routine maintenance and represents an average daily value. The value is assumed to be 10 minutes per day (min/d).

Practice has shown that the equivalent of 2.5 employees can run a plant of this size; this includes administrative, managerial, and operator staff. This estimate is based on communication with a local consulting company. A fully loaded personnel salary of \$80,000 was used, based on current salary and overhead rates for water treatment plants. The electricity cost is assumed to be \$0.1/kWh based on the average industrial electricity rates for 2010 (EIA 2012).

3.2 Variables

The operating condition values are the variables in the cost model (table 3.3). The following is a discussion of the possible ranges of variable values based on regulatory requirements, equipment limitations, and practical considerations. Values from typical practice are also provided for reference.

Table 3.3 Summary of model variables

Name	Description	Units
J	Design flux rate	L/m ² /h
v	Cross-flow velocity	m/s
P _b	Average transmembrane pressure	kPa
F _c	Chemical cleaning frequency	1/d

Flux values for full-scale plants range from 30 to 170 L/m²/h. Some states have regulatory constraints on flux (Crozes, Jacangelo et al. 2001). Cross-flow velocities can range from 0.1 m/s to over 5 m/s for both ceramic and polymeric membranes. Reducing cross-flow velocity decreases the volume of water required for recirculation and the pressure drop due to frictional losses within the membrane channel.

Chemical cleaning frequency ranges from once every 5 years to 50 times per year, with a median of 4 cleanings per year. Each cleaning requires around 6 hours to complete. Cleaning frequency is dependent on the operation of the plant, occurrence of water quality upsets, and the average feed water characteristics. Maintenance cleanings, or more frequent less extensive cleanings, are becoming more common. These cleanings typically last for 30 minutes to 1 hour. The

AWWA MF and UF Knowledge Base reported that about 50% of survey respondents used maintenance cleanings (Adham, Chiu et al. 2005). The median frequency of maintenance cleanings is once per day. Chemical cleaning waste disposal methods are dependent on the type of chemicals used; however, most chemical cleaning waste can be neutralized and discharged to the sewer at standard wastewater costs (which are assumed negligible).

3.3 Engineering Design Equations

The average operating pressure is a function of the initial operating pressure, which is determined by the operating flux and the rate of pressure increase due to membrane fouling. The rate of pressure increase due to fouling was measured experimentally for each membrane for a range of operating conditions; see chapter 6.

The pressure drop across the membrane modules is calculated from classical theory describing fluid flow in a pipe (Perry and Chilton 1991),

$$\Delta P = \frac{2f \cdot L \cdot \rho \cdot v^2}{d} \quad (\text{Equation 3.1})$$

where f is the friction factor, L is the length of the membrane channel, ρ is the density of the feed water, v is the fluid velocity in the channel, and d is the diameter of the channel.

To maintain a high cross-flow velocity through the channels, a sufficient volumetric flow rate is required. This volume is recirculated through the membrane system,

$$Q_r = \pi \left(\frac{d}{2}\right)^2 v N \quad (\text{Equation 3.2})$$

where N is the number of channels per membrane module.

The number of backwash per day is determined by the backwash frequency.

$$N_b = \frac{60 \cdot 24}{F_b} \quad (\text{Equation 3.3})$$

The backwash flux is determined by the backwash pressure and the membrane material. To some extent, it is dependent on the degree of fouling; however, the resistance of the backflow through the membrane is the predominant factor affecting the backwash flux. The following expressions were derived experimentally for backwash flux as a function of pressure,

$$J_b = 1.09 \cdot P_b + 5.39 \quad (\text{Equation 3.4})$$

where P_b is the backwash pressure (kPa).

The volume of water consumed during backwash is determined by the frequency, duration, and water flux of backwashes.

$$V_b = \frac{J_b \cdot A_{mem} \cdot N_b \cdot D_b}{60} \quad (\text{Equation 3.5})$$

The plant downtime due to backwash includes the time required for backwash and the time required to stop and re-start the filtration cycle by stopping and starting the pumps and moving the valves.

$$T_d = (D_b + T_v) \cdot N_b + F_i \cdot D_i + F_c \cdot D_c \quad (\text{Equation 3.6})$$

The membrane area required depends on the design flux, the volume of additional filtrate water required for backwash, and the plant downtime.

$$A_{mem} = \frac{Q_p \left(1 + \frac{T_d}{24}\right) \cdot \frac{1}{24 \cdot J}}{1 - \left(\frac{J_b \cdot D_b \cdot N_b}{1440 \cdot J}\right)} \quad (\text{Equation 3.7})$$

The actual plant feed flow rate, Q , is the amount of feed water supplied to the plant to generate the desired product flow rate based on the design flux and the plant downtime.

$$Q_f = \frac{24 \cdot A_{mem} \cdot J}{(1 - T_d)} \quad (\text{Equation 3.8})$$

3.4 Membrane System Cost

Membrane system costs are most commonly described as the total water production cost (TWPC), defined as the sum of the amortized capital cost and the annual operating and maintenance cost per volume of water produced. Plant design results, power requirements, individual cost components, and the overall cost are the relevant model outputs, summarized in table 3.4.

Table 3.4 Summary of calculated parameters for cost components and plant design results

Name	Description	Units
TPC	total production cost per volume of water produced	\$ m ⁻³
C _a	amortized capital cost per volume of water produced	\$ m ⁻³
C _{om}	annual operating and maintenance cost per volume of water produced	\$ m ⁻³
A _{mem}	total membrane area required	m ²
C _r	annual cost of replacement membranes per volume of water produced	\$ m ⁻³
C _{pf} + C _{pr}	energy required for pumping	\$ m ⁻³

3.4.1 Capital Costs

The capital cost is the sum of the individual purchase costs of all of the capital equipment and includes the cost of the first set of membranes, vessels (if applicable), pipes and valves, instrumentation and controls, tanks and frames, miscellaneous equipment, chemical cleaning skid, feed pump, and recirculation pump.

$$C_{cap} = C_{mem} + C_{v,tot} + C_{PV} + C_{IC} + C_{TF} + C_{MI} + C_{cc} + C_{p,f} + C_{p,r} \text{ (Equation 3.9)}$$

Capital costs often are reported as amortized values over the lifespan of the water treatment plant.

Amortized capital cost, C_a : The amortized capital cost is the yearly payment on the total capital cost over the lifespan of the plant at the annual interest rate.

$$C_a = \left(i \cdot \frac{(1+i)^{Lp}}{(1+i)^{Lp} - 1} \right) \cdot C_{cap} \text{ (Equation 3.10)}$$

3.4.1.1 Membrane-Related Capital Costs

Membrane-related costs include the membrane material itself and the vessels required to hold the membranes, if applicable. The membrane capital cost accounts for the initial set of membranes required for the plant.

$$C_{mem} = C_m \cdot A_{mem} \text{ (Equation 3.11)}$$

The vessel cost, $C_{v,tot}$, is assumed to be a one-time cost; replacing the membranes does not require replacing the vessels. This cost is only applicable to the ceramic membranes because polymeric membranes typically come with housings, and the basic polymeric membrane material cost includes a plastic housing.

$$C_{v,tot} = \frac{A_{mem}}{A} \cdot C_v \text{ (Equation 3.12)}$$

3.4.1.2 Nonmembrane Capital Costs

Typically, capital cost components, for different pieces of equipment, are estimated by correlations based on existing cost data. Capital costs are assumed to scale directly to the plant size or installed membrane area in the form of a power law (Owen, Bandi et al. 1995; Sethi 1997).

$$Cost = k \cdot (size)^n \text{ (Equation 3.13)}$$

The manner in which the cost increases with the size of the parameter determines the value of the exponent n . If $n = 1$, then no economy of scale exists; if n is less than ($<$) 1, then increases in size result in a decrease in the incremental cost. Total capital costs exhibit economies of scale for some cost components, e.g., pumps and plumbing; however, for membrane-related equipment, economies of scale are insignificant ($n = 1$).

The power law relationship was used to estimate the cost of the following components: pipes and valves, instruments and controls, tanks and frames, and miscellaneous costs. Miscellaneous costs include electrical supply and distribution equipment, disinfection facilities, treated water storage and pumping, the building that houses the equipment, and the wash water recovery system (Sethi 1997). The values for the leading coefficient and the exponent were established by Sethi (1997). The following equations describe the costs for pipes and valves, instruments and controls, tanks and frames, and miscellaneous costs.

$$C_{PV} = 5926.13 \cdot (A_{mem})^{0.42} \quad (\text{Equation 3.14})$$

$$C_{IC} = 1445.5 \cdot (A_{mem})^{0.66} \quad (\text{Equation 3.15})$$

$$C_{TF} = 3047.21 \cdot (A_{mem})^{0.53} \quad (\text{Equation 3.16})$$

$$C_{MI} = 7865.02 \cdot (A_{mem})^{0.57} \quad (\text{Equation 3.17})$$

The feed pump is sized so that it delivers the plant feed water to the recirculation pump at the same pressure as the returning recirculation water.

$$C_{p,f} = I \cdot f1 \cdot f2 \cdot L \cdot 81.27 \left(Q_f \cdot \left(P_{avg} - \frac{\Delta P}{2} \right) \right)^{0.39} \quad (\text{Equation 3.18})$$

The recirculation pump is sized so that it pumps the total plant feed and the recirculated volume at a pressure equal to the pressure drop across the modules.

$$C_{p,r} = I \cdot f1 \cdot f2 \cdot L \cdot 81.27 \left((Q_r + Q_f) \cdot \Delta P \right)^{0.39} \quad (\text{Equation 3.19})$$

The cost of the chemical cleaning skid is assumed to be \$25,000, based on typical practice.

3.4.2 Operating and Maintenance Costs

The annual operating and maintenance cost is the sum of the following: annual membrane replacement, energy cost for pumping, personnel cost, chemical cost, and maintenance.

$$C_{om} = C_r + C_{p,f} + C_{p,r} + C_{sal} + C_{maint} + C_{chem} \quad (\text{Equation 3.20})$$

The number of sets of replacement membranes, M_r , is calculated based on the plant lifespan and the anticipated lifespan of the membranes.

$$M_r = \frac{L_p}{L_m} - 1 \quad (\text{Equation 3.21})$$

Note: The initial set of membranes typically is considered part of the capital expense.

The annual cost of replacement membranes, C_r , is calculated from the total cost of the replacement membranes amortized over the lifespan of the plant.

$$C_r = \left(i \cdot \frac{(1+i)^{Lp}}{((1+i)^{Lp}-1)} \right) \cdot M_r \cdot A_{mem} \cdot C_m \quad (\text{Equation 3.22})$$

Feed pump work, W_{pf} , is calculated from the pressure and flow rate of the water to be pumped.

$$W_{pf} = \frac{\left(P_{avg} - \frac{\Delta P}{2} \right) P_f \cdot Q_f}{\eta \cdot \left(1 - \frac{T_d}{1440} \right) \cdot 3,600,000} \quad (\text{Equation 3.23})$$

Recirculation pump work, W_{pr} , is calculated based on the volume and pressure of water to be pumped and the pump efficiency.

$$W_{pr} = \frac{\Delta P \cdot Q_r}{\eta \cdot \left(1 - \frac{T_d}{1440} \right) \cdot 3,600,000} \quad (\text{Equation 3.24})$$

The feed pump energy cost, C_{pf} , is equal to the unit energy cost times the pump work. The recirculation pump energy cost, C_{pr} , is equal to the unit energy cost times the pump work. The chemical cost, C_{chem} , can be calculated based on the dosing requirements and/or the chemical cleaning frequency and volume requirements and the commodity chemical price.

The labor cost is equal to the number of personnel multiplied by the personnel salary per year. Typically, labor costs amount to approximately 30% of operation and maintenance (O&M) cost (Adham, Chiu et al. 2005). Annual maintenance costs are calculated as 1.5% of the nonmembrane capital cost.

Model Assumptions

The following assumptions are used:

- The plant is assumed to operate 24 hours per day, 365 days per year; but for a fraction of that time, the plant will be offline for backwashing, chemical cleaning, integrity testing, and routine maintenance. During normal operation time, additional product water is generated and stored to be used during backwashing cycles.
- Cleaning chemicals are not reused.
- Each vessel houses one ceramic membrane. Polymeric membranes come in housings; no additional vessel purchase is necessary.

4. Membrane Properties and Feed Water Quality

This chapter describes the membranes, feed water sources, and experimental equipment used to conduct the laboratory analyses. Limited characterization measurements were conducted to assess relevant properties of the membrane materials not provided by the manufacturers' specifications.

4.1 Membranes

A ceramic and a polymeric membrane were compared in this study. The ceramic membrane is an alpha-phase alumina composite, tubular, UF membrane (CerCor[®], Corning Inc., Corning, New York) with 208 channels of 1.05 mm diameter with a nominal pore size of 0.01 μm . The polymeric membrane is a polyethersulfone tubular ultrafiltration membrane (WaterSep Technology Corp., Marlborough, Massachusetts) with 160 channels and a diameter of 1.00 mm, and a nominal MWCO of 10,000 g/mol. The membranes hereafter will be referred to as alumina and PES. The membrane specifications are summarized in table 4.1. Figure 4.1 is a photograph of the membrane modules used for experimentation.

Table 4.1 Membrane specifications

Parameter	Alumina	PES
Channel diameter (mm)	1.05	Nominal: 1.00 Measured: 1.02
Channel length (mm)	304.8	304.8
Number of channels	208	135
Total membrane area (m ²), as reported by manufacturer	0.195	0.13



Figure 4.1 End view of alumina (left) and PES (right) modules.

The pure water permeance of the alumina membrane is $1.3 \pm 0.02 \text{ L m}^{-2} \text{ h}^{-1} \text{ kPa}^{-1}$; the pure water permeance of the PES membrane is $1.23 \pm 0.02 \text{ L m}^{-2} \text{ h}^{-1} \text{ kPa}^{-1}$.

Atomic force microscopy (AFM) is a very common technique used to visualize membrane surfaces. A significant downside to using microscopy techniques for tubular ceramic membranes is that destruction of the membrane is necessary to gain access to the membrane surface; therefore, using AFM in this study is limited to characterization of virgin samples. Figure 4.2 shows AFM images of the alumina and PES membranes.

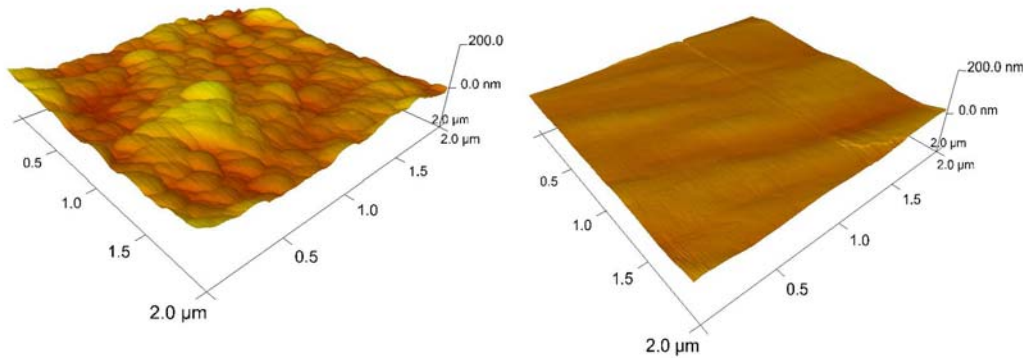


Figure 4.2 AFM of alumina (left) and PES (right) membranes.

The roughness, calculated as the root mean square (RMS), from the AFM measurements on three separate $2\text{-}\mu\text{m} \times 2\text{-}\mu\text{m}$ square samples is 12.8 nm ($\sigma^2 = 4.5 \text{ nm}$) and 6.0 nm ($\sigma^2 = 3.3 \text{ nm}$) for the ceramic and polymeric membranes, respectively. A one-tailed, two-sample t-test on the roughness of the alumina and PES membranes results in a p-value of 0.063; therefore, we can accept that the roughness of the ceramic membrane is greater than that of the polymeric membrane at approximately (\sim) a 94% confidence level.

4.2 Friction Factor

Friction factor is a measure of energy dissipation caused by shear stress (predominantly originating at the membrane surface) resulting in a pressure drop down the length of the membrane. The Fanning friction factor can be calculated using the pressure drop measured at different cross-flow velocities using equation 4.1,

$$f = \frac{2 \cdot \Delta P \cdot d}{\rho \cdot v^2 \cdot L} \quad (\text{Equation 4.1})$$

where, f = friction factor, L = length of channel, v = cross-flow velocity within the channel, and d = the hydraulic diameter of the channel (actual diameter for round channels). The friction factor times Re is referred to as the coefficient of

friction. For laminar flow, this value theoretically is constant and is used to compare the degree of energy dissipation within the channels for the two membranes.

Two test solutions were used: deionized water and 24% sodium chloride (NaCl). The properties of the test solutions are found in table 4.2. The two solutions were chosen to have different densities so that the calculated friction factor could be estimated with greater confidence.

Table 4.2 Liquid solution properties at 20 °C

Parameter	DI water	24% NaCl
Density (kg/m ³)	998	1,180
Viscosity x10 ³ (Pa*s)	1.0	4.2

During the friction factor measurements, the membrane module was turned horizontally to minimize hydrostatic pressure effects on the pressure drop across the module. The back pressure valve on the reject side was fully open, and the permeate valve was closed to ensure that all flow was directed through the membrane channels. The feed solution was pumped through the system from the feed side of the membrane to the reject side. The pressure drop and cross-flow velocity (calculated from the volumetric flow rate) were observed over the range of volumetric flow rates measureable by the installed flow meters and attainable by the pump. This corresponded to velocities ~0.1–0.5 m/s. The procedure was repeated three times for each membrane and each water type.

Figure 4.3 shows the friction factor as a function of the Reynolds number (Re) for the two membranes using the two different liquids. The values obtained for the two liquids are in agreement. Data also were collected for a second alumina membrane, of the same material from the same manufacturer, with 85-mm-diameter channels to confirm the results obtained with the original alumina membrane.

The value of the friction factor obtained from classical theory is shown compared to the value of the friction factor obtained through measurements, see figure 4.3. The observed friction factors for the PES membrane are lower than the theoretical values and higher for the alumina ceramic. Other studies have shown that in small diameter channels, rougher surfaces exhibit friction factors higher than predicted by theory and smoother surfaces may exhibit lower values than predicted by theory (Pfund, Rector et al. 2000; Ghajar, Tam et al. 2010).

The friction coefficient, which is defined as the friction factor times Re, is plotted in figure 4.4. The friction coefficient for the alumina membrane is nearly three times greater than that of the PES membrane.

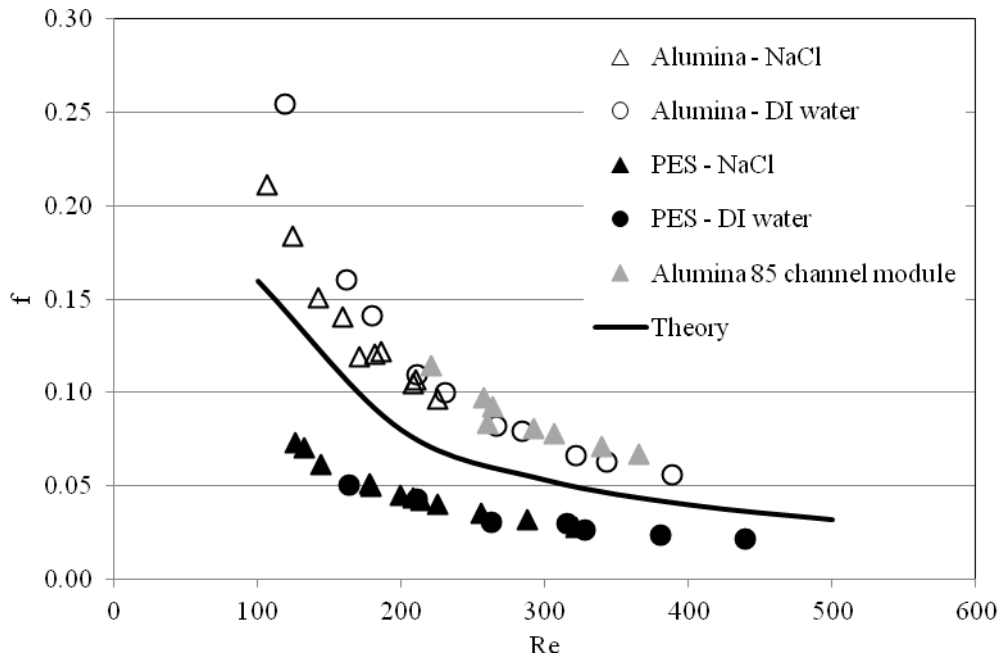


Figure 4.3 Friction factor plotted as a function of Re for alumina and PES membranes.

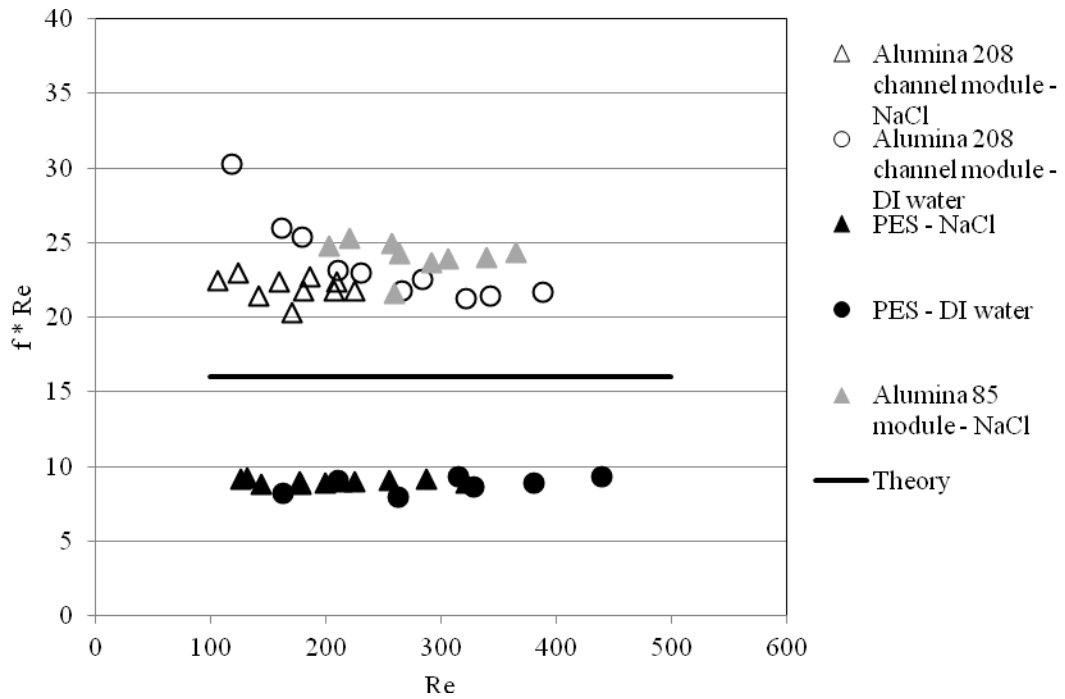


Figure 4.4 Coefficient of friction for alumina and PES membranes.

The values of the friction constant, obtained for both membranes and both feed solutions, are summarized in table 4.3.

Table 4.3 Comparison of coefficient of friction values

Membrane	DI water	24% NaCl
alumina	25 ± 3	22 ± 1
PES	8.7 ± 0.5	9.0 ± 0.1

A two-sample t-test was conducted to ensure that the NaCl and water data yielded consistent friction coefficient results for each membrane. The p-values for the two-sample t-test for a null hypothesis that the two sample means are equal, are 0.003 and 0.019, for the alumina and PES membranes, respectively; therefore, there is greater than 98% confidence that the two liquids produced the same friction coefficient results. The two-sample t-test to determine whether the ceramic and polymeric friction coefficients are different resulted in a p-value of less than 0.001, meaning that there is over 99.9% confidence that the two friction coefficients are different.

The coefficient of friction values obtained in these measurements are used in the cost model to predict the pressure drop across the membrane modules as a function of the cross-flow velocity. They also provide a perspective on possible sources of differences in boundary layer mass transfer coefficients.

4.3 Molecular Mass Cutoff Determination

The molecular mass cutoff of the alumina and PES membranes was determined by measuring the rejection of different molecular mass dextrans, using a previously published and industry-accepted method developed by Tkacik and Michaels (Tkacik and Michaels 1991). The rejection curves for the alumina and PES membranes are shown in figure 4.5.

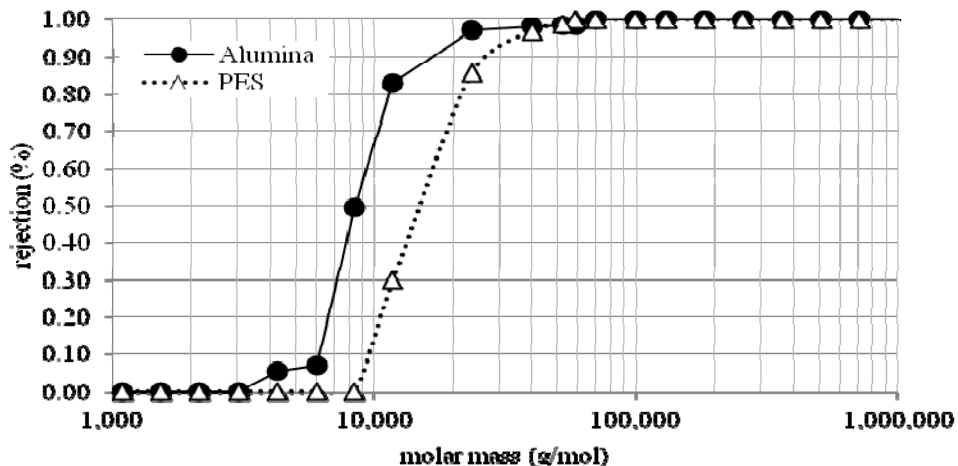


Figure 4.5 Dextran rejection for alumina and PES membranes.

4.4 Feed Water

Surface water, including water from rivers, lakes, and reservoirs are the most commonly treated water types using MF and UF membranes (Crozes, Jacangelo et al. 2001; Adham, Chiu et al. 2005). Initial experiments were conducted using water from Clear Creek, a surface water source that provides municipal drinking water for the city of Golden, Colorado. These experiments were conducted to gain an understanding of relevant operating parameters for ceramic membranes.

Following the initial ceramic membrane experiments, further laboratory studies were conducted in a more controlled manner, using synthetic feed waters. Two synthetic feed water types were chosen for this work to represent the types of water commonly treated with MF and UF membranes. A bentonite suspension was chosen to simulate particulate matter in feed waters. A complex feed mixture consisting of natural organic matter, algae, and particulates, was used to provide a reproducible simulcrum for a surface water source.

4.4.1 Clear Creek Surface Water

The feed water used in the initial studies was surface water collected from Clear Creek in Golden, Colorado, and is used in this study to represent low turbidity surface waters.

contains water quality data measured for the Clear Creek river water. Water was collected in 1,000 liter (L) batches during nonweather events over the winter months to ensure the most consistent water quality. The water samples were used within 5 days of collection to minimize water quality changes due to storage. The experiments were randomized to account for uncontrolled differences in water quality of the different batches of water. Each water sample was kept in the laboratory for 24 hours prior to testing to allow the water temperature to rise to the laboratory's ambient temperature, approximately 19 °C. The flux data collected during the experiments were normalized to 25 °C to account for changes in the feed water temperature. Turbidity was the only water quality parameter used to compare the feed water quality between different collected samples. The average turbidity of the samples was 3.1 Nephelometric Turbidity Units (NTU). The water was pre-filtered using a 200- μ m strainer before contacting the membrane.

Table 4.4 Clear Creek feed water characteristics

Parameter	Average Value ¹
hardness	100 (\pm 35)
alkalinity	39 (\pm 9)
pH	7.7 (\pm 0.2)
TOC (mg/L)	1.6 (\pm 0.9)
turbidity (NTU)	3.1 (\pm 1.1)

¹ The numbers in parenthesis are standard deviations.

4.4.2 Bentonite Suspension

The bentonite suspension used for the fouling experiments was 100 mg/L bentonite (Sigma Aldrich, CAS# 1302789) in tap water. The suspension simulates waters containing a high concentration of particulates and was chosen because it is easily reproducible, easy to dispose of in an environmentally friendly manner, and easy to obtain in the large volumes required for this testing. The bentonite particle size was measured by dynamic light scattering using a Zetasizer Nano (Malvern Instruments, Inc.). The average diameter was found to be 1,436 nm with three distinct size fractions of individual average diameters of 286, 1,328, and 5,455 nm, respectively; see figure 4.6. Even the smallest size fraction of the bentonite is over one order of magnitude greater in size than the nominal pores size of the membrane; therefore, almost complete rejection of the bentonite is expected. The feed suspension was stirred continuously and monitored throughout the experiments to ensure that no settling occurred and that the turbidity remained constant.

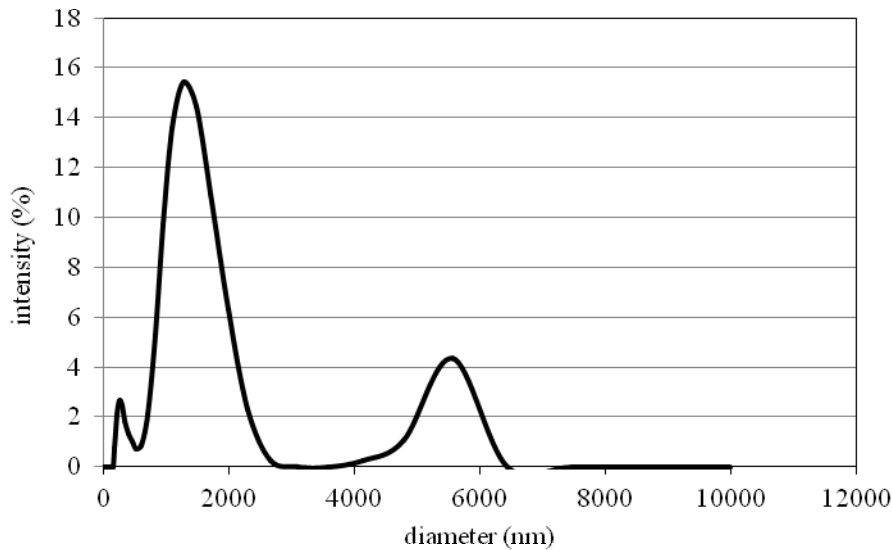


Figure 4.6 DLS results for bentonite feed solution.

4.4.3 Complex Mixture

The complex mixture is representative of a surface water under the influence of wastewater and contains constituents similar to those in the complex mixture developed by the Bureau of Reclamation for testing low-pressure membranes (Chapman 2010). The recipe for the mixture is as follows: 10 parts per million (ppm) Klamath blue-green algae, 40 ppm bentonite, and 5 ppm humic and fulvic organic matter (from Orchid Pro plant food). Water quality parameters for the complex mixture are presented in table 4.5.

Table 4.5 Complex feed mixture characteristics¹

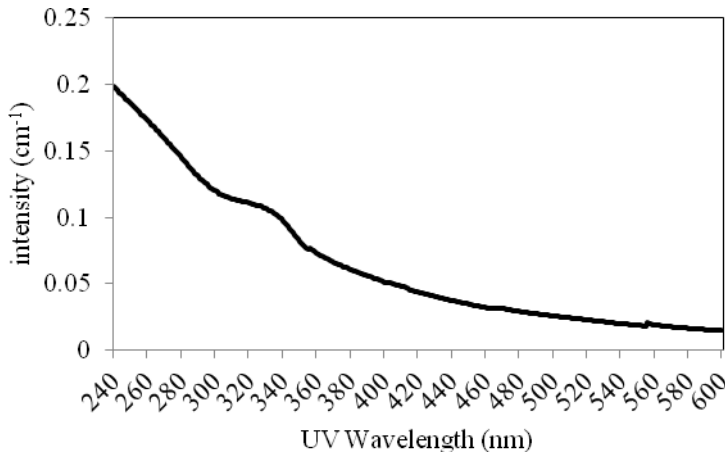
Parameter	Units	Average Value ²
pH	–	7.7(± 0.2)
turbidity	NTU	21.5 (± 0.6)
conductivity	mS/cm	260 (± 30)
DOC	mg/L	4.2 (± 0.6)
UV ₂₅₄	cm ⁻¹	0.146 ± 0.008
SUVA	mg/L/cm	3

¹ mS/cm = microSiemens per centimeter; cm = centimeter; SUVA = specific ultraviolet absorbance; mg/Lcm = milligram per liter per centimeter.

² The numbers in parenthesis are standard deviations.

A measurement of the absorbance of the complex mixture over both UV and visible light regions was conducted; see figure 4.7. The complex mixture also was characterized using fluorescence spectroscopy. Fluorescence measurements are widely used to characterize complex mixtures containing dissolved organic matter (Her, Amy et al. 2003). Figure 4.8 is the excitation-emission matrix (EEM) spectra for the complex mixture.

The EEM of the complex mixture shows the presence of large amounts of humic acids and smaller amounts of microbial by-products and fulvic acids. Figure 4.9 shows the relative percentage of the different types of organic matter in the complex mixture.

**Figure 4.7 UV-Vis spectrum of complex mixture.**

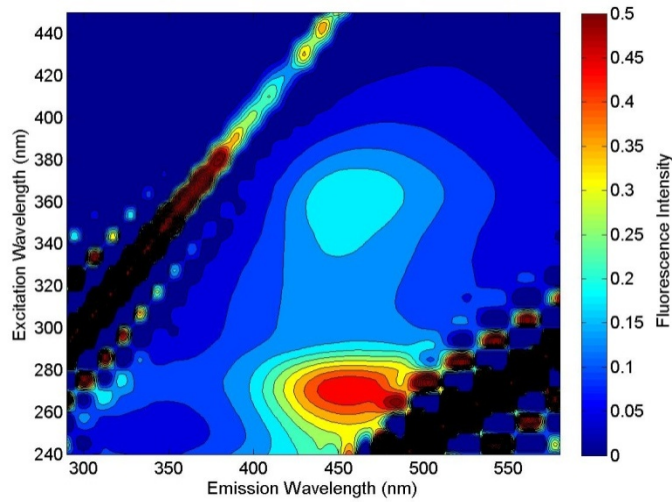


Figure 4.8 EEM of complex mixture.

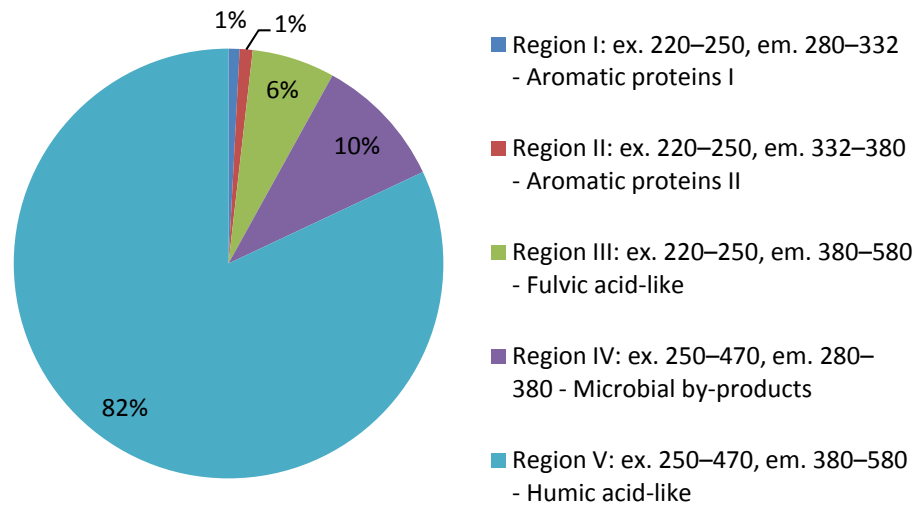


Figure 4.9 Analysis of complex feed water composition.

4.5 Experimental Equipment

A schematic diagram of the experimental apparatus is illustrated in figure 4.10. The apparatus was configured so that it could accommodate both the ceramic and polymeric membrane modules; however, only one membrane is tested at a time. The treatment system is equipped with a 200- μm strainer, feed pump (Hydra Cell™ model M03BAPGSFSHA), and a peristaltic pump to maintain constant flux during experiments. There is also instrumentation to monitor the flow rate

(GF Signet PN 321002L) and pressure of the feed (GF Signet 2450-1H), filtrate (Cole Parmer model 67356-53), and retentate (Cole Parmer model 67356-53) process streams and the feed water temperature (GF Signet 2350). LabVIEW™ was used to collect data, manipulate values to direct flow for backwashes and chemical cleaning, and adjust the pump speed to maintain the desired cross-flow velocity for each experiment. Experimental data were collected every 3 seconds, and the data were reduced using the average of every 10 data points. The filtrate water quality was measured using a handheld turbidimeter (Hach® 2100P).

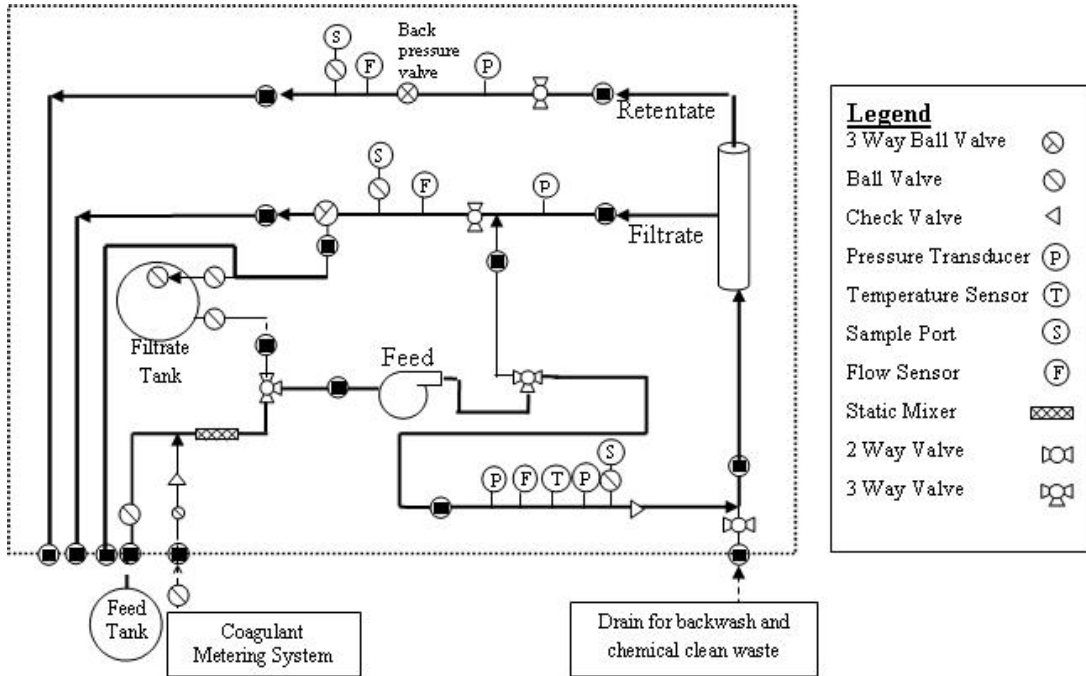


Figure 4.10 Schematic diagram of filtration equipment.

5. Preliminary Ceramic Membrane Study

Previous research studies using ceramic membranes for water treatment applications have been inconsistent with respect to the operating conditions and module configurations used. This chapter describes an experimental effort to determine relevant operating conditions for ceramic membranes in the context of the economic model. This chapter has been published in *Separation and Purification Technology* (Guerra, Pellegrino et al. 2012).

5.1 Identification of Operating Condition Ranges

For ceramic membranes commercially available today, there is no standard channel diameter, number of channels per module, or channel shape. Circular is the most common shape for membrane channels; however, square and star-shaped channels are also commercially available. Past research studies have used ceramic membrane products with 1 (Hilal, Ogunbiyi et al. 2008), 7 (Rajca, Bodzek et al. 2009), 19 (Konieczny, Bodzek et al. 2006), or 55 (Lerch, Panglisch et al. 2005; Lerch, Panglisch et al. 2005; Loi-Brugger, Panglisch et al. 2007) channels ranging in diameter from 1–10 mm. Decreasing the channel diameter reduces the feed flow required to maintain the desired cross-flow velocity (CFV) and increases the packing density (area per volume) of the membrane module.

Based on literature data, a wide range of values for CFV have been used. In some studies, ceramic membranes have been operated in dead-end mode (normal filtration) (Lerch, Panglisch et al. 2005; Lerch, Panglisch et al. 2005; Lehman, Adham et al. 2007; Loi-Brugger, Panglisch et al. 2007). Others have operated at a moderately low CFV of less than 1 m/s (Koltuniewicz, Field et al. 1995; Mueller, Cen et al. 1997; Kim, Davies et al. 2008). Some studies have operated ceramic membranes at very high CFV, 3–4 m/s (Bodzek and Konieczny 1998; Klomfas and Konieczny 2004; Konieczny, Bodzek et al. 2006; Cremades, Rodriguez-Grau et al. 2007; Rajca, Bodzek et al. 2009; Vincent Vela, Álvarez Blanco et al. 2009; Waeger, Delhaye et al. 2010). The channel diameter and CFV provide the Re , which correlates with boundary layer mass transfer efficiency and parasitic energy consumption for pumping. Re for the previously mentioned studies have ranged from 100 to over 10,000.

Typical operating pressures for ceramic membranes in the literature range from 100–400 kPa (Mueller, Cen et al. 1997; Konieczny, Bodzek et al. 2006; Cremades, Rodriguez-Grau et al. 2007; Hilal, Ogunbiyi et al. 2008; Nandi, Das et al. 2009; Rajca, Bodzek et al. 2009; Vincent Vela, Álvarez Blanco et al. 2009; Nandi, Moparthi et al. 2010). Up to a point, increasing transmembrane pressure will increase the productivity of the membrane system and reduce the number of

membrane elements required to treat a given volume of water. However, increasing the pressure or flux past a critical value will increase the fouling rate leading to a reduction in productivity. Even though the ceramic membrane material has a high mechanical strength and can withstand greater pressures, other membrane module components, such as seals and housing, may have lower pressure limitations (Cheryan 1998).

A common strategy to enhance particulate and TOC removal by ceramic MF/UF membranes is in-line coagulation (Lerch, Panglisch et al. 2005; Konieczny, Bodzek et al. 2006; Meyn and Leiknes 2010). Ferric chloride, aluminium sulfate, and polyaluminum chloride have been used with ceramic membranes to improve TOC rejection (Lerch, Panglisch et al. 2005; Konieczny, Bodzek et al. 2006; Rajca, Bodzek et al. 2009). Literature also indicates that alum, at a concentration of 1 to 4.1 mg Al³⁺/L, may be used as a coagulant for low turbidity waters (Konieczny, Bodzek et al. 2006; Rajca, Bodzek et al. 2009).

Backwashing is an effective strategy for recovering flux in ceramic membrane systems (Sondhi, Lin et al. 2000; Sondhi and Bhave 2001; Lerch, Panglisch et al. 2005; Kumar, Madhu et al. 2007; Mourouzidis-Mourouzidis and Karabelas 2008). Because backwashing consumes product water and typically results in plant downtime, there may also be a tradeoff between flux improvement and increased plant size.

Previous studies that varied operating parameter values independently are inadequate to evaluate the interaction effects between operating parameters. In this study, values of operating conditions (Re, transmembrane pressure, in-line coagulant addition, and backwash) were varied systematically and simultaneously in a series of controlled experiments to determine the effects of the operating conditions on permeate flux and degree of fouling for the ceramic membrane system. A cost model was used to evaluate the total plant investment and operating costs for the different operating conditions.

5.2 Experimental Approach

A factorial experimental design, which systematically varies the value of experimental factors using a minimum number of experiments and with minimal effect of uncontrolled sources of variability, was used to quantitatively measure the effects of operating parameters on the permeate flux decline for the ceramic membrane system. By systematically varying factor levels, it is possible to detect interactions between different experimental factors and to identify optimal solutions other than those tested. The set of experiments was designed to evaluate the significant factors (or system operating conditions) at three levels to determine the optimal level for each factor using JMP[®] statistical analysis software, Version 8.0.2 from SAS Institute Inc., Cary, North Carolina.

5.2.1 Experimental Factors

The following levels of the experimental factors (system operating conditions) were used for the experiments:

- Re: 100, 200, 300, 400, and 500
- TMP: 207, 310, and 414 kPa.
- Coagulant dose: 1–2.5 mg Al³⁺/L. The low level of the coagulant was determined as the dose required to generate the smallest visible flocs. The high level coagulant dose produced significantly larger flocs.
- Backwash flow: Backwashes were conducted at a fixed flow rate of 68 liters per hour (L/h) and a pressure of 414 kPa. The backwash frequency and duration were combined into a single factor expressed as total backwash volume per hour—either 13.6 L/h (based on backwash every 5 minutes for 60 seconds), or 4.5 L/h (based on backwash every 15 minutes for 60 seconds), or 0 L/h for no backwash. Backwash was conducted by flowing water from the permeate side of the membrane to the feed side. Because the backwash consumes product water, the overall recovery ranged from 10–75% for the different conditions tested.

5.2.2 Response Variables

The flux decline and the moving average flux were the measured (derived) response variables for this study. The flux decline, or J/J_0 , is calculated as the ratio of the temperature and pressure-corrected-flux (denoted by J) at the end of the experiment to the flux at the beginning of the experiment. The flux (J) is calculated by equation 5.1,

$$J = \frac{Q_t}{A} * \frac{TMP_r}{TMP_t} * \frac{TCF_r}{TCF_t} \quad (\text{Equation 5.1})$$

where Q_t is the permeate flow rate at time, t (L/h), and A is the membrane area (m^2), TMP_r is the target transmembrane pressure for the experiment (i.e., 207, 310, or 414 kPa), TMP_t is the TMP at time t , and TCF is the temperature correction factor. TCF_r is 1, and $TCF_t = TCF$ at time, t . TCF is calculated by the following equation,

$$TCF = (1.0202)^{(25-T)} \quad (\text{Equation 5.2})$$

where, T is the temperature ($^{\circ}C$) (Cremades, Rodriguez-Grau et al. 2007).

The moving average flux (J_{avg}), is calculated as the average flux over the duration of the experiment and, when considered with the specific flux decline, is indicative of overall productivity. The response variable values after filtration of 400 L/ m^2 were used in the experimental design analysis.

5.2.3 Data Analysis

Response surface methodology (RSM) is often used in industrial practice as a mathematical optimization tool (Montgomery 2001). RSM is used to determine the values of experimental variables that maximize or minimize the response variables. RSM is useful when the response variable of interest is influenced by several variables and the objective is to optimize the response (Montgomery 2001). In this study, RSM was conducted, using Minitab[®], Version 16.1.1 from Minitab, Inc., State College, Pennsylvania. The software was used to determine the experimental factor values, or the operating conditions, that result in the maximum value of J/J_0 and J_{avg} (used as individual objective functions).

5.3 Results and Discussion

The system was operated at the desired operating conditions, described in table 5.1, until 400 L/m² of filtrate was produced. The response values were calculated based on the experimental data.

5.3.1 Filtration Experiments

The moving average flux is plotted versus the volume of filtrate produced per unit area of membrane material for a selected set of experiments; see figure 5.1. The experimental conditions, the values of the average flux, and the flux decline after filtration of 400 L/m² are presented in table 5.1.

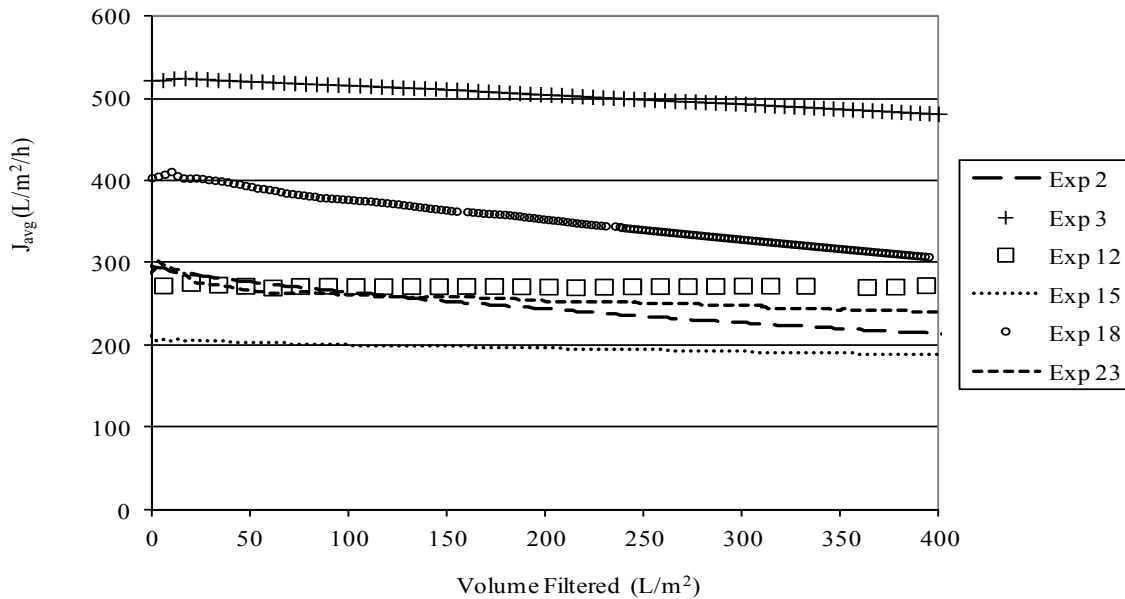


Figure 5.1 Average flux versus volume filtered for select set of experiments.

Table 5.1 Summary of experimental conditions, response variables, and TPC¹

#	Re	TMP	Coagulant dose (mg Al ³⁺ /L)	BW flow rate (L/h)	Response variables (at 400 L/m ² filtered)		TPC (\$/m ³)
					J/J _o	J _{avg} (L/m ² /h)	
1	300	414	2.5	4.5	0.81	399	0.124
2	300	207	1	0	0.57	213	0.149
3	500	414	1	0	0.84	481	0.118
4	200	207	2.5	4.5	0.86	259	0.128
5	300	207	2.5	0	0.93	237	0.129
6	300	414	1	4.5	0.80	417	0.130
7	300	414	2.5	4.5	0.76	402	0.132
8	300	207	1	0	0.75	196	0.144
9	300	414	1	4.5	0.75	387	0.125
10	300	207	2.5	0	0.78	203	0.154
11	200	414	2.5	0	0.85	378	0.122
12	500	207	1	13.6	0.95	274	0.134
13	500	207	2.5	4.5	0.85	207	0.159
14	200	414	1	0	0.58	308	0.133
15	200	207	1	4.5	0.82	187	0.155
16	500	414	2.5	0	0.92	417	0.126
17	200	207	2.5	4.5	0.78	360	0.152
18	100	414	2.5	4.5	0.53	264	0.143
19	100	310	1	13.6	0.70	294	0.136
20	100	207	1	13.6	0.77	220	0.203
21	100	207	2.5	0	0.92	217	0.130
22	200	414	2.5	0	0.76	337	0.123
23	400	310	2.5	13.6	0.71	235	0.225

¹ TPC = total production cost; BW = backwash; \$/m³ = dollars per cubic meter.

Experiment 3 resulted in the highest average flux and experiment 15 the lowest. Experiments 18 and 12 resulted in the greatest and least flux decline, respectively.

5.3.2 Filtrate Water Quality

The Safe Drinking Water Act (SDWA) requires that water treatment systems, using filtration, monitor turbidity daily and that all filtrate water samples have a turbidity less than 1.0 NTU (United States Environmental Protection

Agency 2002). The filtrate water quality from all experiments was less than 0.1 NTU, the detection limit of the handheld meter.

5.3.3 Response Surface Methodology

Response surface methodology was conducted for each response variable to identify the values of the experimental factors that result in the most favorable response variable value (the maximum value of J/J_0 and J_{avg}). The optimal TMP, Re, coagulant dose, and backwash volume for minimizing flux decline (or maximizing J/J_0) are 207, 500, 1 mg Al^{3+}/L coagulant dose, and 13.6-L/m²/h backwash flow rate, respectively. Figure 5.2 illustrates the response curve generated to describe the impact of TMP and Re on J/J_0 . The operating conditions that generate the highest average flux are 414 kPa TMP, Reynolds number of 500, 1 mg Al^{3+}/L coagulant dose, and 13.6-L/m²/h backwash flow rate. The TMP was the only variable that differed between the optimal results for the two objective function responses. The impact of TMP and Re on average flux is shown in figure 5.3.

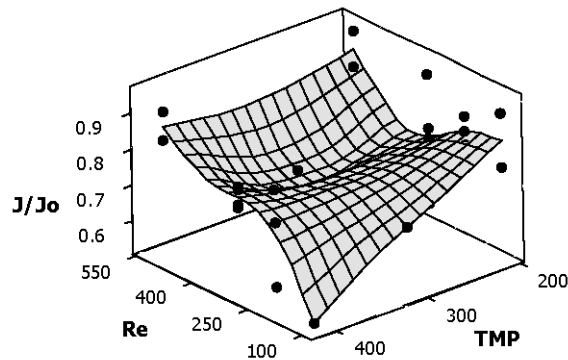


Figure 5.2 Response surface for J/J_0 .

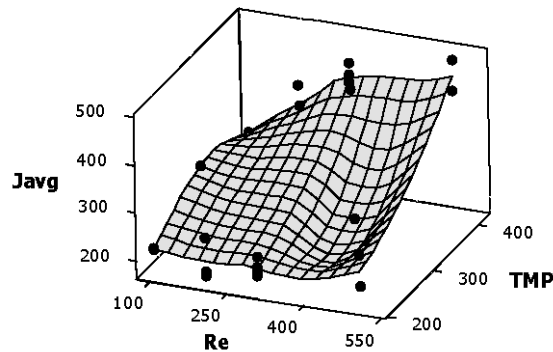


Figure 5.3 Response surface for J_{avg} .

Optimization of each response variable identified the highest value of Re and backwash flux and the lowest coagulant dosage tested. High values of Re represent hydrodynamic conditions that are less conducive to mass accumulation at the membrane surface, which is beneficial for maintaining high flux. However, increased Re also means increasing the CFV for a given membrane channel size, which also requires more energy for pumping. Thus, there is a tradeoff that can only be rationalized with an economic analysis.

Not surprisingly, increased backwash flow rate resulted in the best flux conditions; however, because backwashing consumes filtrate water, the overall recovery is reduced, and a larger plant capacity is required to produce the extra filtrate for the backwash and to compensate for the plant not producing filtrate while executing backwashes. To better evaluate the optimum Re , transmembrane pressure, and backwash flow rate, the effect of these variables, in terms of their contribution to the total investment (or annualized capital charge), also has been calculated.

In addition, the coagulant dose should be kept at the lowest level that results in acceptable TOC reduction. Increasing the coagulant dose can contribute to fouling (Kimura, Maeda et al. 2008; Wang, Guan et al. 2008; Lee, Choo et al. 2009) and increases the chemical demand for the plant—thus, increasing the O&M cost. Thus, the full annualized production cost is another useful (derived) response variable.

5.3.4 Production Cost Analysis

The operating conditions identified in table 5.1 were used as the inputs to the cost model. The cost model was used to calculate the TPC for a full-scale plant corresponding to each experiment (table 5.1) operating with the indicated conditions and experiencing the corresponding average flux. Table 5.2 presents the membrane area and costs associated with the optimum operating condition within our experimental levels. Because operating at a higher flux requires less membrane area to produce the same volume of product water, the maximum average flux conditions required ~40% of membrane area that the minimum flux decline case requires. Because the membrane material cost is the major component of the capital cost, the highest average flux case has a lower annualized capital cost. Interestingly, maximum J_{avg} also provides for lower annual O&M cost even with higher pressures that require more energy because of the amortized cost of membrane replacement.

Table 5.2 Membrane area and annualized cost for optimal operating conditions

	Maximize J_{avg}	Maximize J/J_o
Membrane area (m ²)	1,693	3,539
Annualized capital (\$/m ³)	0.052	0.063
Annualized O&M (\$/m ³)	0.066	0.071
Total annualized cost (\$/m ³)	0.118	0.134

A parametric analysis was conducted using the membrane material cost and the two separate scenarios of maximizing average flux versus minimizing flux decline. These results are presented in figure 5.4. The cost of ceramic membrane material has been reported to range from \$500/m² to over \$1,000/m² (Sethi 1997; Nandi, Uppaluri et al. 2008). As mentioned above, the maximum average flux case results in a lower annual cost for all values of the material cost because it requires less membrane area. However, as lower values for ceramic membrane material cost are assumed, the gap narrows, especially in the contribution of the O&M costs where the sensitivity to energy cost is the greatest.

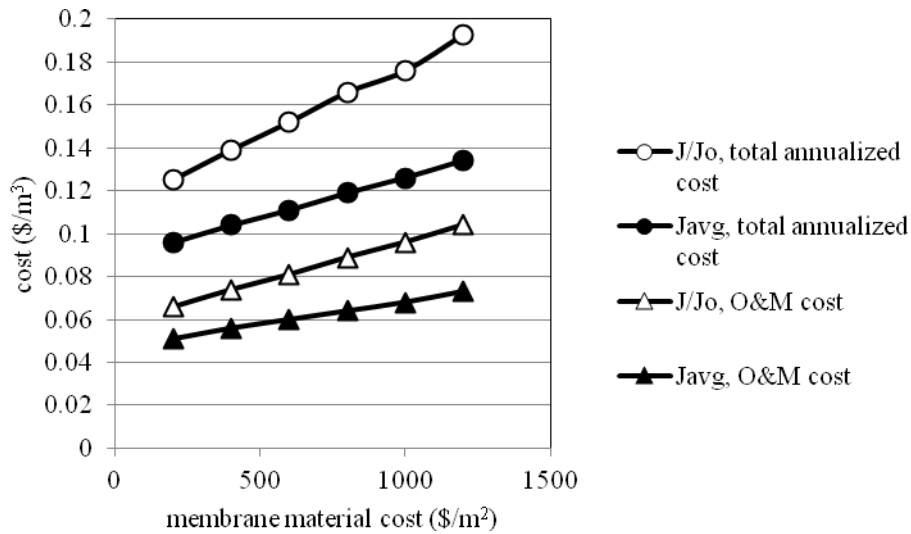


Figure 5.4 Membrane material cost parametric analysis results

A common goal of membrane research and plant design is to minimize flux decline (Song 1998; Aydinler, Demir et al. 2005; Vela, Blanco et al. 2007). The belief is that minimum flux decline results in the lowest plant cost. The cost modeling results from this study show that, for the feed water used in this testing and the design parameters chosen, minimizing flux decline is less important than maximizing average flux for producing the lowest annualized plant cost.

5.4 Summary

Ceramic membranes are very adaptable with regard to the possible values of the important operating parameters: TMP, Re, coagulant dose, and backwash flow rate. RSM, a statistical analysis tool, was used to identify the operating conditions that resulted in the least amount of flux decline and the highest average flux. The total plant costs were estimated for a ceramic membrane system designed to operate at the set of operating conditions that resulted in a) the least flux decline and b) the highest average flux over the experimental period for the specific membrane evaluated to treat Clear Creek river water.

The optimal values of Re , coagulant dose, and backwash flow rate were found to be 500, 1 mg Al^{3+}/L , and 13.6 L/h for both cases (least flux decline and highest average flux). The optimal values were the limits of the range of values tested; therefore, further studies could be conducted at values outside of the range tested. Operation at a TMP of 207 kPa resulted in the least amount of flux decline, while operation at a TMP of 414 kPa resulted in the highest average flux.

Due to the high material cost of ceramic membranes, the total plant cost can be reduced by operating under conditions that produced higher relative flux decline but greater moving average flux. Increasing the backwash volume was found to be beneficial; however, backwashing consumes product water, which requires that the plant be designed for a larger flow rate. Further detailed studies are necessary to determine the optimal backwash conditions to minimize flux decline and irreversible fouling while maintaining the system recovery and maximizing the amount of usable product water.

The conclusion that increased fouling results in reduced plant costs is only valid for membrane materials and water types in which the foulant is easily and efficiently removed. Therefore, these results emphasize the need for studies on membrane cleaning efficiency to evaluate strategies for restoring flux lost due to fouling using a systematic experimental design tied to an economics-based objective function, rather than focusing efforts on minimizing flux decline. These modeling efforts also showed that the techno-economic model was sufficient for evaluating the effect of different operating conditions on total water production cost; therefore, this modeling approach can be adapted to compare the economic benefits of different types of materials with different performance characteristics.

6. Comparison of Membrane Fouling Tendency

Experiments were conducted to quantify the degree of fouling for the alumina and PES membranes at carefully controlled hydrodynamic conditions. The results of these experiments are used in the cost model to calculate the average system operating pressure and the pumping requirements as a function of the cross-flow velocity and flux and the rate of pressure increase. Experiments were conducted using the bentonite suspension and the complex mixture described in chapter 4.

6.1 Membrane Conditioning

A new polymeric membrane was used for each set of experiments with a different feed water type. Each new polymeric membrane was conditioned prior to its first use, using the protocol established by the membrane manufacturer. The polymeric membrane was flushed with DI water at 70-kPa transmembrane pressure until 40 L/m² of filtrate were produced.

Due to the high cost of ceramic membranes, the ceramic membranes were cleaned and reused. The pure water permeance of the ceramic membrane was evaluated before each experiment and determined to be within 0.02 L/m²/h/kPa, equivalent to one standard deviation on multiple measurements on the membrane at the beginning of the experiments, of the initial membrane permeance of 1.13 L/m²/h/kPa.

6.2 Fouling Conditions

For both the alumina and PES membranes described in chapter 4, a series of filtration experiments were conducted over a range of hydrodynamic conditions. The series of experiments were conducted using both the bentonite suspension and the complex mixture. During the filtration experiments, constant flux conditions were maintained; therefore, an increase in the transmembrane pressure over the duration of the experiment was used to quantify the extent to which fouling occurred. The filtrate flux and the cross-flow velocity were monitored and controlled during the experiments. The difference in the transmembrane pressure at time, t , and the initial transmembrane pressure was recorded as a function of the volume of filtrate produced per membrane area. The series of experiments for each membrane covered a range of apparent Pe from 2 to 12.5 for both feed mixtures.

6.3 Results

Results are presented for both the bentonite suspension and complex mixture feed solutions over a range of Pe values. The increase in transmembrane pressure as a function of the cumulative volume of filtrate produced is presented.

6.3.1 Bentonite Suspension

The flux of the membrane at different transmembrane pressures was measured for both the alumina and PES membranes, figures 6.1 and 6.2, respectively. The alumina membrane has a higher permeance to the bentonite suspension than the PES membrane— $1.13 \text{ L/m}^2/\text{h/kPa}$ compared to $1.09 \text{ L/m}^2/\text{h/kPa}$. The permeance of the alumina membrane to the bentonite suspension is equal to its pure water permeance. The permeance for the PES membrane to the bentonite suspension is 10% lower than its pure water permeance. This is likely due to hydrophobic interactions between the membrane and the bentonite suspension.

The increase in TMP over the duration of the filtration experiments is presented in Figures 6.3 and 6.4 for the alumina and PES membrane, respectively.

For the alumina membrane, minimal TMP increase occurred for $Pe < 7.8$; however, for $7.8 < Pe < 11.4$, a slight TMP increase was observed during the filtration; runs. At $Pe > 11.4$, a significant increase in TMP is measured; however, the rate of TMP increase is less than that for the polymeric membrane at corresponding values of Pe ; see figure 6.4.

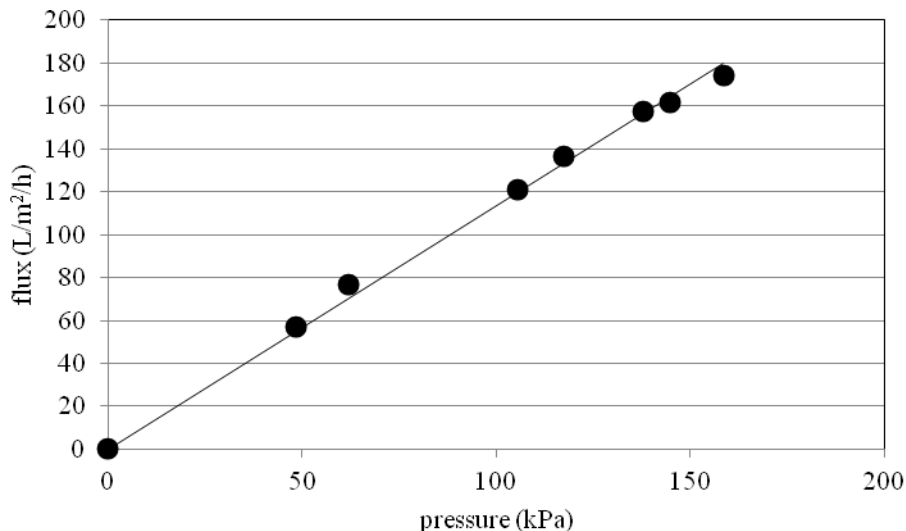


Figure 6.1 Alumina membrane permeance for bentonite suspension.

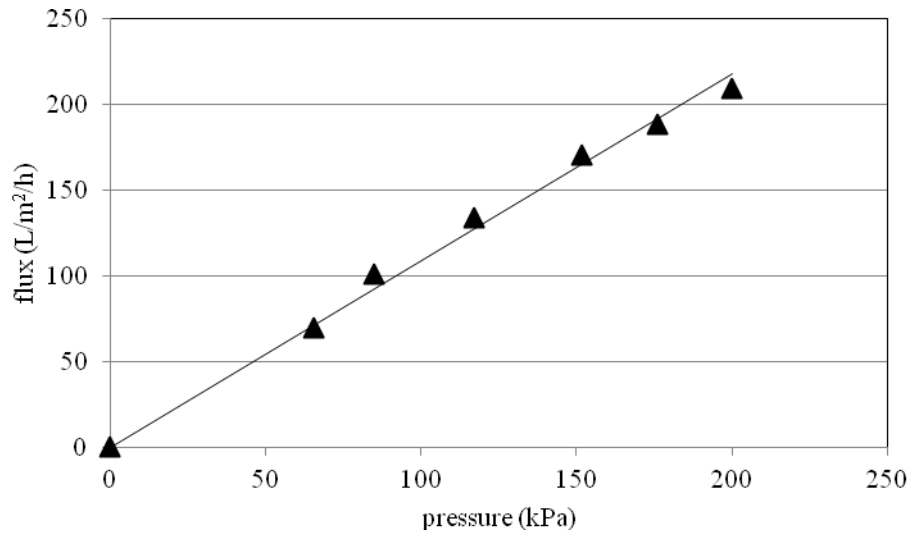


Figure 6.2 PES membrane permeance for bentonite suspension.

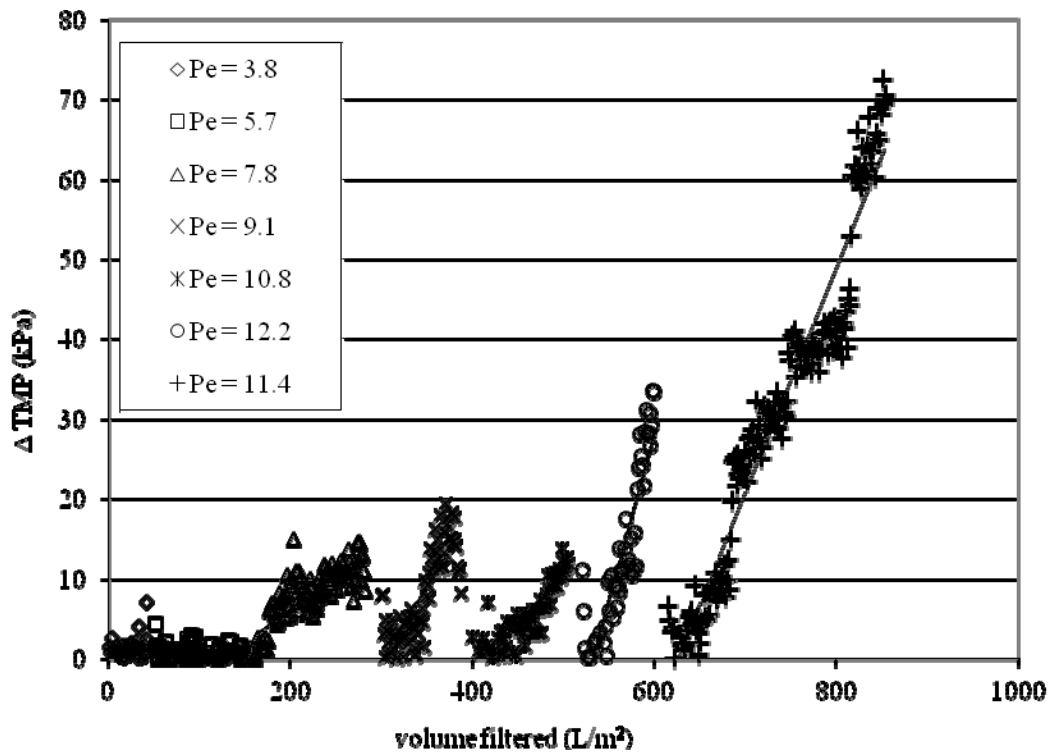


Figure 6.3 Alumina membrane permeance at different Pe.

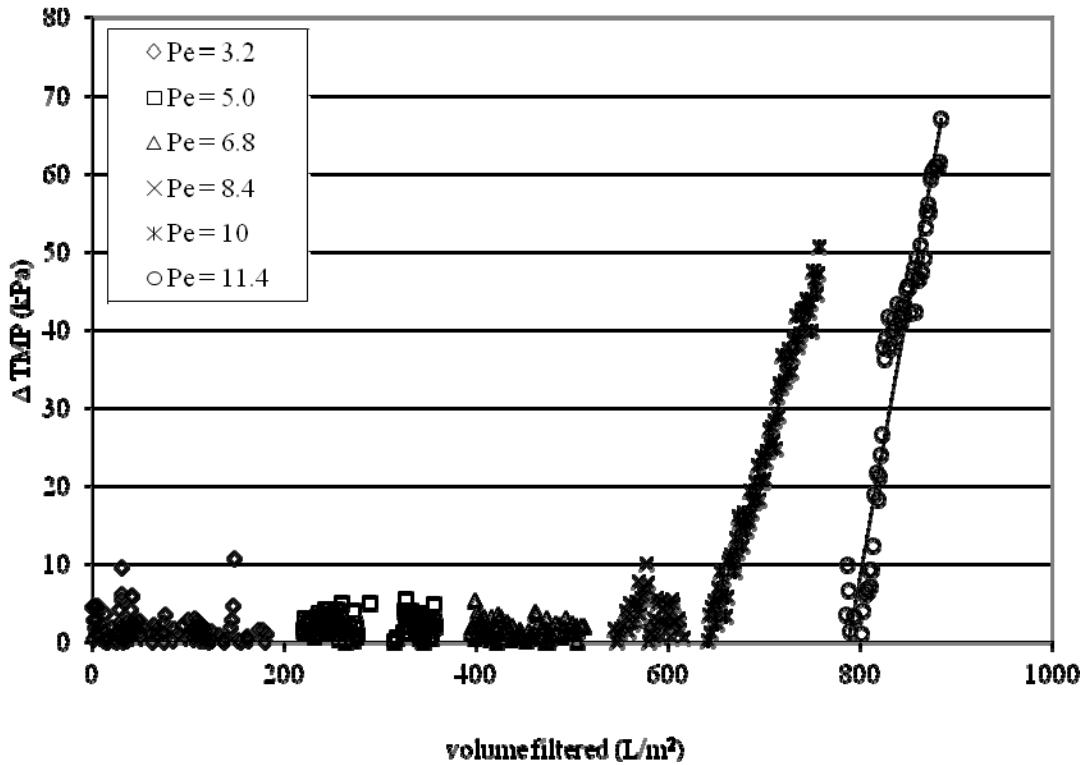


Figure 6.4 Polymeric membrane performance at different Pe.

The PES membrane experienced no measurable increase in transmembrane pressure for experiments at Pe less than 8.4. At Pe > 8.4, substantial TMP increase was observed. A critical Pe exists near 8.4 for the system with the PES membrane.

The slopes of the TMP increase over the duration of each filtration experiment are shown in figure 6.5 for both membranes to facilitate direct comparison. The alumina membrane shows a gradual increase in the rate of TMP increase; whereas, the PES membrane shows negligible increase until the distinct Pe value nears 8.4.

6.3.2 Complex Mixture

The flux of the membrane at different transmembrane pressures was measured for both the alumina and PES membranes for filtration of the complex feed mixture. The results are shown in figures 6.6 and 6.7 for the alumina and PES membranes, respectively.

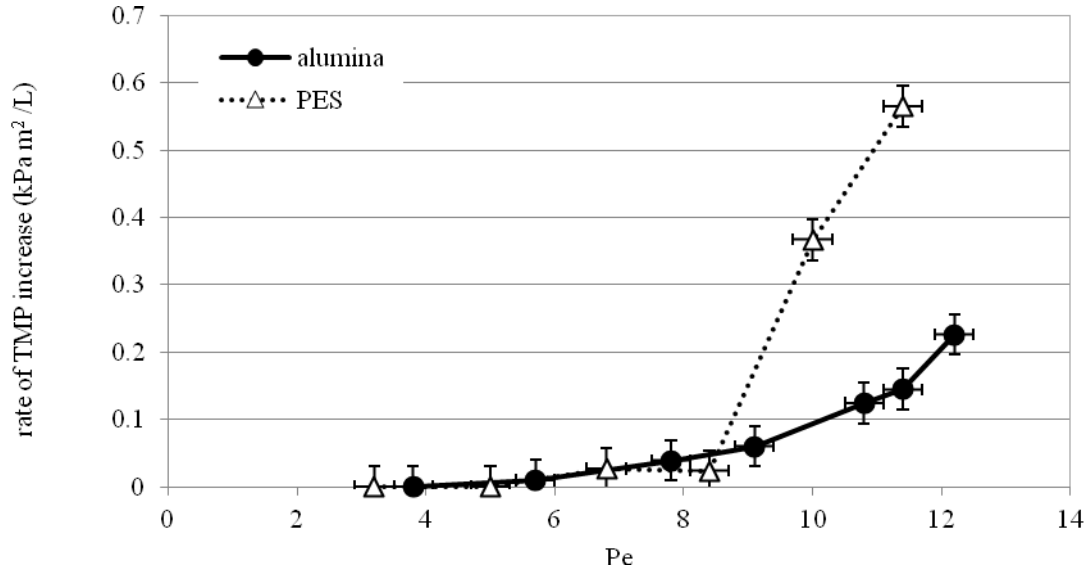


Figure 6.5 Rate of pressure increase versus Pe for the alumina and PES membranes.

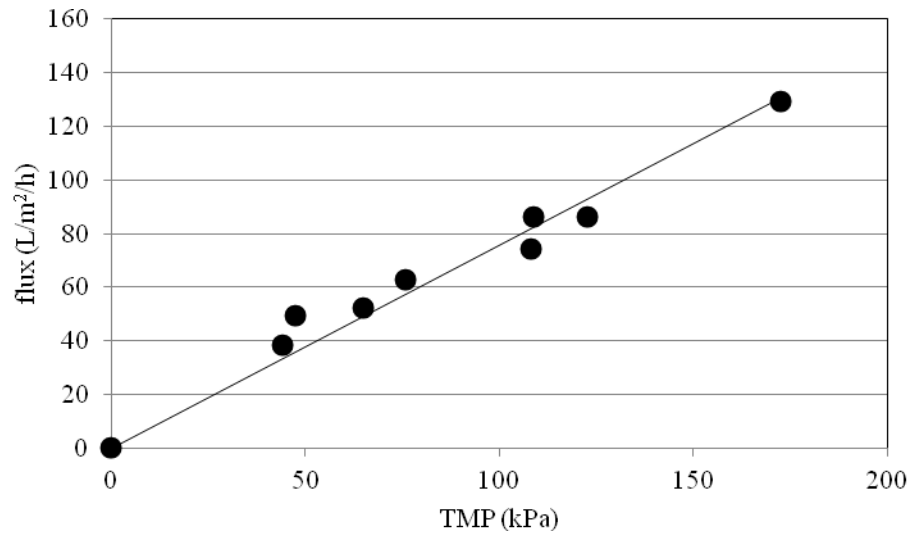


Figure 6.6 Alumina membrane permeance to complex mixture.

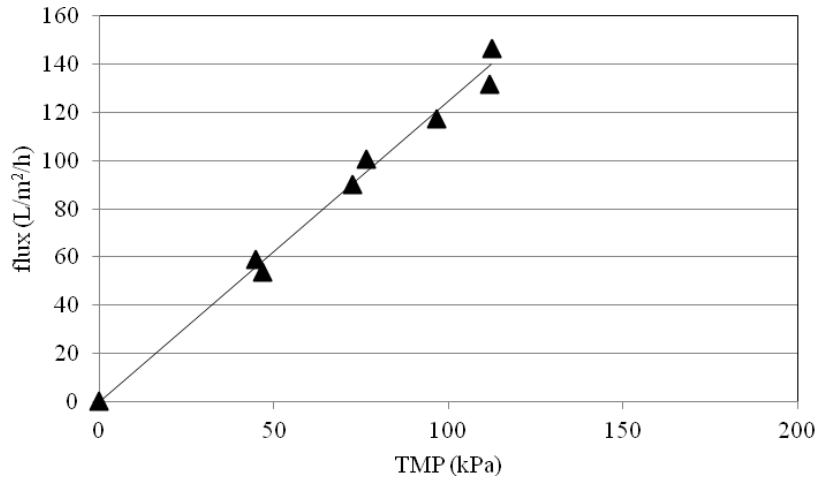


Figure 6.7 PES membrane permeance to complex feed mixture.

For the complex mixture, the permeance of the alumina membrane was significantly less than the PES membrane, 0.76 and 1.20 L/m²/h/kPa, respectively. Contrary to the results for the bentonite permeance, the PES membrane permeance is not statistically different from its pure water permeance; whereas, the alumina membrane permeance is 32% lower than its pure water permeance.

The difference in transmembrane pressure as a function of water filtered per area of membrane is plotted in figures 6.8 and 6.9 for the alumina and PES membranes, respectively. The alumina membrane exhibited negligible fouling for $Pe < 3.6$. At $Pe > 3.6$, the fouling rate increased with increasing Pe . The PES membrane showed a minimal fouling for $Pe < 4.5$. For $Pe > 4.5$, the rate of fouling increased with increasing Pe . The fouling rate as a function of Pe is shown in figure 6.10 for both membranes to facilitate comparison of results.

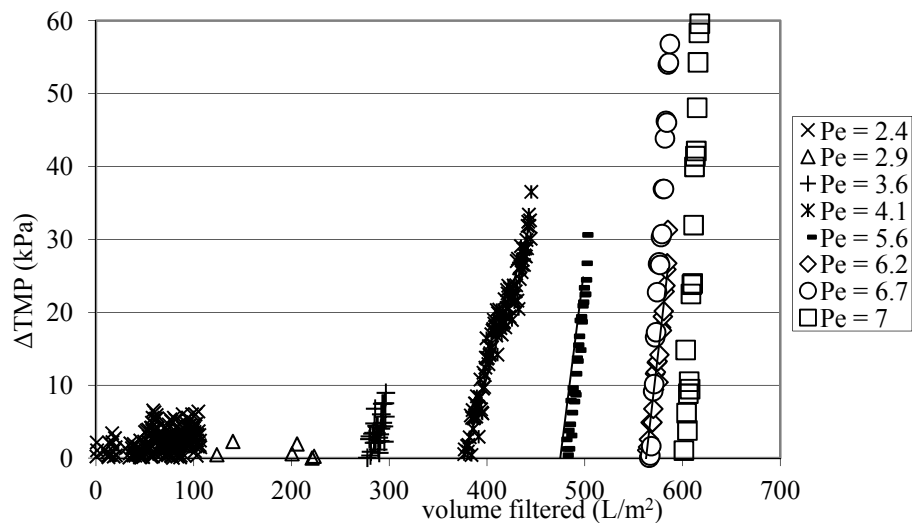


Figure 6.8 Alumina membrane fouling rate for different values of Pe .

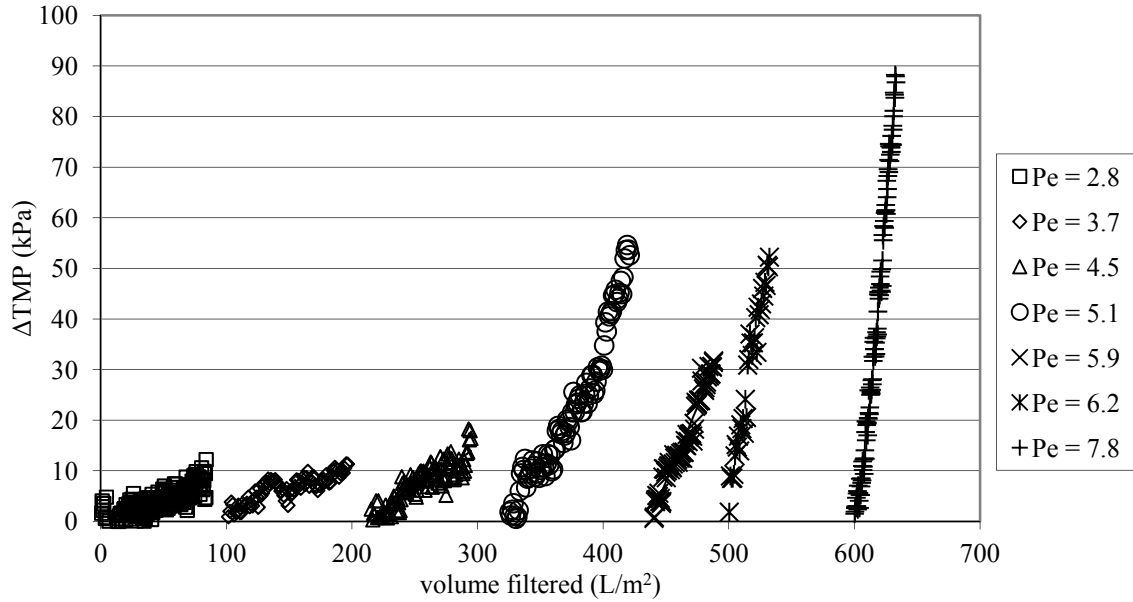


Figure 6.9 PES membrane fouling rate at different values of Pe.

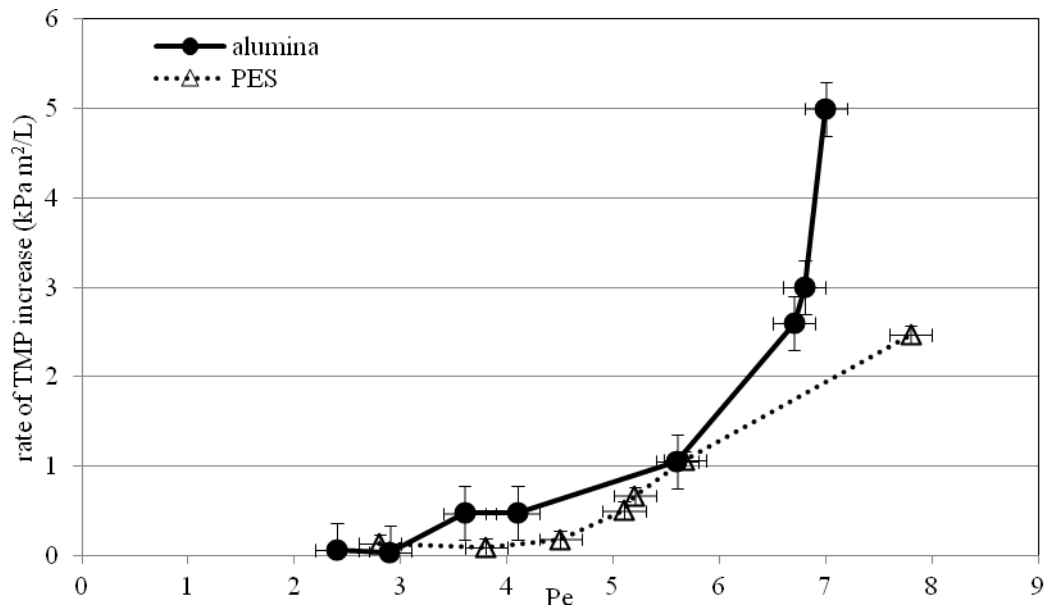


Figure 6.10 Comparison of alumina and PES membrane fouling as a function of Pe.

At low values of Pe ($Pe < 3.6$), the fouling rates were negligible for both membranes. At moderate values of Pe, $3.6 < Pe < 5.6$, the two membranes have similar fouling rates. At $Pe > 6$, the fouling rate for the alumina membrane is higher than that for the PES membrane.

The observed solute rejection was calculating using the following equation,

$$R_{obs} = \frac{(C_f - C_p)}{C_f} \quad \text{(Equation 6.1)}$$

Where C_f and C_p refer to the DOC concentrations in the feed and permeate streams, respectively. The observed rejection is shown in figure 6.11 for the two membranes.

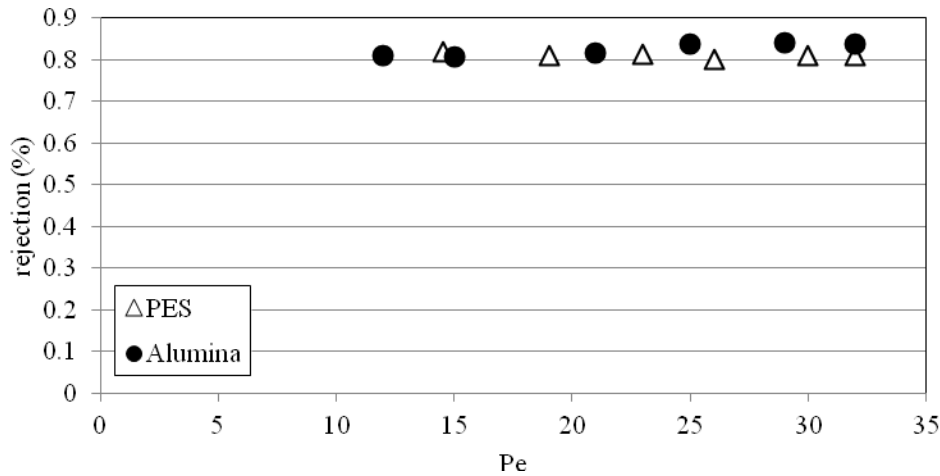


Figure 6.11 Observed DOC rejection for alumina and PES membranes.

The polymeric membrane rejection was independent of Pe ; however, the alumina membrane rejection increased slightly at Pe values, which caused large amounts of membrane fouling. The rejection for the alumina and PES membranes at $Pe = 6.2$ were 84 and 81%, respectively. The increased rejection for the alumina membrane is likely due to cake filtration or pore constriction because foulant accumulated on the membrane surface and in the pores.

Figures 6.12 and 6.13 are EEMs of the filtrate from the alumina and PES membrane, respectively.

Filtrates from both the alumina and PES membrane were similar in the EEM spectra signatures. The calculated regional fractions were also very similar. The overall fluorescence intensity, calculated as the sum of the matrix intensities, was slightly higher in the PES filtrate than that in the alumina filtrate, consistent with the lower rejection observed for the PES membrane.

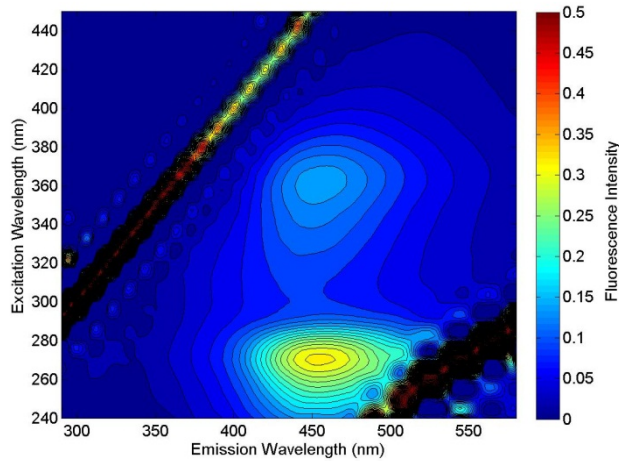


Figure 6.12 Ceramic membrane filtrate.

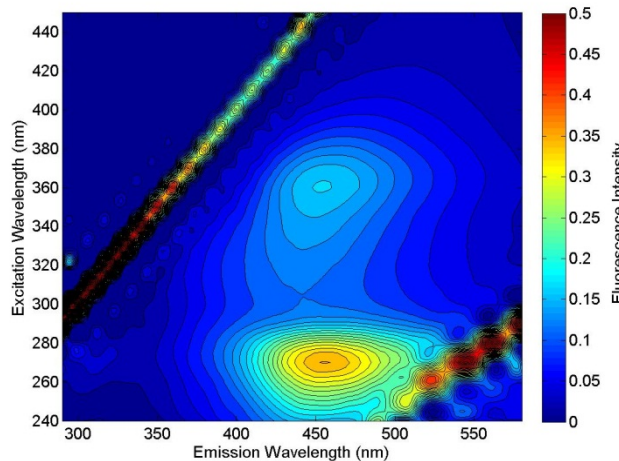


Figure 6.13 Polymeric membrane filtrate.

6.4 Discussion of Results for Bentonite Suspension

For filtration of the bentonite suspension, lower fouling rates were observed for the alumina membrane as compared to the PES membrane at values of $Pe > 8.7$. At higher values of Pe , less accumulation of solute on the membrane surface is observed at the same apparent value of Pe . This result implies that back-diffusion is greater for the alumina membrane as compared to the PES membrane. The intrinsic surface roughness of the alumina membrane increases the shear-induced diffusion, or the diffusion due to deflection of solute from streamlines due to interaction with the membrane surface. Additionally, membrane roughness increases the membrane surface area; therefore, the apparent flux may be higher than the actual flux, resulting in an apparent Pe that is higher than the actual.

6.5 Discussion of Results for Complex Mixture

The Hermia model is a commonly used empirical model with model parameters that have a physical interpretation. The following represents the characteristic form of the model for constant flux filtration:

$$\frac{d^2\Delta P}{dV^2} = k \left(\frac{d\Delta P}{dV} \right)^n \quad (\text{Equation 6.2})$$

where ΔP is the transmembrane pressure, V is the cumulative volume of filtrate produced, and n and k are the model parameters. The value of n identifies the mode of fouling, where $n = 0$ corresponds to cake formation, $n = 1$ to intermediate blocking, $n = 3/2$ to standard blocking, and $n = 2$ to complete blocking. The fouling mechanisms are depicted in figure 6.14.

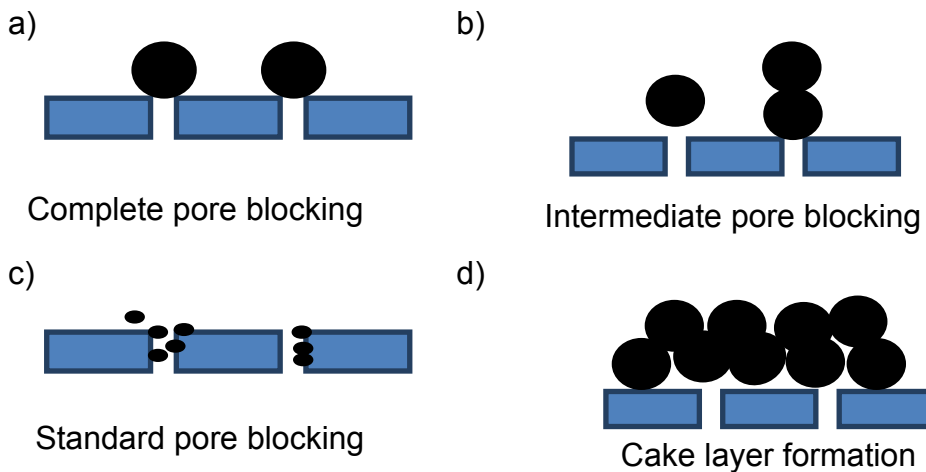


Figure 6.14 Illustration of the four modes of fouling described by the Hermia model.

Linear expressions have been developed for each of the modes of fouling for constant flux filtration under cross-flow conditions, (Huang, Young et al. 2008) by defining the value j_s as the normalized specific flux, which is the pressure normalized flux as time, t , divided by the pressure normalized flux at time zero, see table 6.1.

Table 6.1. Linear expressions of revised Hermia model (Huang, Young et al. 2008)¹

Fouling Mechanism	n	k	Linear Expression
Cake formation	0	$C_f R_c / R_m$	$\frac{1}{j_s} = 1 + kV$
Intermediate blocking	1	$C_f \sigma$	$\ln j_s = -kV$
Standard blocking	3/2	$2C_f / L\rho$	$j_s^{1/2} = 1 + \frac{k}{2V}$
Complete blocking	2	$C_f \sigma$	$j_s = 1 - kV$

¹ C_f = mass concentration of foulant in the feed, R_c = specific cake resistance, R_m = hydraulic resistance of clean membrane, L = pore length, σ = project area of unit mass of particles on membrane, ρ = density of foulants.

The alumina and PES filtration data were used to calculate j_s using the flux and transmembrane pressure data from the experiments wherein fouling occurred for the complex mixture. The values of j_s , $1/j_s$, $\ln j_s$, and $j_s^{1/2}$ were calculated and plotted versus the cumulative volume of filtrate produced. The results are shown in figure 6.15 for the alumina membrane and in figure 6.16 for the PES membrane. A regression analysis was conducted on the linear expressions to determine the model with the best fit. The results of the regression analysis are shown in table 6.2.

The fouling mode that produced the highest value of the F-statistic (and R^2) is determined to be the best fit and; therefore, the dominant fouling mechanism. The fouling mechanism is cake formation for the alumina membrane and standard blocking for the PES membrane.

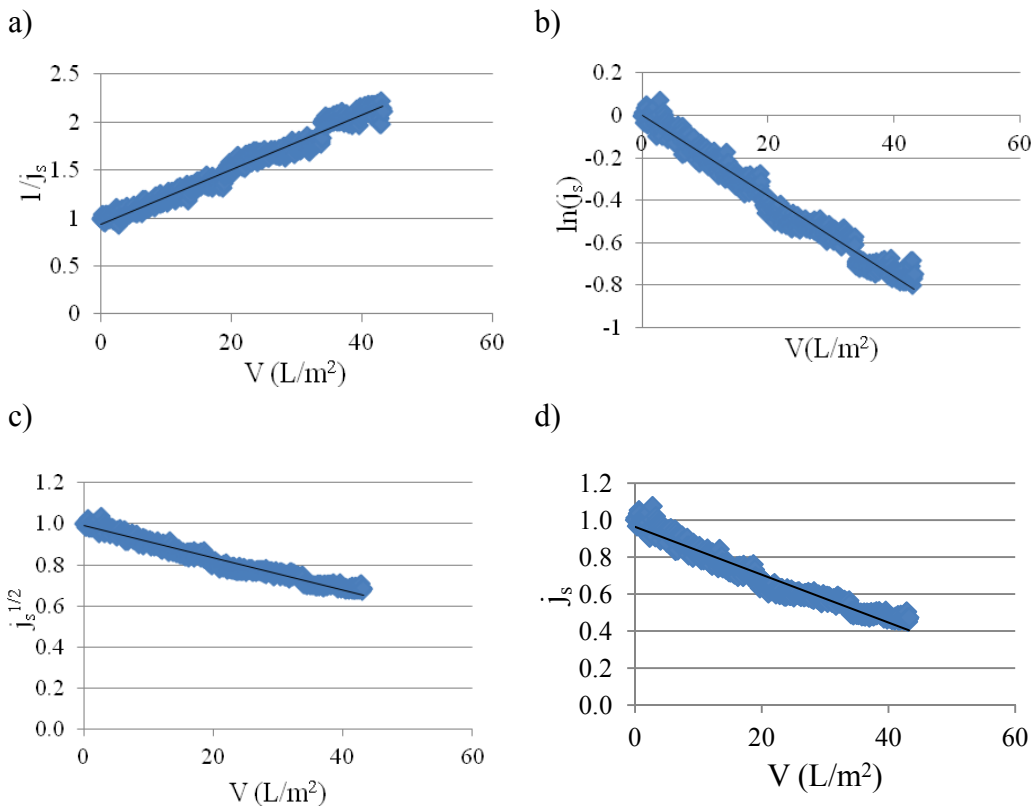


Figure 6.15 Plots of linear expressions for the alumina membrane for a) cake formation, b) intermediate blocking, c) standard blocking, and d) pore plugging.

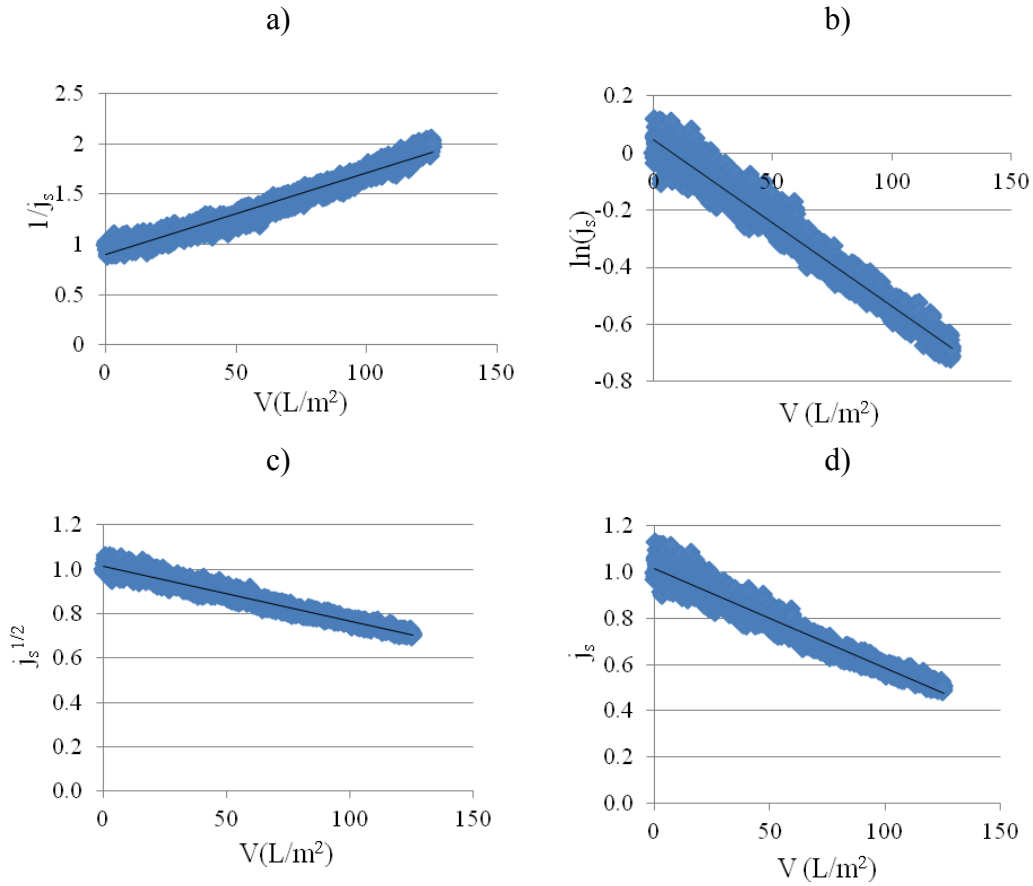


Figure 6.16 Plots of linear expressions for the PES membrane for a) cake formation, b) standard blocking, c) intermediate blocking, and d) pore plugging.

Table 6.2 Results of regression analysis comparing Hermia model fits

Membrane	Fouling Mechanism	R2	Standard Error	F-Value
alumina	cake formation	0.97	0.045	14467
alumina	intermediate blocking	0.96	0.035	12681
alumina	standard blocking	0.96	0.017	10683
alumina	complete blocking	0.95	0.032	8664
PES	cake formation	0.97	0.054	50244
PES	intermediate blocking	0.97	0.15	60119
PES	standard blocking	0.98	0.033	67703
PES	complete blocking	0.96	0.029	46572

6.6 Effect of Surface Energy on Filtration Results

For the bentonite mixture, the rate of the fouling was less for the alumina membrane than for the PES membrane, whereas the opposite was true for the complex mixture. Surface energy is a likely explanation for these results. Ceramic membranes are known to have high surface energy compared to polymeric membranes. The complex mixture, as shown in figure 4.9, is dominated by humic substances. Functional groups such as carboxylic acids and hydroxyl groups attached to aromatic rings make humic acids hydrophilic. It is likely that the hydrophilic fraction of the organic matter is interacting with the alumina membrane. The results presented in this chapter are consistent with other studies finding that hydrophobic membranes experience less natural organic matter fouling than hydrophilic membranes (Choo and Lee 2000; Maximous, Nakhla et al. 2009).

The results presented here may help to explain the seemingly inconsistent results in the literature with respect to ceramic and polymeric membranes. The observation that the ceramic membrane experienced less fouling than the polymeric membrane for hydrophobic feed solutions is consistent with the findings of Mueller and Davis who reported that the resistance of the fouling layer formed on the polymeric membrane is higher than that formed on the ceramic membrane during filtration of oily water emulsions (Mueller, Cen et al. 1997). Reed et al. also showed a higher average flux for ceramic versus polymeric membranes when treating oily wastes (Reed, Lin et al. 1997).

During filtration of the complex feed mixture, the ceramic membrane experienced more fouling than the polymeric membrane at $Pe > 5.6$ for filtration of the complex mixture. This result is consistent with the results from Bodzek et al. that showed that the polymeric membrane was more favorable (Bodzek and Konieczny 1998) for treatment of water containing natural organic matter. The result that the ceramic and polymeric membranes experienced similar fouling rates (for $Pe < 5.6$) for the complex mixture is in agreement with Hofs et al., who found that an alumina ceramic membrane exhibited similar reversible fouling as a polymeric membrane (Hofs, Ogier et al. 2011) for treatment of surface water.

6.7 Integration of Performance Results into Cost Model

Integrating the results for the performance comparison into the cost model allows for consideration of differences in performance due to operating conditions in terms of total process cost so that the costs are more representative of a real application in which fouling affects the average transmembrane pressure. The results from these experiments are quantified in the cost model in two ways: (1) the fouling rates ($\text{kPa}/\text{L}/\text{m}^2$) are used in conjunction with the feed water quality and the membrane area to calculate the average operating pressure; and

(2) the fouling rates, as a function of Pe , are used to calculate full-scale membrane operating conditions that result in similar fouling rates to those observed during laboratory experiments using smaller modules.

6.7.1 Calculating Average Operating Pressure

The fouling rates obtained through experiments are expressed as a pressure increase per time, calculated from the water production rate and the membrane area. The fouling rates are used in the cost model to calculate the average operating pressure for the full-scale system.

6.7.2 Calculating Operating Conditions for Full-Scale Membranes

Full-scale membrane modules typically contain more fibers or channels with a longer length than modules used in laboratory testing. The membrane geometry of the full-scale modules was used to calculate the cross-flow velocity and flux that corresponded to Pe values from the laboratory experiments; see appendix B for the cross-flow velocity and flux values corresponding to Pe that were used in the cost model simulations.

While it is important to consider the cost results in the context of commercially available products, it also is necessary to understand the differences in cost due to the material properties and characteristics of each membrane type; therefore, a hypothetical module size was developed to illustrate the cost of the alumina and PES membranes that is independent of module geometry. The hypothetical module size has a channel diameter of 1 mm and a length of 0.864 m. Cost model simulations were conducted for the commercially available module and the hypothetical module for both membrane materials to illustrate the effects of module geometry on TPC.

According to the AWWA Membrane Knowledgebase, 63% of responding utilities conducted pilot testing (Adham, Chiu et al. 2005). Of those that pilot tested, the majority responded that pilot testing accurately predicted full-scale operation; however, overpredicting full-scale performance was far more common than underpredicting full-scale performance. This may be due to scale-up issues related to the actual length of module used in pilot testing. Pilot test modules are never longer than full-scale modules. Using only cross-flow velocity and pressure as the operating variables, figure 2.4 shows that a longer module length requires a higher cross-flow velocity to keep the Pe constant; therefore, a difference in module length may be one factor leading to overprediction of performance based on pilot scale results. Other factors, such as time and unplanned water quality events at full-scale, also can contribute to differences.

6.8 Summary

Theoretically, the critical value of Pe that caused the onset of fouling should be 1, as described in chapter 2. In the experiments presented here, the critical values of Pe are greater than 1 for both membranes and for both feed water types. This indicates that the mass transfer correlation used underpredicts the back transport of solute (from the membrane surface to the bulk flow). The most likely source of error in the calculation of the mass transfer coefficient is the estimation of the solute diffusion coefficient. Measurements of the diffusion coefficient were outside of the scope of this study; therefore, this value was estimated based published diffusion coefficients for natural organic matter. This value is difficult to estimate due to the complex, colloidal physics acting at the membrane surface within the concentration boundary layer.

If the two materials tested in this study were exactly the same, we would expect the fouling behavior to be the same. Since differences in performance do exist, they are due either to differences in hydrodynamic conditions or material property differences. Every effort was made to control the hydrodynamic conditions, thereby minimizing the impacts of hydrodynamic conditions and increasing the confidence in attributing performance differences to differences in material properties and membrane-solute interactions.

Since the pore size, permeance, and rejection of the membranes are similar, based on results presented in chapter 4, other material properties such as surface energy, surface charge, and roughness are most likely responsible for the observed performance differences. The surface charge of both membranes is expected to be negative at pH 7 (the pH of the water types tested); therefore, electrostatic effects are expected to be similar. The surface energy and roughness are the two material properties that likely are influencing the differences in measured performance.

7. Comparison of Membrane Cleaning Efficiency

A cleaning study was conducted on the alumina and PES membranes to identify the time and volume of chemicals required to efficiently clean the membranes. Multiple cycles of fouling and cleaning were conducted to determine whether any trends of long-term irreversible fouling or membrane degradation due to cleaning occurred. The experimental results are used in the cost model to estimate chemical cleaning costs of a full-scale plant.

7.1 Experimental Procedure

The membranes were fouled and cleaned multiple times to evaluate whether long-term effects of degradation due to cleaning or irreversible fouling could be detected. In this chapter, the membrane fouling procedure is described, and a new cleaning procedure is presented and demonstrated.

7.1.1 Fouling

The complex feed mixture was used to foul both of the membranes at a Pe of 5.7 ± 0.3 . This value of Pe was chosen because it resulted in a measurable increase in TMP within only a few hours of operation for both membranes. The membranes were fouled until the same percentage decrease in pure water permeance was observed. The value of the PWP decrease during the fouling run was $45 \pm 5\%$. The pure water permeance was measured before and after each fouling cycle. Table 7.1 describes the conditions used for fouling and PWP measurements for the two membranes.

7.1.2 Cleaning

The most commonly employed strategy for cleaning membranes is to recirculate cleaning chemicals for a prescribed length of time (see chapter 2). Static cleaning, or soaking, is commonly used in conjunction with the latter. The downside to the conventional cleaning procedure is that it is difficult to ascertain the optimal amount of time to conduct each cleaning step because there is no visual indication of when cleaning is complete. Each membrane was cleaned one time with a conventional cleaning procedure, which consisted of recirculating cleaning solutions (citric acid following by a mixture of sodium hydroxide at pH 11 and sodium hypochlorite at 400 ppm) for up to 2 hours, checking the pure water permeance in between sequential cleaning steps.

In an attempt to increase the efficiency and shorten the duration of chemical cleaning, a slight modification was made to the conventional cleaning strategy. In

the modified cleaning strategy, the cleaning solution was allowed to permeate the membrane under 70 kPa TMP. This approach allows for the monitoring of the membrane permeance as cleaning progressed. An increase in permeance was observed in the first few minutes of recirculation. After the permeance stabilized, the membrane was backwashed and flushed with filtrate water. After flushing with clean water, the second cleaning solution, sodium hydroxide plus sodium hypochlorite, was introduced into the system. The same steps were repeated for the caustic cleaning solution. The conditions used for each step in the cleaning sequences are shown in table 7.1.

Table 7.1 Experimental conditions for fouling and cleaning cycles

	TMP (kPa)	t (min)	Solution
PWP	100	5	tap water
Fouling	130–275	100	complex feed mixture
Rinse	70	5	tap water
Acid cleaning	70	~5	citric acid (pH 2.75)
Backwash	70	~5	tap water
Caustic cleaning	70	~5	NaOH (pH 11) + NaOCl (400 ppm)
Rinse	70	5	tap water

During the cleaning with the caustic solution, the initial volumes of filtrate were colorless; and after a few minutes of filtration with the cleaning solution, the filtrate exhibited color similar to the complex feed mixture during normal filtration. After another few minutes, the filtrate was colorless again; see figure 7.1.



Figure 7.1 Color of the filtrate during caustic cleaning (pH 11, 400 ppm NaOCl); initial (left); after 4 minutes (middle); after 5 minutes (right).

Following the caustic cleaning, the membrane was backwashed. The color of the backwash effluent was used as an indicator for the progress of the cleaning. When the color of the backwash effluent diminished, the backwashing portion of the cleaning was deemed to be complete; see figure 7.2.



Figure 7.2 Backwash effluent after 1 minute (left), 4 minutes (middle), and 5 minutes (right); color evolution indicates complete cleaning has been accomplished.

This technique of monitoring the progress of chemical cleaning is not widely practiced in full-scale membrane plants, mainly because established cleaning protocols work relatively well, are supplied by the membrane manufacture, and are guaranteed in the membrane product warranty. In the past, membranes were cleaned in full-scale practice one to two times per year; and reducing cleaning time from hours to minutes does not dramatically affect the total water production cost. More plants are moving toward short duration and more frequent maintenance cleanings (Adham, Chiu et al. 2005), so the cleaning technique presented here may be more practical when frequent maintenance cleanings are employed, allowing for operation of the plant at more aggressive productivity conditions.

7.2 Results

The results of multiple cycles of fouling and cleaning are presented. The PWP was measured before and after each fouling cycle for both the alumina and PES membranes as shown in figure 7.3 and figure 7.4, respectively. The initial PWP represents the PWP at the beginning of the fouling cycle and is also the PWP at the end of the previous cleaning cycle. The final PWP represents the PWP at the end of each filtration cycle and the PWP at the beginning of that cycle's cleaning sequence. Error bars represent one standard deviation based on five measurements of PWP for each cycle.

The alumina membrane PWP at the start of each fouling cycle remained constant for all cycles, indicating that no irreversible fouling was observed. The PES membrane showed a decrease in PWP (approximately 30%) after the first cleaning cycle (PWP at the start of experiment 2). Some of this fouling was recovered by implementing the modified cleaning procedure so that there was only a 12% decrease in PWP (cycle 1 compared to cycle 4). From cycle 3 on, the initial PWP was recovered after each cleaning cycle.

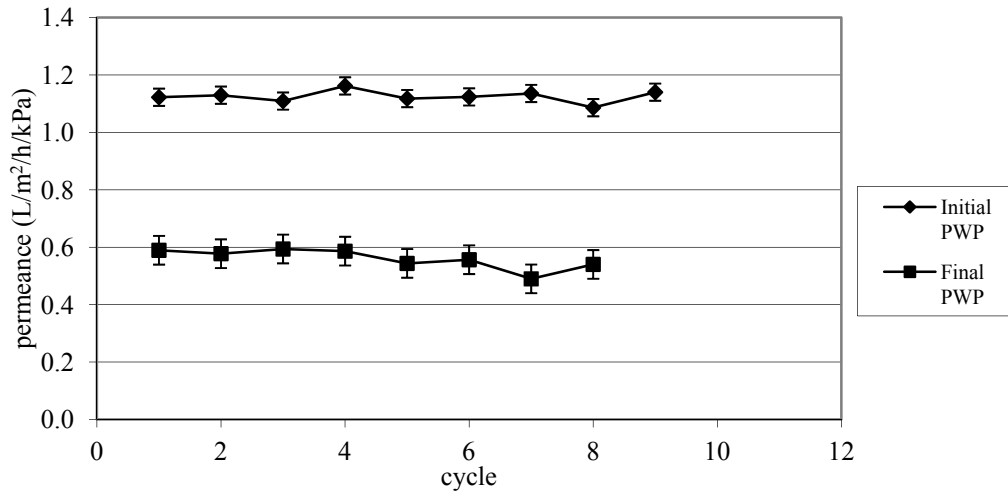


Figure 7.3 PWP before and after fouling cycles for the alumina membrane.

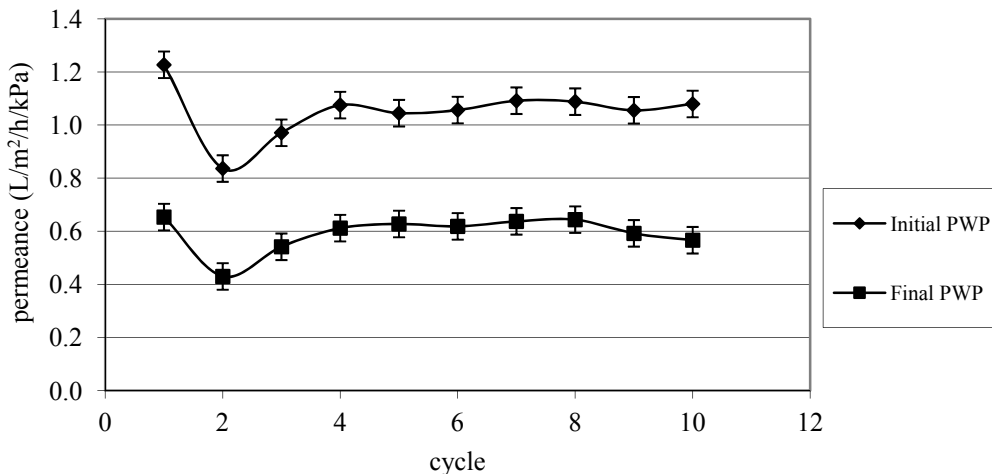


Figure 7.4 Initial and final PWP for multiple fouling and cleaning cycles for the PES membrane.

The membrane rejection was monitored during the fouling and cleaning cycles to ensure that the membrane integrity was not compromised during the fouling and cleaning cycles. The average rejection, based on measurements of turbidity and absorbance at 340 nm, are shown in figure 7.5 and figure 7.6 for the alumina and PES membranes, respectively.

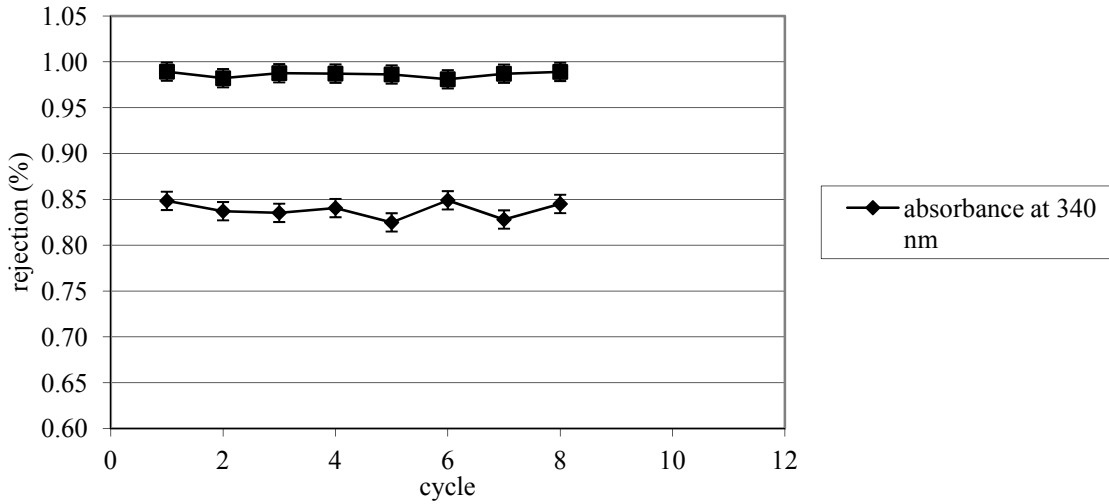


Figure 7.5 Alumina membrane rejection for each fouling and cleaning cycle.

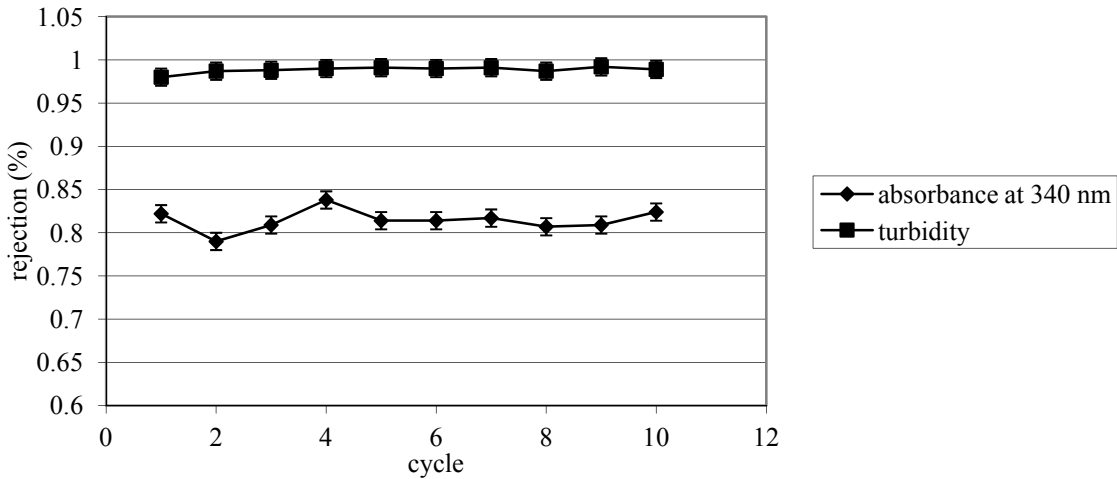


Figure 7.6 PES membrane rejection over fouling and cleaning cycles.

Cleanings were conducted after each fouling cycle. Figure 7.7 and figure 7.8 illustrate the cleaning time for each cleaning cycle for the alumina and PES membranes, respectively. The first cleaning cycle was conducted using a conventional cleaning protocol consisting of re-circulating the cleaning solution. The time required to execute the conventional cleaning protocol was 9 times longer for the PES membrane and 3 times longer for the alumina membrane.

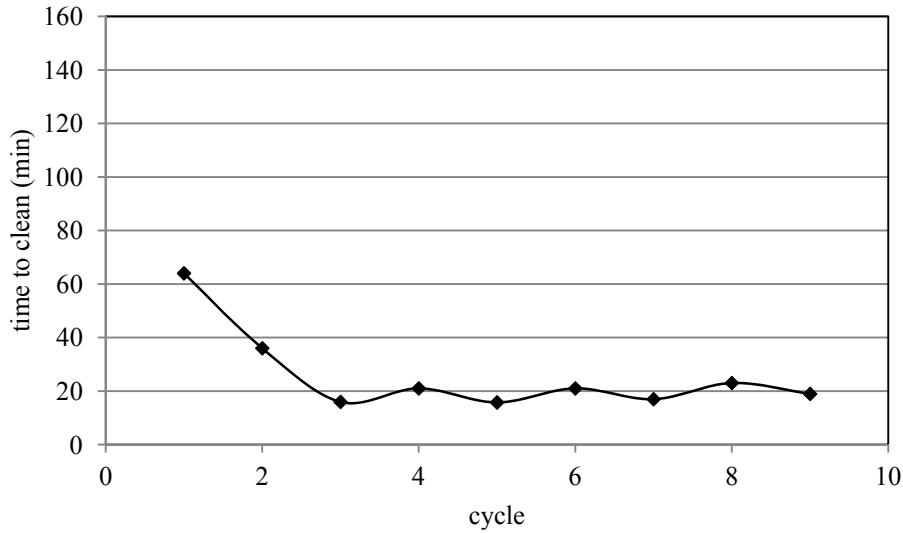


Figure 7.7 Alumina membrane cleaning duration for each cycle.

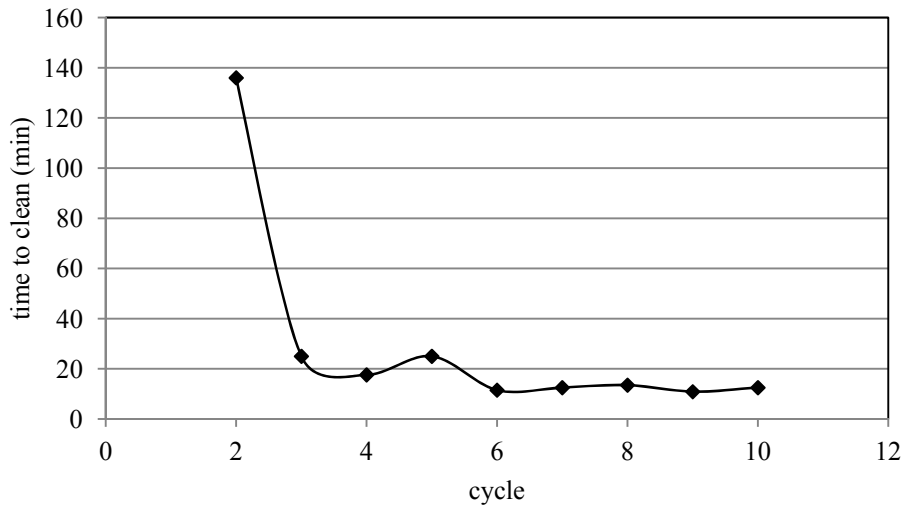


Figure 7.8 Cleaning time for the PES membrane.

Figure 7.9 is an EEM of the filtrate during the cleaning cycle corresponding to the time during cleaning which produced filtrate with enhanced color (approximately 4 minutes into the caustic cleaning).

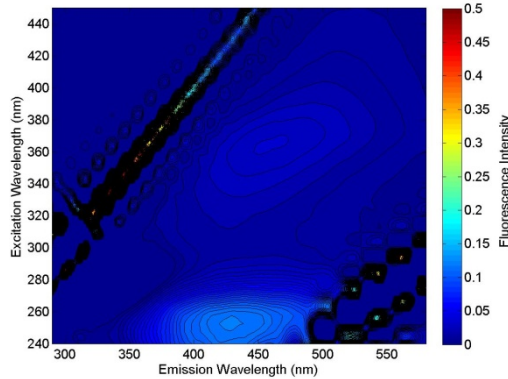


Figure 7.9 EEM of cleaning filtrate sample.

The EEM of a cleaning sample indicates that humic and fulvic acids are removed during cleaning, suggesting that these are the constituents that are leading to fouling.

Table 7.2 summarizes the time and chemical volume requirements for cleaning the membranes.

Table 7.2 Summary of cleaning time and chemical consumption for each membrane

	Total Cleaning Time (min)	Citric Acid Consumption (L/m²)	Caustic Soda Consumption (L/m²)
alumina	18 ± 3	2.2 ± 0.3	5 ± 1
PES	15 ± 5	1.3 ± 0.6	1.6 ± 0.4

7.3 Integration of Cleaning Results into Cost Model

The cleaning results were incorporated in the cost model in the following two ways: to estimate the cost per chemical cleaning event based on the time and chemical requirements for cleaning and to estimate the impact of long-term irreversible fouling on the total water production cost.

7.3.1 Chemical Cleaning Cost

To estimate the cost of chemical cleaning, the following parameters are required:

- Cleaning time – to determine off-line time and additional water production capacity to account for off-line time.
- Chemical usage – to estimate cost of chemicals consumed during cleaning.
- Cleaning efficiency – to determine the amount of pressure recovery following cleaning and account for long-term fouling.

The results from the cleaning studies were used to determine the volume of chemicals consumed per square meter (table 7.2) and, therefore, can be scaled up based on the membrane area of a full-scale plant.

7.3.2 Long-Term Irreversible Fouling

Multiple fouling and cleaning cycles were conducted during the laboratory assessment; however, these tests were not sufficient to determine whether long-term irreversible fouling was occurring and to quantify the degree of long-term fouling.

7.4 Summary

Cleaning of the two membranes was conducted after the membranes had been fouled under similar hydrodynamic conditions and experienced a comparable decrease in PWP, indicative of similar level or degree of fouling. Since the membranes were fouled in a similar manner, differences in cleaning (efficiency, time, and chemical consumption) can be attributed to differences in material properties and module geometry.

After an initial reduction in pure water permeance (after the first fouling and cleaning cycle), the PES membrane experienced no irreversible fouling. The alumina membrane was previously used, so it was not possible to determine whether this initial loss of permeance occurred for the ceramic membrane. The time to clean the alumina membrane was 20% longer than the PES membrane, and the alumina consumed significantly more caustic cleaning solution, 5 L compared to 1.6 L, than the PES membrane. The volume-to-area ratio (V/A) is one factor that influences the volume of chemicals required for cleaning. A higher V/A ratio means that there is more holdup volume in the system relative to the membrane area, resulting in more chemical lost during flushing of the module between cleaning steps. The V/A is 10% higher for the ceramic membrane, which alone does not account for the difference in cleaning time or chemical consumption.

The conventional cleaning protocol, consisting of recirculating cleaning solutions, was not as effective as the modified cleaning protocol; the time required to clean was substantially longer, the pure water permeance following cleaning was not as high, and the membrane rejection was reduced during the filtration cycle following conventional cleaning.

The modified cleaning protocol was effective at cleaning the membranes completely in a shorter period of time with less chemical consumption. Another benefit of the modified cleaning protocol is that it allows for a visual indication of the progress of cleaning by observing the color of the filtrate during cleaning and backwash. This method could be used at full-scale with a visual light monitoring system to reduce cleaning time and cleaning chemical consumption.

The results from the chemical cleaning experiments provided the data necessary to estimate cleaning costs for the two membranes. The cleaning times and chemical consumption were estimated for the two membranes. A method was developed for estimating the effects of long-term fouling on total water production cost. The cost model will be modified to incorporate differences in the cleaning requirements and long-term, irreversible fouling rates for the two membranes.

8. Cost Model Simulation Results

This chapter presents results from simulations using the cost model to determine whether differences in membrane performance and cleaning efficiency for ceramic and polymeric membranes are significant in terms of the total water production cost.

8.1 Cost Comparison for Operation Under Similar Hydrodynamic Conditions

The experimental results of fouling propensity were used to evaluate the cost of the two types of membranes under different hydrodynamic conditions. Three different scenarios were evaluated, representing low, medium, and high fouling rates. Table 8.1 summarizes the fouling rates for the two membranes used in the cost scenarios.

Table 8.1 Summary of fouling rates for the alumina and PES membranes

Pe	Fouling Rate (kPa m ² L ⁻¹)	
	Alumina	PES
5.5	0	0
9.1	0.18	0.18
11.4	0.28	0.68

The values in table 8.1 were chosen to represent the following three cases:

1. Both membranes experience no fouling.
2. Both membranes experience the same rate of fouling.
3. The alumina membrane exhibits less fouling than the PES membrane.

The fouling rates for each membrane at the different hydrodynamic conditions were used to calculate the average operating pressure and the frequency of backwashing events.

The first scenario for the economic comparison was conducted using the experimental data at $Pe = 5.5$ for a water with similar membrane performance to the bentonite feed. No fouling was observed during the operation at $Pe = 5.5$ for either the alumina or the PES membrane. While, in theory, no cleaning or backwashing would be required if no fouling occurs, provisions were made for a

maintenance backwash every 60 seconds and a chemical cleaning twice per year. This assumption affects both membranes similarly.

The TPC—the sum of the amortized capital cost and the annual operating and maintenance cost—is shown in figure 8.1 for a range of fluxes with $Pe = 5.5$. Results are shown for two different module geometries of both the alumina and PES membrane. Both membranes exhibit the same characteristic of having a higher cost at higher values of flux; this is consistent with the findings of Owen et al. (Owen, Bandi et al. 1995).

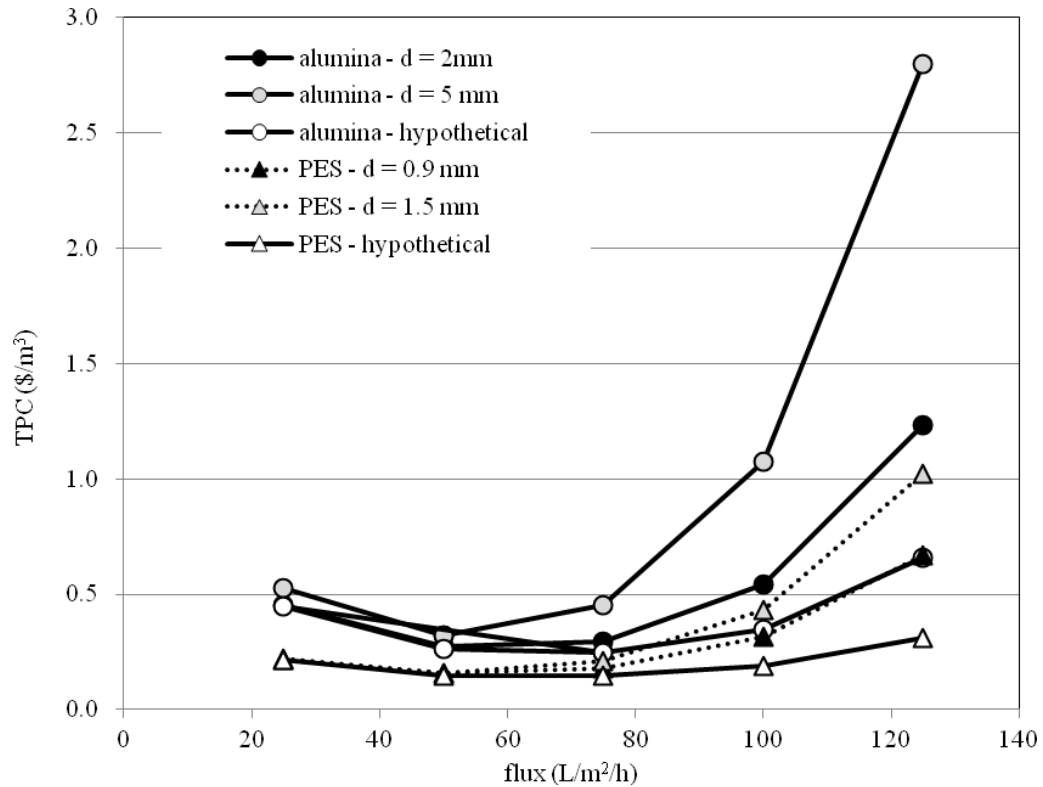


Figure 8.1 Economic comparison at $Pe = 5.5$.

The minimum TPC for the commercially available alumina membrane, $0.268 \text{ } \$/\text{m}^3$, is substantially higher than the minimum TPC, $0.156 \text{ } \$/\text{m}^3$, for the PES membrane. The value of flux that produced the local minimum cost was $50 \text{ L}/\text{m}^2/\text{h}$ for both membranes. For both the alumina and PES materials, the membrane modules with smaller diameter channels resulted in lower TPC. The hypothetical modules, defined such that the geometry of the modules was similar for both types of membranes with a length equal to 0.86 m and a channel diameter of 0.9 mm , resulted in lower costs than the commercially available modules. The minimum TPC values calculated for the alumina and PES hypothetical modules are 0.245 and $0.145 \text{ } \$/\text{m}^3$, respectively, and occur at a flux of $75 \text{ L}/\text{m}^2/\text{h}$. Table 8.2 summarizes the results of the cost modeling for $Pe = 5.5$. Tables of the

entire cost model (including parameters, inputs, and outputs) for the scenarios in table 8.2 are provided in appendix C.

Table 8.2 Cost model results for $Pe = 5.5$

	Alumina			PES		
	2 mm	5 mm	0.9 mm (hyp)	0.9 mm	1.5 mm	0.9 mm (hyp)
TPC ($\$/m^3$)	0.268	0.320	0.245	0.156	0.160	0.145
Capital ($\$/m^3$)	0.138	0.170	0.113	0.058	0.059	0.055
O&M ($\$/m^3$)	0.130	0.150	0.132	.098	0.101	0.090

The characteristic shape of the cost curves illustrates the tradeoff between the increased membrane area required to meet the plant design capacity at low flux values and the increased pumping costs due to the high cross-flow velocity required to maintain the same value of Pe at high flux values. This tradeoff is more apparent (by the greater concavity in the cost curve) for the alumina membrane because the cost is 10 times higher for the alumina material than the PES material and because the two-fold higher membrane roughness increases the pressure drop at high cross-flow velocities. The right side of the cost curve, corresponding to high flux values, is shallower for both of the hypothetical membranes geometries because the pumping requirements are lower for a smaller diameter channel.

The same cost comparison was conducted for operation of the system at $Pe = 9.1$. Under these conditions, fouling occurs, making backwash or cleaning necessary for long-term, sustainable operation. The slope of the pressure increase during the laboratory assessment for filtration at $Pe = 9.1$ was used for each membrane to estimate the frequency of backwash. The fouling rates were equal for the two membranes at this value of Pe . The fouling rate is 0.18 kPa/min. The fouling rate is used to determine the backwash frequency. Backwash is assumed to completely regenerate the membrane. The limit of pressure increase between backwashes for the PES membrane was set to 138 kPa, the maximum transmembrane pressure specified by the PES membrane manufacturer. The effect of choosing different values of the TMP increase that triggers backwash was investigated for the alumina membrane; see figure 8.2.

Figure 8.2 shows that the optimal pressure increase between backwashes is ~ 32 kPa. When backwashes are more frequent, or occur at a lower pressure increase, the membrane area required for the plant increases because of the water consumed during backwash and the downtime required to conduct backwashes. When backwashes are conducted after larger pressure increases, the average pressure is higher, requiring more energy for pumping. A pressure limit between backwashes of 32 kPa will be used for the alumina membrane.

The costs for the commercially available and hypothetical modules for the alumina and PES membranes at $Pe = 9.1$ are shown in figure 8.3.

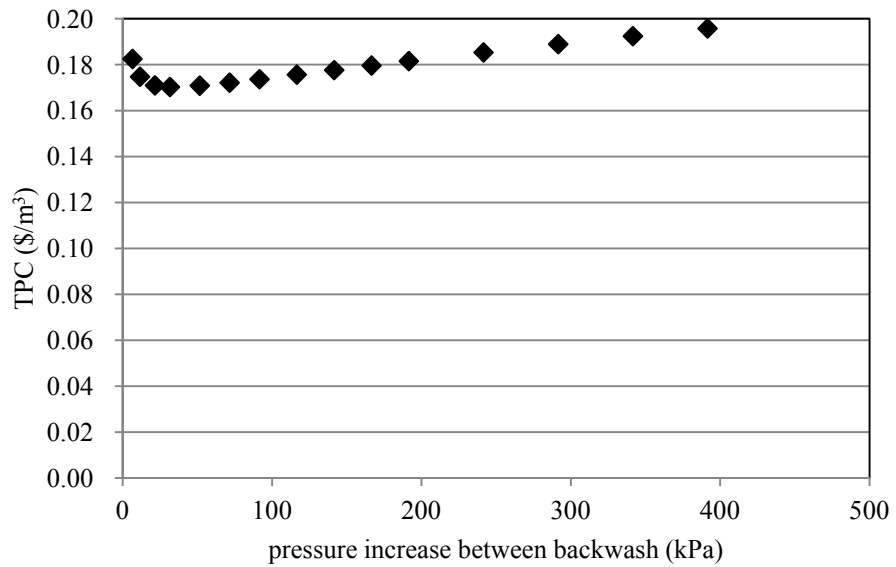


Figure 8.2 TPC as a function of pressure increase between backwashes for the alumina membrane at a flux of 125 at a $Pe = 9.1$.

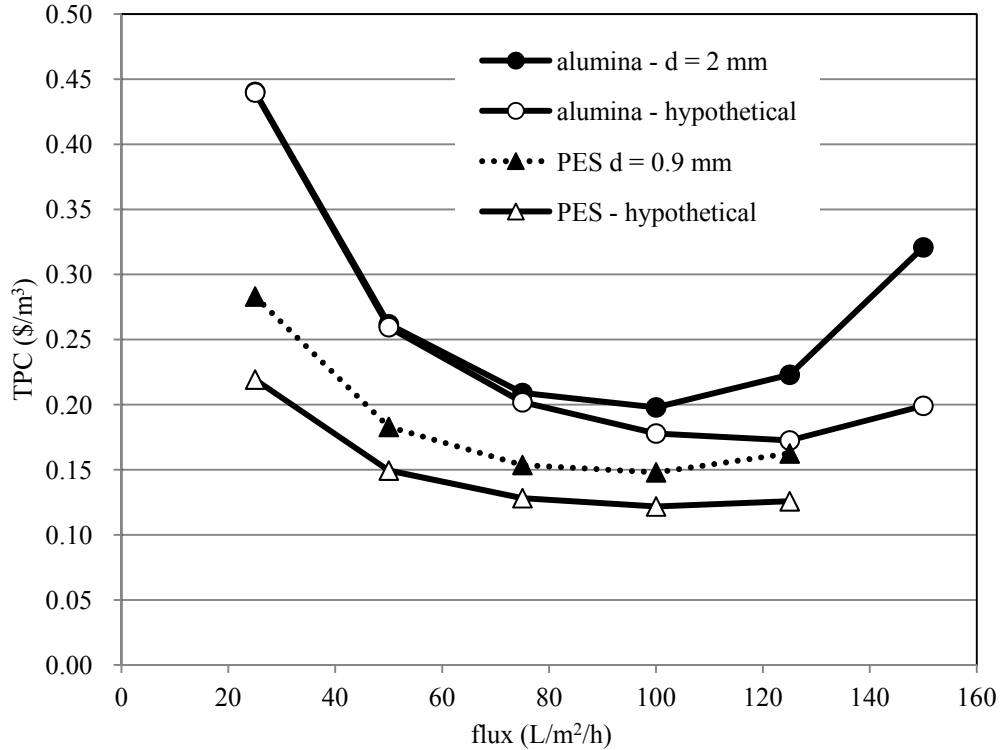


Figure 8.3 Economic comparison at Pe = 9.1.

At Pe = 9.1, the TPC for both membranes (commercially available modules) was lower than for Pe = 5.5, 0.198 \$/m³ and 0.148 \$/m³ for the alumina and PES membranes, respectively; and both had the most economically favorable flux at 100 L/m²/h. The most economically favorable flux for the hypothetical alumina membrane is 125 L/m²/h, resulting in a cost of 0.173 \$/m³. The most economically favorable flux for the hypothetical PES membrane is 100 L m⁻² h⁻¹ with a TPC of 0.122 \$/m³. Table 8.3 summarizes the cost results for Pe = 9.1.

Table 8.3 Cost model results for Pe = 9.1

	Alumina		PES	
	2 mm	0.9 mm (hyp)	0.9 mm	0.9 mm (hyp)
TPC (\$/m ³)	0.198	0.173	0.148	0.122
Capital (\$/m ³)	0.091	0.080	0.051	0.047
O&M (\$/m ³)	0.107	0.092	.097	0.074

The TPC is lower at Pe = 9.1 than for Pe = 5.5 because the higher Pe requires less cross-flow velocity, which translates into lower pumping costs. The fouling rate at Pe = 9.1 is so high that the increase in the average operating pressure offsets the pumping cost savings of the reduced cross-flow velocity.

To fully use the advantages of the alumina membrane's mechanical strength and the fact that the alumina membrane exhibited less fouling (with bentonite) at higher values of Pe , the alumina membrane system was evaluated at $Pe = 11.4$. The same economic comparison is made for the two membranes at $Pe = 11.4$ in figure 8.4. The fouling rate for the PES and alumina membranes at $Pe = 11.4$ are 0.28 kPa/min and 0.68 kPa/min, respectively. The fouling rate for the PES membranes is 2.5 times higher than the alumina membrane's fouling rate; therefore, for this scenario, the chemical cleaning frequency is assumed to be 2.5 times higher.

At $Pe = 11.4$, the minimum TPC, for a commercially available alumina membrane, is 0.188 $\$/m^3$ and is lower than for $Pe = 9.1$; however, the TPC for the commercially available PES membrane, 0.152 $\$/m^3$, is higher than for $Pe = 9.1$. This is due to the 2.5-times higher fouling rate for the PES membrane compared to the alumina membrane at $Pe = 11.4$, triggering more frequent backwash events. The minimum TPC for the hypothetical modules are 0.151 $\$/m^3$ and 0.137 $\$/m^3$ for the alumina and PES membranes, respectively. Table 8.4 summarizes the results for the cost model simulations at $Pe = 11.4$.

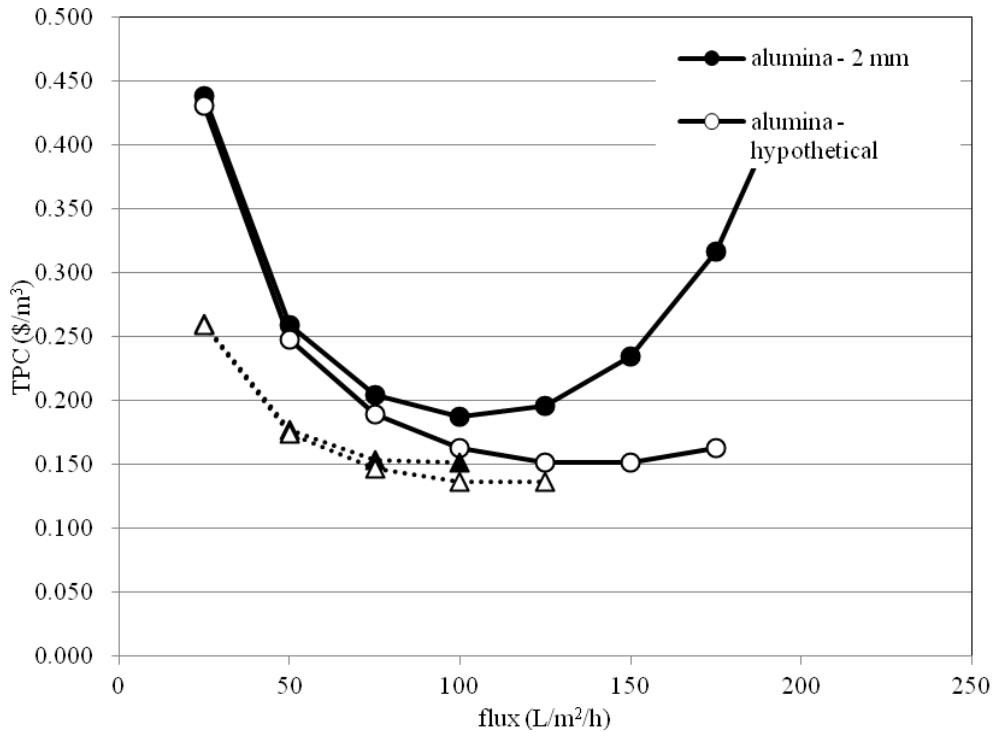


Figure 8.4 Economic comparison for bentonite suspension at Pe = 11.4.

Table 8.4 Cost model results for Pe = 11.4

	Alumina		PES	
	2 mm	0.9 mm (hyp)	0.9 mm	0.9 mm (hyp)
TPC (\$/m³)	0.188	0.151	0.152	0.137
Capital (\$/m³)	0.089	0.068	0.057	0.051
O&M (\$/m³)	0.099	0.084	0.095	0.086

8.2 Identification of Key Economic Leverage Points

To identify the reasons for the cost differences between the alumina and PES membrane systems, the contribution of each cost component is shown for the capital cost components (membranes, vessels, pipes and valves, instrumentation and controls, tanks and frames, miscellaneous items, feed pump, and recirculation pump) and the annual O&M costs (replacement membranes, power, maintenance, and cleaning); see figures 8.5 and 8.6, respectively. The values in the figures represent the data for the lowest-cost scenarios for each type of membrane; therefore, results are shown for the PES membrane at Pe = 9.1 and a flux of 100 L/m²/h, and the alumina membrane data are for Pe = 11.4 and a flux of 125 L/m²/h for the bentonite feed suspension.

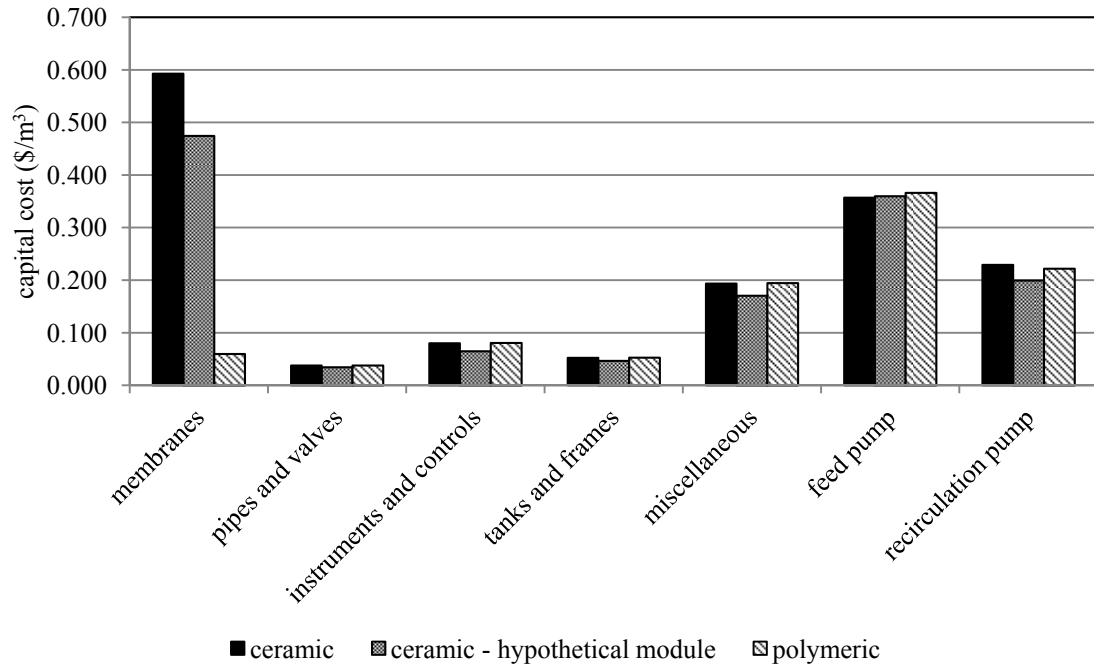


Figure 8.5 Comparison of capital cost components (not amortized).

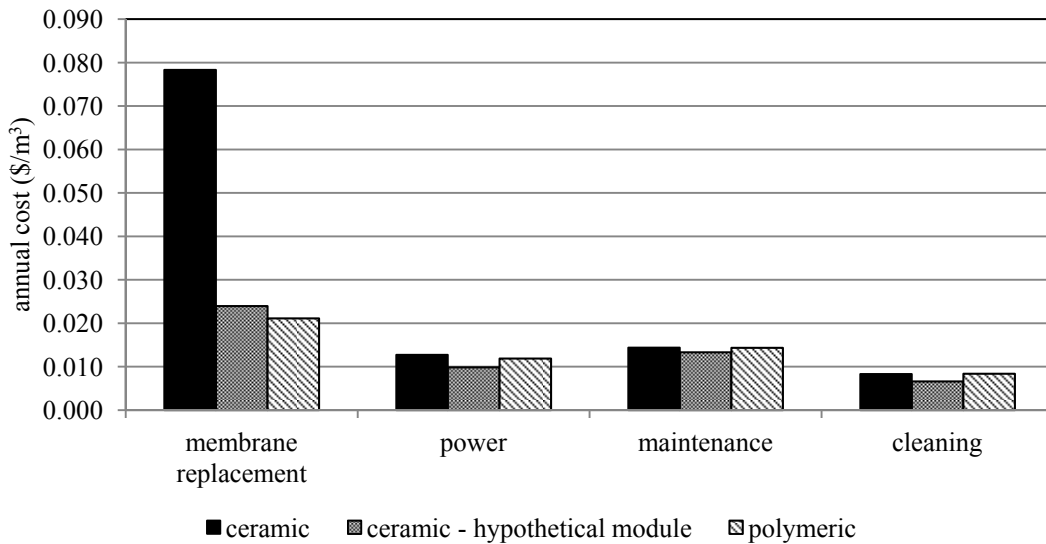


Figure 8.6 Comparison of O&M cost components.

The cost for pipes and valves, instruments and controls, tanks and frames, and miscellaneous are all based on the membrane area; therefore, large differences are not expected for these cost components between the two membrane types. The capital expense for the purchase of the initial set of membranes is roughly

10 times higher for the alumina membrane system compared to the PES system, since the material cost is 10 times higher. The cost of the recirculation pump is slightly higher for the alumina membrane. The recirculation pump flow rate is roughly five times higher for the ceramic membrane ($d = 2 \text{ mm}$) due to the larger channel size; however, the pressure drop along the membrane channel is 3.5 times lower for the alumina membrane (even though the friction factor is larger) due to the larger channel diameter.

Even though the membrane material cost is 10 times higher for the alumina membrane than the PES membrane, the longer operational life for the alumina membrane results in an annual membrane replacement cost that is only 39% higher than the PES membrane replacement cost.

The power requirement for the alumina membrane is slightly higher than the PES membrane due to electricity costs associated with pumping the five times higher recirculation volume. Because maintenance costs are commonly calculated as a percentage of the total capital cost, the ceramic membrane maintenance cost is higher than the PES membrane maintenance cost.

Figures 8.7 and 8.8 show the breakdown of capital and O&M costs for the lowest cost alumina membrane condition ($Pe = 11.4$). The cost of the initial set of membranes accounts for 38% of the total capital expenditures for a full-scale plant. The feed pump and recirculation pump represent another 38% of the capital costs, and miscellaneous represents 13%. Replacement membranes comprise 31% of the annual O&M costs, and labor represents 30%. Maintenance and energy costs represent 18% and 13%, respectively. Cleaning accounts for 8% of the O&M costs. Therefore, reducing the cost of the following cost components will make the greatest impact on the economic value proposition for alumina membranes: membrane material cost and labor, maintenance, and pumping requirements (capital cost of pumps and energy cost).

To identify the conditions under which alumina membrane systems are cost competitive with PES membrane systems, further cost calculations were conducted to identify the material costs (membrane and vessel) that would make the cost of the two systems equal, using the hypothetical alumina module configuration. Using the hypothetical module geometry, the minimum TPC is $0.151 \text{ \$/m}^3$ compared to $0.188 \text{ \$/m}^3$, a 20% cost savings. Therefore, subsequent cost comparison will use the hypothetical alumina membrane geometry.

Currently, ceramic membrane systems use stainless steel housings; however, MF and UF systems do not require high pressures that normally preclude using PVC housings. A PVC housing would cost approximately \$50 per vessel rather than \$2,000 for stainless steel vessels. The TPC for the alumina membrane system with PVC vessels is $0.140 \text{ \$/m}^3$, which is 7% less than the cost with stainless steel housings ($0.151 \text{ \$/m}^3$) but still higher than the cost of the PES membrane system. The following cost scenarios will use the cost of PVC housings for the alumina membrane.

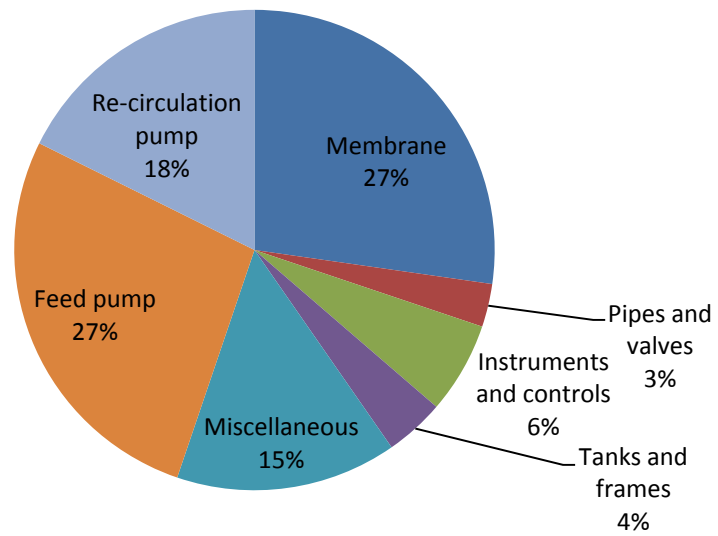


Figure 8.7 Capital cost components for alumina membrane at $Pe = 11.4$.

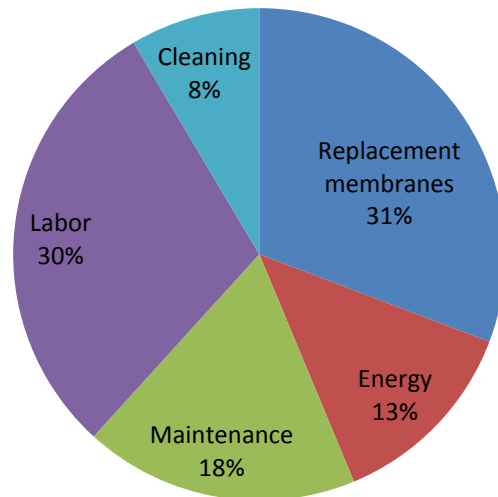


Figure 8.8 Operating and maintenance costs for alumina membrane at $Pe = 11.4$.

Integrity issues are commonly encountered with polymeric membranes. An average number of 24 fiber breakages per year is estimated per MF/UF membrane water treatment plant. Plugging broken fibers requires significant membrane operator time, but no quantitative estimates are available for the average amount of time per year spent plugging broken fibers. Because fiber breakages are not a concern with ceramic membranes, cost reductions could be realized in the amount of labor required to operate the plant. The effect of reducing the number of full time employees (FTE) required to operate the plant on TPC is shown in figure 8.9. Reducing the personnel requirement by 0.5 FTE to 2.0 FTE is sufficient to make the cost competitive with the PES membrane at 0.122 $\$/\text{m}^3$.

The majority of the capital cost differences are due to the higher cost of the alumina membrane material (membrane) and that the alumina membranes require the use of separate, stainless steel vessels. Differences in the O&M costs for the two systems are primarily due to the higher membrane replacement cost of the alumina membrane and higher maintenance cost (calculated as 1.5% of the membrane cost).

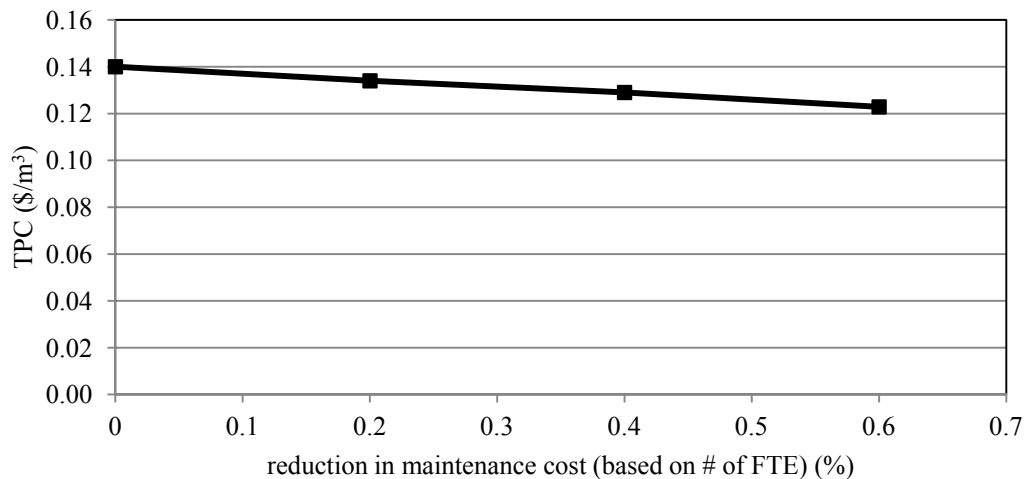


Figure 8.9 Effect of reducing the number of plant operators on TPC for hypothetical alumina membrane at $Pe = 11.4$.

Even though the lifespan of the alumina membrane is four times longer than the PES, this isn't enough to offset the higher material cost. Other researchers have reported that membrane material costs represent approximately 27% of the total plant cost (Sethi 1997), therefore, it is not surprising that the effect of the higher material cost comprises a significant portion of the difference in cost for the two systems. As ceramic membranes become more widely used, their cost likely will be reduced due to economies of scale in production. The effect of reducing the ceramic membrane material cost also is shown in figure 8.10.

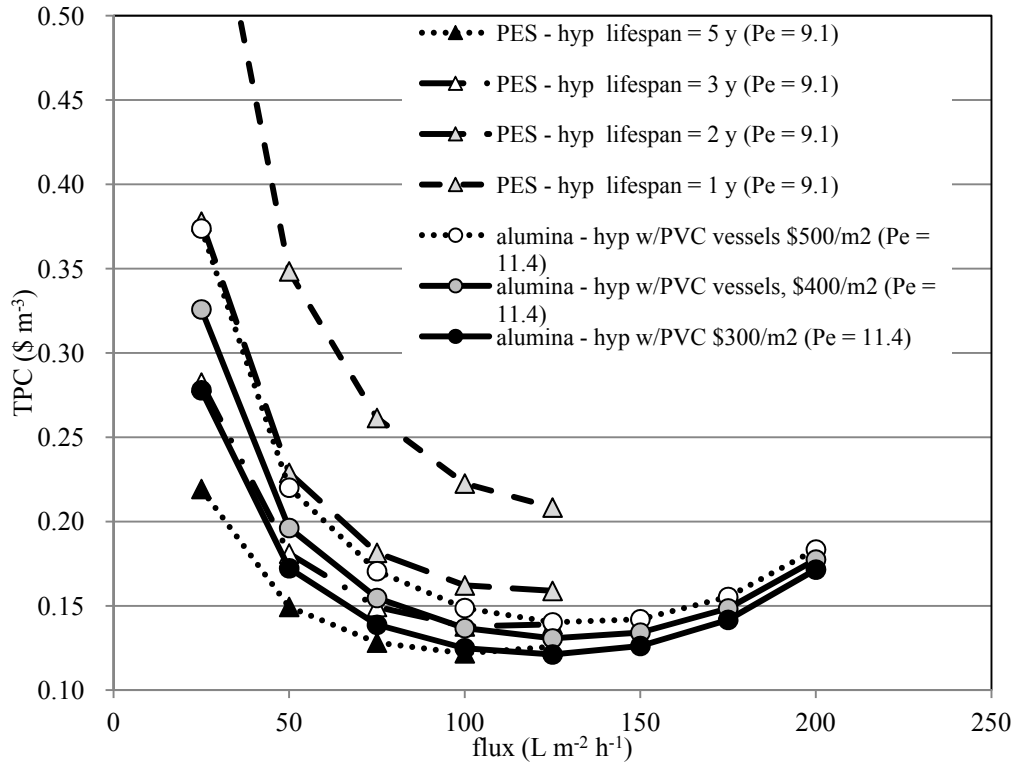


Figure 8.10 Effect of reducing polymeric membrane lifespan and reducing ceramic membrane material cost.

The lifespan of the polymeric membrane was assumed to be 5 years; however, in many applications, this lifespan can be greatly reduced due to irreversible fouling or integrity issues. The effect on TPC of varying the lifespan of the polymeric membrane and the ceramic membrane material cost is illustrated in figure 8.10.

The alumina membrane cost is competitive with the PES membrane cost when either the lifespan of the PES membrane is reduced to 3 years or the cost of ceramic membrane material decreases to 300 \$/m². See table 8.5 for a summary of the cost results for the different scenarios that were considered.

8.3 Summary

The results of the cost modeling effort show that the cost of full-scale implementation of ceramic membranes is 12% greater than the cost for a polymeric membrane system. For water types in which ceramic membranes experience less fouling than polymeric membranes, operation at more aggressive filtration conditions, i.e., higher Pe, result in more competitive costs. Aggressive filtration conditions, reduced labor requirements, PVC rather than stainless steel vessels, and a reduced membrane material cost all lead to ceramic membranes being more cost competitive with polymeric membranes.

Table 8.5 Summary of results for the cost comparison

	PES hyp.	PES hyp.	Alumina with PVC vessels	Alumina with PVC vessels	Alumina with PVC vessels
Material cost (\$/m ²)	50	50	500	300	500
Channel diameter (mm)	0.9	0.9	0.9 (hyp)	0.9 (hyp)	0.9 (hyp)
Pe	9.1	9.1	11.4	11.4	11.4
Membrane lifespan (y)	5	3	20	20	20
Flux (L/m ² /h)	100	100	125	125	125
FTE	2.5	2.5	2.5	2.5	1.5
Total production cost (\$/m ³)	0.122	0.138	0.140	0.122	0.122
Amortized capital cost per volume produced (\$/m ³)	0.047	0.047	0.059	0.050	0.059
O&M cost (\$/m ³)	0.074	0.090	0.081	0.072	0.063

9. Conclusions

The increasing demand for expanding water supplies will drive the need for more technologically efficient, cost-effective water treatment technologies. Low-pressure membrane technologies will continue to be a widely used technology to remove particulates, bacteria and viruses, and other contaminants from impaired water sources as a stand alone treatment process and as pretreatment technology for desalination. Because water is treated as a commodity, the cost of water remains extremely low despite the advanced technology that is used to treat it. Reductions in cost and improvements in performance of low-pressure membrane systems are needed to employ these technologies in competitive water markets. This research has shown that a techno-economic model can be used to investigate the effect of different membrane materials, operating conditions, fouling tendency, and application-specific parameters on total water production cost.

A techno-economic model was developed using previously published correlations and engineering design equations to describe the total water production cost in terms of operating conditions and membrane performance for a full-scale UF membrane treatment process. The model allows the input of experimental data to describe the fouling rate, which is used to compute the average operating pressure, the pumping power requirement, and the cleaning efficiency, which is used to calculate chemical demand.

A scoping study was conducted to identify relevant ranges of operating conditions for the alumina membrane. This study investigated the effects of varying ceramic membrane operating conditions on membrane flux decline and total water production cost. The results of this portion of the study indicated that operating the alumina membrane at conditions, which minimized fouling, did not produce the lowest water production cost. This finding represents a contradiction to the conventional wisdom in the membrane community, that minimizing membrane fouling minimizes total water production cost. The rationale for this observation is that the ceramic membrane material cost is very high compared to polymeric membrane material costs, and this cost contribution outweighs maintenance expenses. This work was also significant because it showed that the techno-economic model was an effective tool for evaluating the effects of operating conditions and membrane performance on total water production costs.

A performance comparison was made for an alumina and PES membrane using two types of feed waters: a bentonite suspension and a complex mixture consisting of natural organic matter, algae, and bentonite. This performance comparison illustrated that the hydrodynamic conditions in which the membranes are operated, characterized by the apparent Peclet number, are important when comparing performance. These results indicated that, at low values of Pe , both membranes experience insignificant pressure increases due to fouling. At moderate levels of Pe , the PES membrane exhibited a lower rate of fouling than

the alumina membrane. At high values of Pe for the bentonite suspension, the alumina membrane experienced significantly less flux decline than the PES membrane; whereas for the complex mixture, the PES membrane exhibited lower fouling. These findings illustrate the importance of membrane-solute interactions in identifying which membrane is best suited for a given application and help rationalize the somewhat variable findings from past studies comparing ceramic and polymeric membrane performance.

Previous cost modeling efforts did not include the effects of cleaning chemical requirements and cleaning frequency. The cleaning characteristics of the alumina and PES membranes were compared using multiple fouling and cleaning cycles. The PES membrane experienced some irreversible fouling after the first filtration cycle, and no further irreversible fouling was observed for subsequent filtration and cleaning cycles. No irreversible fouling was observed for the alumina membrane. The time required to clean the membrane was 20% higher for the alumina membrane, and the volume of chemicals consumed during cleaning was nearly three times higher for the alumina membrane than that for the PES membrane.

A modification was made to the conventional cleaning strategy of recirculating cleaning chemicals for a prescribed amount of time. The modified cleaning protocol consisted of monitoring the permeance of the membrane to the cleaning solution to determine when the maximum cleaning efficiency has been reached. The modified approach reduced the cleaning time from 1–2 hours to fewer than 20 minutes for both membrane materials. This new cleaning protocol is efficient because it minimizes the chance for re-deposition of foulant onto the membrane and allows for visual inspection of the progress of cleaning. The conventional cleaning method also was not able to recover all of the permeance lost during the first filtration cycle; however, subsequent cleanings with the modified cleaning strategy were able to recover what was initially believed to be irreversible fouling.

Using the apparent Peclet number to describe the fouling rate in terms of hydrodynamic conditions allows the techno-economic model to be used to evaluate the tradeoffs between different combinations of operating conditions that result in the same degree of membrane fouling and, therefore, the subsequent cleaning frequency and cost. This approach identified an optimal flux that balanced the tradeoff between membrane area (determined by flux) and pumping requirements (determined by required cross-flow velocity for a given module design) at a given value apparent Pe . The optimal flux increased as Pe increased. The optimal apparent Pe for the alumina membrane is higher than for the PES membrane due to the reduced fouling tendency of the alumina membrane at higher values of Pe .

The cost model was used to identify cost scenarios in which ceramic membranes result in a lower cost than polymeric membranes. Currently, the material cost of polymeric membranes is very low—approximately 10 times lower than ceramic membrane materials. The longer operational life of the ceramic membrane makes

up for much of the increased material cost; however, the total water production cost for a ceramic membrane is still over 30% higher. Another major capital cost difference between ceramic and polymeric membranes is the vessels required to house ceramic membranes. Polymeric membranes are supplied with a housing and do not require the purchase of a vessel. Currently, ceramic membrane vessels are made of stainless steel. For most MF and UF membrane applications, plastic vessels, such as PVC, would be appropriate and would significantly reduce the TPC for ceramic membranes. Also, as ceramic membranes become more widely used for water treatment applications, the cost may be expected to decrease. The use of PVC vessels, along with a reduction in material cost from 500 $\$/m^2$ to 340 $\$/m^2$, would make ceramic membranes cost competitive with polymeric membranes.

Loss of integrity and loss of productivity are the most common reasons for replacement of polymeric membranes. Using the bentonite feed suspension as an example, reducing the lifespan of the polymeric membrane to 3 years instead of 5 years, makes the ceramic membrane cost competitive.

Currently, ceramic membranes are not cost competitive with polymeric membranes for commodity water treatment applications; however, use in specialized applications may provide niche applications in which ceramic membranes are cost competitive. Based on the results of this work, the following application specific attributes will favor the use of ceramic membranes over polymeric membranes:

- The rate of fouling is significantly less for the ceramic membrane compared to the polymeric membrane.
- The lifespan of the polymeric membrane is reduced due to aggressive cleaning or membrane degradation.
- The maintenance cost is high due to lack of skilled personnel onsite.

The techno-economic model is a novel tool that can be used to identify the economic benefit of one material compared to another when the optimal operating conditions and performance characteristics for the two materials are different. The capability of the model to identify the technical and economic factors that impact the overall system cost for each material was demonstrated. Conditions that lead to the selection of one membrane type over another were identified.

While the quantitative results presented in this report are specific to the water types and membranes tested; the main contributions of this work are the methods developed, membrane testing protocol, and data-driven cost model. The testing protocol and data-driven model can be used to evaluate the performance and cost of other types of membranes for feed water types other than those tested in this work. When using these methods to evaluate other membranes and feed water types, the data required are the time rate of change of transmembrane pressure at corresponding values of apparent P_e .

10. Recommendations

Future research relating to the comparison of ceramic and polymeric membranes should focus:

- Material characterization such that performance differences can be definitively attributed to **specific** material properties. This **also** would require the following:
 - Comparison of ceramic and polymeric membranes using different feed water compositions.
 - More direct observation and/or postmortem analysis of fouling to quantify the mechanisms.

10.1 Material Characterization

The membranes used in this study were tubular or hollow fiber modules. While these modules were suitable for making measurements on fouling tendency and scaling up the laboratory results to full-sized modules, they were not conducive to conducting characterization of the membrane surface. More studies are necessary to characterize the membrane materials in terms of hydrophobicity, zeta potential, pore size distribution, and surface morphology. The feed water also should be adequately characterized. Conducting performance comparison using ceramic and polymeric membranes that are well characterized will make it more likely that performance differences can be attributed to specific material properties.

Previous literature has indicated that hydrophobicity and roughness together influence fouling. An interesting focused study would be to investigate this link in terms of fouling potential for different feed waters. Additional work also may focus on membrane surface modification to improve performance for a specific water treatment application.

10.2 Fouling Studies with Other Water Types

Ceramic membranes have been suggested for other water types, including oil and gas exploration's produced water. Produced water is a broad classification of water types associated with the oil and gas industry. Performance and cost comparisons should be conducted with other water types to identify other applications and economic lever points that are significant for membrane material selection. This work did not address feed water types with the potential to cause biofouling; this would be an interesting water type on which to focus future efforts.

10.3 Modeling Membrane Fouling of Ceramic and Polymeric Membranes

This effort only focused on quantifying differences in membrane fouling for the alumina and PES membranes. Developing a model to describe the degree of fouling in terms of membrane material properties and solute characteristics to predict membrane fouling that can adequately predict fouling for different types of materials would be a valuable screening tool for different water treatment applications.

11. References Cited

- Adham, S., K.-P. Chiu, et al. (2005). *Development of a Microfiltration and Ultrafiltration Knowledge Base*. Denver, American Water Works Association.
- Almecija, M.C., A. Martinez-Ferez, et al. (2009). "Influence of the cleaning temperature on the permeability of ceramic membranes." *Desalination* **245**(1-3): 708-713.
- AWWA (1996). *Water Treatment: Membrane Processes*, McGraw Hill.
- Aydiner, C., I. Demir, et al. (2005). "Modeling of flux decline in crossflow microfiltration using neural networks: the case of phosphate removal." *Journal of Membrane Science* **248**(1-2): 53-62.
- Bacchin, P. and P. Aimar (2005). "Critical fouling conditions induced by colloidal surface interaction: from causes to consequences." *Desalination* **175**(1): 21-27.
- Bacchin, P., P. Aimar, et al. (2006). "Critical and sustainable fluxes: Theory, experiments and applications." *Journal of Membrane Science* **281**(1-2): 42-69.
- Bartlett, M., M. R. Bird, et al. (1995). "An experimental study for the development of a qualitative membrane cleaning model." *Journal of Membrane Science* **105**(1-2): 147-157.
- Belfort, G., R. H. Davis, et al. (1994). "The behavior of suspensions and macromolecular solutions in crossflow microfiltration." *Journal of Membrane Science* **96**(1-2): 1-58.
- Bird, M. R. and M. Bartlett (2002). "Measuring and modelling flux recovery during the chemical cleaning of MF membranes for the processing of whey protein concentrate." *Journal of Food Engineering* **53**(2): 143-152.
- Blanpain-Avet, P., J. F. Migdal, et al. (2004). "The Effect of Multiple Fouling and Cleaning Cycles on a Tubular Ceramic Microfiltration Membrane Fouled with a Whey Protein Concentrate: Membrane Performance and Cleaning Efficiency." *Food and Bioproducts Processing* **82**(3): 231-243.
- Bodzek, M. and K. Konieczny (1998). "Comparison of ceramic and capillary membranes in the treatment of natural water by means of ultrafiltration and microfiltration." *Desalination* **119**(1-3): 191-197.

- Bodzek, M. and K. Konieczny (1998). "Comparison of various membrane types and module configurations in the treatment of natural water by means of low-pressure membrane methods." *Separation and Purification Technology* **14**(1–3): 69–78.
- Booker, R. (2010). Ceramic membranes: A pilot evaluation of an emerging reuse technology. *Water Reuse Symposium*. Washington, D.C.
- Chapman, M. (2010). Synthetic feed water recipe.
- Chen, J.P., S.L. Kim, et al. (2003). "Optimization of membrane physical and chemical cleaning by a statistically designed approach." *Journal of Membrane Science* **219**(1–2): 27–45.
- Cheryan, M. (1998). *Ultrafiltration and Microfiltration Handbook, 2nd Edition*. Boca Raton, CRC Press.
- Choo, K.-H. and C.-H. Lee (2000). "Understanding Membrane Fouling in Terms of Surface Free Energy Changes." *Journal of Colloid and Interface Science* **226**(2): 367–370.
- Cornelissen, E.R., B. Hofs, et al. (2009). Direct and hybrid ceramic membrane filtration in water treatment. *TECHNEAU: Safe Drinking Water from Source to Tap, State of the Art & Perspectives*. T.v.d. Hoven and C. Kazner. London, IWA Publishing.
- Cremades, L.V., E. Rodriguez-Grau, et al. (2007). "Comparative study of the performance of three cross-flow ceramic membranes for water treatment." *Water Sa* **33**(2): 253–259.
- Crozes, G.F., J.G. Jacangelo, et al. (2001). Low pressure membrane filtration for pathogen removal: application, implementation, and regulatory issues. O.o. Water. Cincinnati, United States Environmental Protection Agency.
- Cussler, E.L. (2009). *Diffusion: Mass Transfer in Fluid Systems*. Cambridge, Cambridge University Press.
- Du, J.R., S. Peldszus, et al. (2009). "Modification of poly(vinylidene fluoride) ultrafiltration membranes with poly(vinyl alcohol) for fouling control in drinking water treatment." *Water Research* **43**(18): 4559–4568.
- EIA. (2012). "United States Electricity Profile 2010." Retrieved February 6, 2012, from <http://www.eia.gov/electricity/state/unitedstates/>.
- Elimelech, M., Z. Xiaohua, et al. (1997). "Role of membrane surface morphology in colloidal fouling of cellulose acetate and composite aromatic polyamide reverse osmosis membranes." *Journal of Membrane Science* **127**(1): 101–109.

- Gan, Q., J.A. Howell, et al. (1999). "Synergetic cleaning procedure for a ceramic membrane fouled by beer microfiltration." *Journal of Membrane Science* **155**(2): 277–289.
- Gaulinger, S.I. (2007). Coagulation Pre-Treatment for Microfiltration with Ceramic Membranes. *TECHNEAU*. Nieuwegein, KWR Watercycle Research Institut: 1–71.
- Gekas, V., K.M. Persson, et al. (1992). "Contact angles of ultrafiltration membranes and their possible correlation to membrane performance." *Journal of Membrane Science* **72**(3): 293–302.
- Ghajar, A.J., L.M. Tam, et al. (2010). The Effect of Inner Surface Roughness on Friction Factor in Horizontal Micro-tubes. *2nd International Conference on Mechanical and Electronics Engineering*, IEEE. **1**: 59–63.
- Gilbert, E. (2010). *Kruger Ceramic Membrane*. Ceramic Membranes for Water Treatment - Technical Status and Economic Update, Webinar, Infocast.
- Gourley, L., M. Britten, et al. (1994). "Characterization of adsorptive fouling on ultrafiltration membranes by peptides mixtures using contact angle measurements." *Journal of Membrane Science* **97**: 283–289.
- Guerra, K., J. Pellegrino, et al. (2012). "Impact of operating conditions on permeate flux and process economics for cross flow ceramic membrane ultrafiltration of surface water." *Separation and Purification Technology* **87**(0): 47–53.
- Her, N., G. Amy, et al. (2003). "Characterization of DOM as a function of MW by fluorescence EEM and HPLC-SEC using UVA, DOC, and fluorescence detection." *Water Research* **37**(17): 4295–4303.
- Hilal, N., O.O. Ogunbiyi, et al. (2008). "Neural network modeling for separation of bentonite in tubular ceramic membranes." *Desalination* **228**(1–3): 175–182.
- Hofs, B., J. Ogier, et al. (2011). "Comparison of ceramic and polymeric membrane permeability and fouling using surface water." *Separation and Purification Technology* **79**(3): 365–374.
- Huang, H., T. Young, et al. (2008). "Unified membrane fouling index for low pressure membrane filtration of natural waters: Principles and methodology." *Environmental Science and Technology* **42**(3).
- Huang, H., T. Young, et al. (2009). "Novel approach for the analysis of bench-scale, low pressure membrane fouling in water treatment." *Journal of Membrane Science* **334**(1–2): 1–8.

- Jacangelo, J., R. Trussel, et al. (1997). "Role of membrane technology in drinking water treatment in the United States." *Desalination* **113**(2–3): 119–127.
- Kabsch-Korbutowicz, M. and A. Urbanowska (2010). "Comparison of polymeric and ceramic ultrafiltration membranes for separation of natural organic matter from water." *Environmental Protection Engineering* **36**(1): 125–135.
- Katsoufidou, K., S.G. Yiantsios, et al. (2005). "A study of ultrafiltration membrane fouling by humic acids and flux recovery by backwashing: Experiments and modeling." *Journal of Membrane Science* **266**(1–2): 40–50.
- Katsoufidou, K., S.G. Yiantsios, et al. (2007). "Experimental study of ultrafiltration membrane fouling by sodium alginate and flux recovery by backwashing." *Journal of Membrane Science* **300**(1–2): 137–146.
- Katsoufidou, K., S.G. Yiantsios, et al. (2008). "An experimental study of UF membrane fouling by humic acid and sodium alginate solutions: the effect of backwashing on flux recovery." *Desalination* **220**(1–3): 214–227.
- Katsoufidou, K.S., D.C. Sioutopoulos, et al. "UF membrane fouling by mixtures of humic acids and sodium alginate: Fouling mechanisms and reversibility." *Desalination* **264**(3): 220–227.
- Kim, J., S.H.R. Davies, et al. (2008). "Effect of ozone dosage and hydrodynamic conditions on the permeate flux in a hybrid ozonation-ceramic ultrafiltration system treating natural waters." *Journal of Membrane Science* **311**(1–2): 165–172.
- Kimura, K., T. Maeda, et al. (2008). "Irreversible membrane fouling in microfiltration membranes filtering coagulated surface water." *Journal of Membrane Science* **320**(1–2): 356–362.
- Klomfas, G. and K. Konieczny (2004). "Fouling phenomena in unit and hybrid processes for potable water treatment." *Desalination* **163**(1–3): 311–322.
- Koltuniewicz, A.B., R.W. Field, et al. (1995). "Cross-flow and dead-end microfiltration of oily-water emulsion. Part I: Experimental study and analysis of flux decline." *Journal of Membrane Science* **102**: 193–207.
- Konieczny, K., M. Bodzek, et al. (2006). "A coagulation-MF system for water treatment using ceramic membranes." *Desalination* **198**(1–3): 92–101.
- Koyuncu, I., A. Lüttge, et al. (2008). "Interferometric observations and kinetic modeling of the chemical cleaning of humic materials deposited on membranes." *Journal of Membrane Science* **313**(1–2): 127–134.

- Kumar, S.M., G.M. Madhu, et al. (2007). "Fouling behaviour, regeneration options and on-line control of biomass-based power plant effluents using microporous ceramic membranes." *Separation and Purification Technology* **57**(1): 25–36.
- Lee, B.-B., K.-H. Choo, et al. (2009). "Optimizing the coagulant dose to control membrane fouling in combined coagulation/ultrafiltration systems for textile wastewater reclamation." *Chemical Engineering Journal* **155**(1–2): 101–107.
- Lee, H., G. Amy, et al. (2001). "Cleaning strategies for flux recovery of an ultrafiltration membrane fouled by natural organic matter." *Water Research* **35**(14): 3301–3308.
- Lee, S. and J. Cho (2004). "Comparison of ceramic and polymeric membranes for natural organic matter (NOM) removal." *Desalination* **160**(3): 223–232.
- Lehman, S.G., S. Adham, et al. (2007). *Performance of New Generation Ceramic Membranes Using Coagulation and Ozonation Pretreatment*. American Water Works Association Membrane Technology Conference, Tampa, FL, American Water Works Association.
- Lerch, A., S. Panglisch, et al. (2005). "Direct river water treatment using coagulation/ceramic membrane microfiltration." *Desalination* **179**(1–3): 41–50.
- Lerch, A., S. Panglisch, et al. (2005). "Research experiences in direct potable water treatment using coagulation/ultrafiltration." *Water Science and Technology* **51**(6): 221–229.
- Liu, C., S. Caothien, et al. (2001). Membrane chemical cleaning: From art to science. *2000 AWWA Water Quality Technology Conference*. Denver, CO.
- Loi-Brugger, A., S. Panglisch, et al. (2007). Open Up New Doors in Water Treatment with Ceramic Membranes. *American Water Works Association Membrane Technology Conference*. Tampa, FL, American Water Works Association.
- Lozier, J., Ed. (2005). *Microfiltration and Ultrafiltration Membranes for Drinking Water*. Manual of Water Supply Practices. Denver, American Water Works Association.
- Lozier, J., L. Cappucci, et al. (2008). Natural Organic Matter Fouling of Low-Pressure Membrane Systems. *AWWA Research Foundation*.

- Maximous, N., G. Nakhla, et al. (2009). "Comparative assessment of hydrophobic and hydrophilic membrane fouling in wastewater applications." *Journal of Membrane Science* **339**(1–2): 93–99.
- Mercadé-Prieto, R. and X.D. Chen (2005). "Caustic-induced gelation of whey deposits in the alkali cleaning of membranes." *Journal of Membrane Science* **254**(1–2): 157–167.
- Meyn, T. and T. Leiknes (2010). "Comparison of optional process configurations and operating conditions for ceramic membrane MF coupled with coagulation/flocculation pre-treatment for the removal of NOM in drinking water." *Journal of Water Supply Research and Technology* **59**(2–3): 81–91.
- Montgomery, D.C. (2001). *Design and Analysis of Experiments*. Hoboken, NJ, John Wiley and Sons, Inc.
- Mourouzidis-Mourouzis, S.A. and A.J. Karabelas (2008). "Whey protein fouling of large pore-size ceramic microfiltration membranes at small cross-flow velocity." *Journal of Membrane Science* **323**(1): 17–27.
- Mueller, J., Y. Cen, et al. (1997). "Crossflow microfiltration of oily water." *Journal of Membrane Science* **129**(2): 221–235.
- Mueller, U., R. Schaefer, et al. (2008). Interim report of Removal of particulate matter by ceramic membranes during surface water treatment. *TECHNEAU*, TZW: DVGW - Technologiezentrum Wasser.
- Mulder, M.H.V. (2003). *Basic Principles of Membrane Technology*. Norwell, Kluwer Academic Publishers.
- Muthukumar, S., D.A. Nguyen, et al. (2011). "Performance evaluation of different ultrafiltration membranes for the reclamation and reuse of secondary effluent." *Desalination* **279**(1–3): 383–389.
- Nabe, A., E. Staude, et al. (1997). "Surface modification of polysulfone ultrafiltration membranes and fouling by BSA solutions." *Journal of Membrane Science* **133**(1): 57–72.
- Nandi, B.K., B. Das, et al. (2009). "Microfiltration of mosambi juice using low cost ceramic membrane." *Journal of Food Engineering* **95**(4): 597–605.
- Nandi, B.K., A. Moparthy, et al. (2010). "Treatment of oily wastewater using low cost ceramic membrane: Comparative assessment of pore blocking and artificial neural network models." *Chemical Engineering Research and Design* **88**(7): 881–892.

- Nandi, B.K., R. Uppaluri, et al. (2008). "Preparation and characterization of low cost ceramic membranes for micro-filtration applications." *Applied Clay Science* **42**(1–2): 102–110.
- NRC (2008). *Desalination: A National Perspective*. Washington, D.C.
- Owen, G., M. Bandi, et al. (1995). "Economic assessment of membrane processes for water and waste water treatment." *Journal of Membrane Science* **102**(0): 77–91.
- Perry, R.H. and C.C. Chilton, Eds. (1991). *Chemical Engineers' Handbook*, McGraw-Hill Book Company.
- Pfund, D., D. Rector, et al. (2000). "Pressure Drop Measurements in a Microchannel." *AIChE Journal* **46**(8): 1496–1507.
- Popović, S.S., M.N. Tekić, et al. (2009). "Kinetic models for alkali and detergent cleaning of ceramic tubular membrane fouled with whey proteins." *Journal of Food Engineering* **94**(3–4): 307–315.
- Porcelli, N. and S. udd (2010). "Chemical cleaning of potable water membranes: A review." *Separation and Purification Technology* **71**(2): 137–143.
- Rajca, M., M. Bodzek, et al. (2009). "Application of mathematical models to the calculation of ultrafiltration flux in water treatment." *Desalination* **239**(1–3): 100–110.
- Reed, B., W. Lin, et al. (1997). *Treatment of concentrated oil wastes using the SpinTek rotary ultrafiltration system*. Advances in Filtration and Separation Technology: American Filtration and Separations Society, Minneapolis, MN.
- Sethi, S. (1997). Transient permeate flux analysis, cost estimation, and design optimization in crossflow membrane filtration. PhD Thesis. R. University. Houston.
- Sondhi, R. and R. Bhave (2001). "Role of backpulsing in fouling minimization in crossflow filtration with ceramic membranes." *Journal of Membrane Science* **186**(1): 41–52.
- Sondhi, R., Y.S. Lin, et al. (2000). "Crossflow filtration of chromium hydroxide suspension by ceramic membranes: fouling and its minimization by backpulsing." *Journal of Membrane Science* **174**(1): 111–122.
- Song, L. (1998). "Flux decline in crossflow microfiltration and ultrafiltration: mechanisms and modeling of membrane fouling." *Journal of Membrane Science* **139**(2): 183–200.

- Susanto, H. and M. Ulbricht (2005). "Influence of ultrafiltration membrane characteristics on adsorptive fouling with dextrans." *Journal of Membrane Science* **266**(1–2): 132–142.
- Tan, L.L. (2010). Trends in water sector. *Innovation*. Singapore, World Scientific Publishing Co. **9**.
- Tkacik, G. and S. Michaels (1991). "A Rejection Profile Test for Ultrafiltration Membranes & Devices." *Nat Biotech* **9**(10): 941–946.
- United States Environmental Protection Agency (2002). Safe Drinking Water Act. *National Primary Drinking Water Regulation*. CFR. **Title 40, Chapter 1**.
- Vela, M.C.V., S.A. Blanco, et al. (2007). *Modelling of flux decline in crossflow ultrafiltration of macromolecules: comparison between predicted and experimental results*, Elsevier Science Bv.
- Vincent Vela, M.C., S. Álvarez Blanco, et al. (2009). "Analysis of membrane pore blocking models adapted to crossflow ultrafiltration in the ultrafiltration of PEG." *Chemical Engineering Journal* **149**(1–3): 232–241.
- Waeger, F., T. Delhaye, et al. (2010). "The use of ceramic microfiltration and ultrafiltration membranes for particle removal from anaerobic digester effluents." *Separation and Purification Technology* **73**(2): 271–278.
- Wang, J., J. Guan, et al. (2008). "Characterization of floc size and structure under different monomer and polymer coagulants on microfiltration membrane fouling." *Journal of Membrane Science* **321**(2): 132–138.
- Weis, A., M.R. Bird, et al. (2005). "The influence of morphology, hydrophobicity and charge upon the long-term performance of ultrafiltration membranes fouled with spent sulphite liquor." *Desalination* **175**(1): 73–85.
- Zondervan, E. and B. Roffel (2007). "Evaluation of different cleaning agents used for cleaning ultra filtration membranes fouled by surface water." *Journal of Membrane Science* **304**(1–2): 40–49.

APPENDIX A

Data Acquisition and Experimental Protocol

An experimental test skid was designed and constructed to collect the performance and cleaning data for the alumina and PES membranes. A schematic diagram of the experimental apparatus is illustrated in figure A.1. The apparatus was configured so that it could accommodate both the ceramic and polymeric membrane modules. Only one membrane is tested at a time. The treatment system is equipped with a 200-micrometer (μm) strainer, feed pump (Hydra Cell™ model M03BAPGSFSHA) and a peristaltic pump to maintain constant flux during experiments. There is also instrumentation to monitor the flow rate (GF Signet PN 321002L) and pressure of the feed (GF Signet 2450-1H), filtrate (Cole Parmer model 67356-53), and retentate (Cole Parmer model 67356-53) process streams and the feed water temperature (GF Signet 2350). LabVIEW™ was used to collect data, manipulate values to direct flow for backwashes and chemical cleaning, and adjust the pump speed to maintain the desired cross-flow velocity for each experiment. Experimental data were collected every 3 seconds, and the data were reduced using the average of every 10 data points. The filtrate water quality was measured using a handheld turbidimeter (Hach® 2100P).

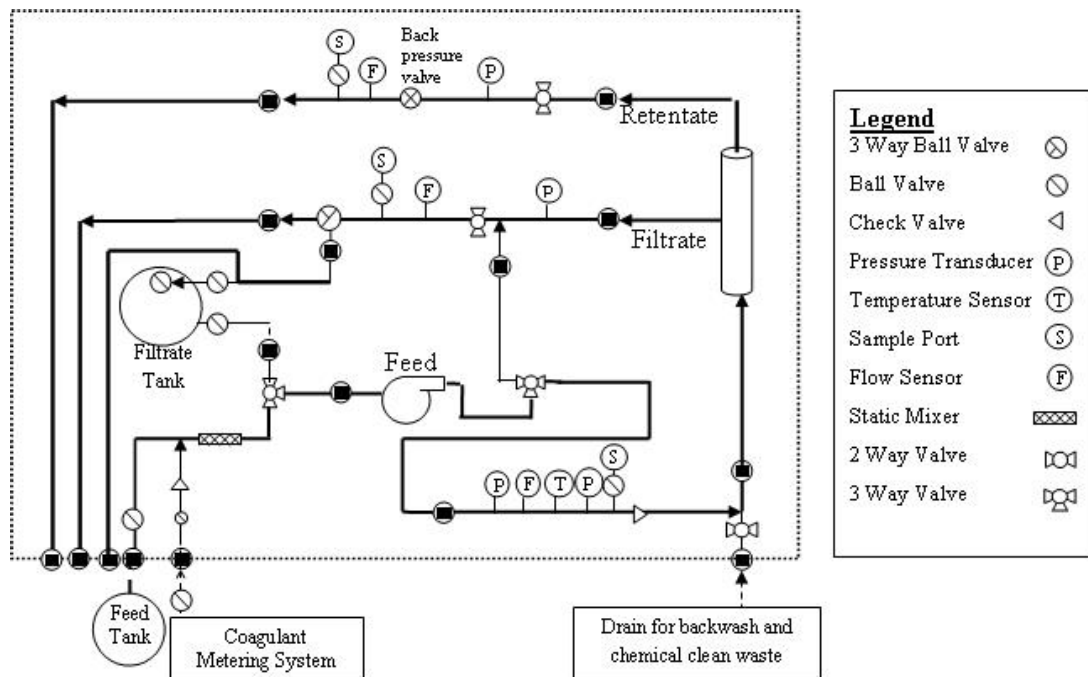


Figure A.1 Schematic diagram.

LabVIEW™ was used to monitor and record process data and to operate the pump and valves during the experiments. Simple calculations also are carried out in LabVIEW to facilitate real-time monitoring of relevant operating parameters such as cross-flow velocity and transmembrane from measured values. The front panel in LabVIEW was used to monitor process variables and ensure that experiments were conducted under controlled conditions; see figure A.2.

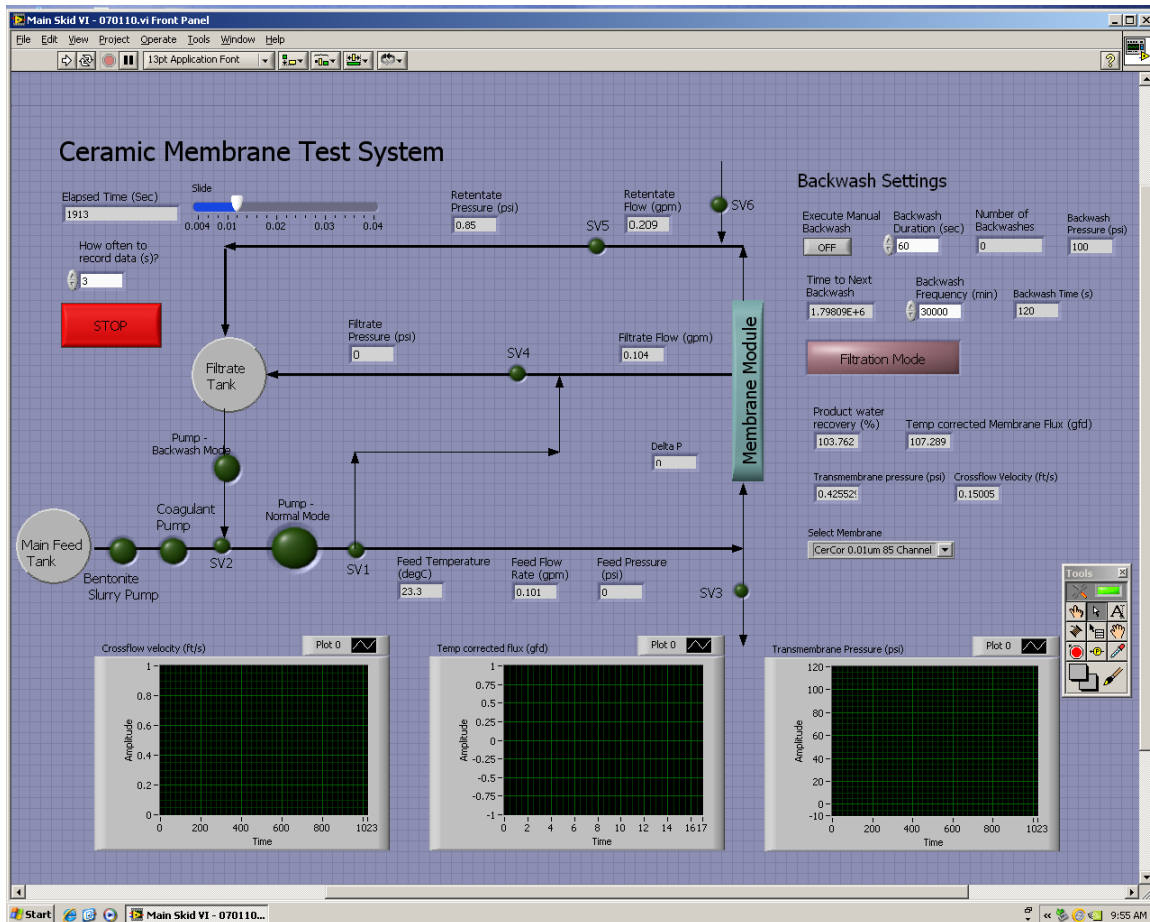


Figure A-2. Front panel of LabVIEW program.

The LabVIEW code was programmed as a timed loop that executes once per second. Each execution of the loop samples one data point from each of the instruments. Data was written to a data file once every 3 seconds. Three seconds was found to be appropriate time between recording data points so that the datafiles were of manageable size.

Functionality also was included to automate backwash cycles to occur at a specified frequency or when instigated manually. The sequence loop structure was used to program the backwash cycles. The sequence consisted of eight steps:

1. Stop the feed pump (to end filtration cycle).

2. Switch valves from filtration positions to backwash position.
3. Switch from filtration pump controller to backwash pump controller (so that the same pump can be used at two different speeds for filtration and backwash).
4. Run pump for prescribed length of time.
5. Stop pump (to end backwash).
6. Switch valves back to filtration positions.
7. Switch pump controllers.
8. Start pump in filtration mode.

A 2- second delay was written into the loop in between valve movements to account for the electrically actuated valves requiring a few seconds to switch positions.

Measurement and Automation Explorer™, a subprogram within LabVIEW™, was used to communicate between the hardware and software, to identify the location to which each sensor is wired on the data acquisition cards. All of the instruments have 4- to 20-milliampere (mA) inputs, the pump controllers were digital outputs (LabVIEW™ was used to turn pumps on and off, pump speed was set manually), and valves were digital outputs. Measurement and Automation Explorer was used to map the 4- to 20-mA inputs to the ranges of the instruments, i.e., 0–100 pounds per square inch for pressure and 0–1 gallon per minute for flow rates.

Over time, the LabVIEW™ program was modified so that alternative backwash strategies, air scour, chemical cleaning, and reverse flow could be evaluated. Because LabVIEW is a visual programming language, all of the added functionality increased the size of the wiring diagram so that it could not fit onto one page. The following screen shots show different portions of the program; see figures A.3–A.5.

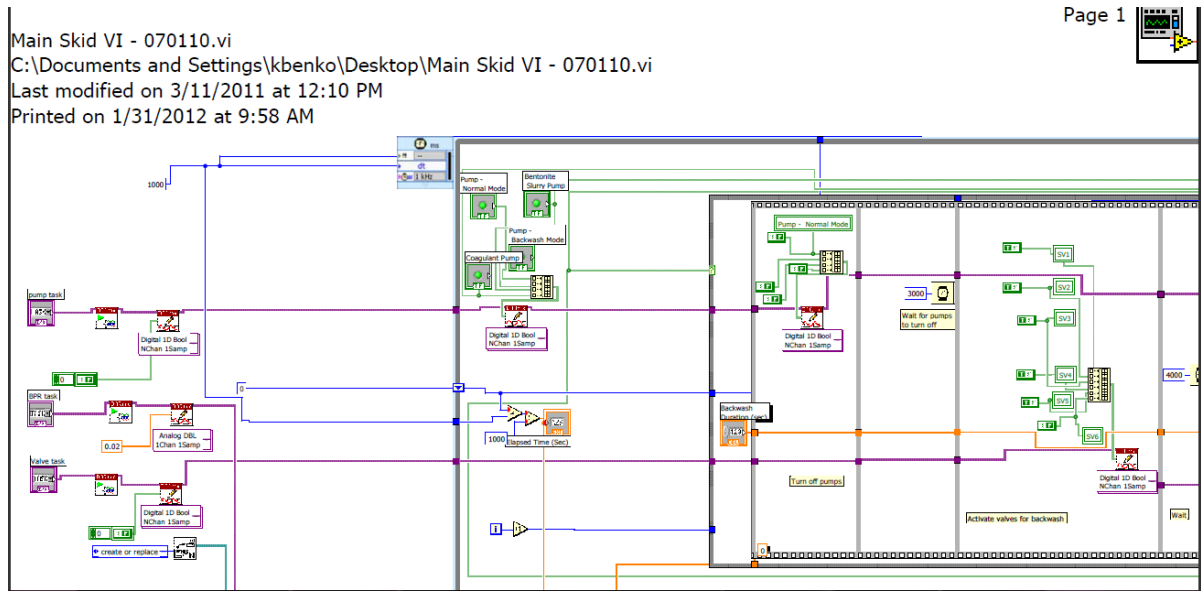


Figure A.3. Upper left portion of LabVIEW™ wiring diagram showing the timed loop initialization, task definitions, and a portion of the backwash sequence.

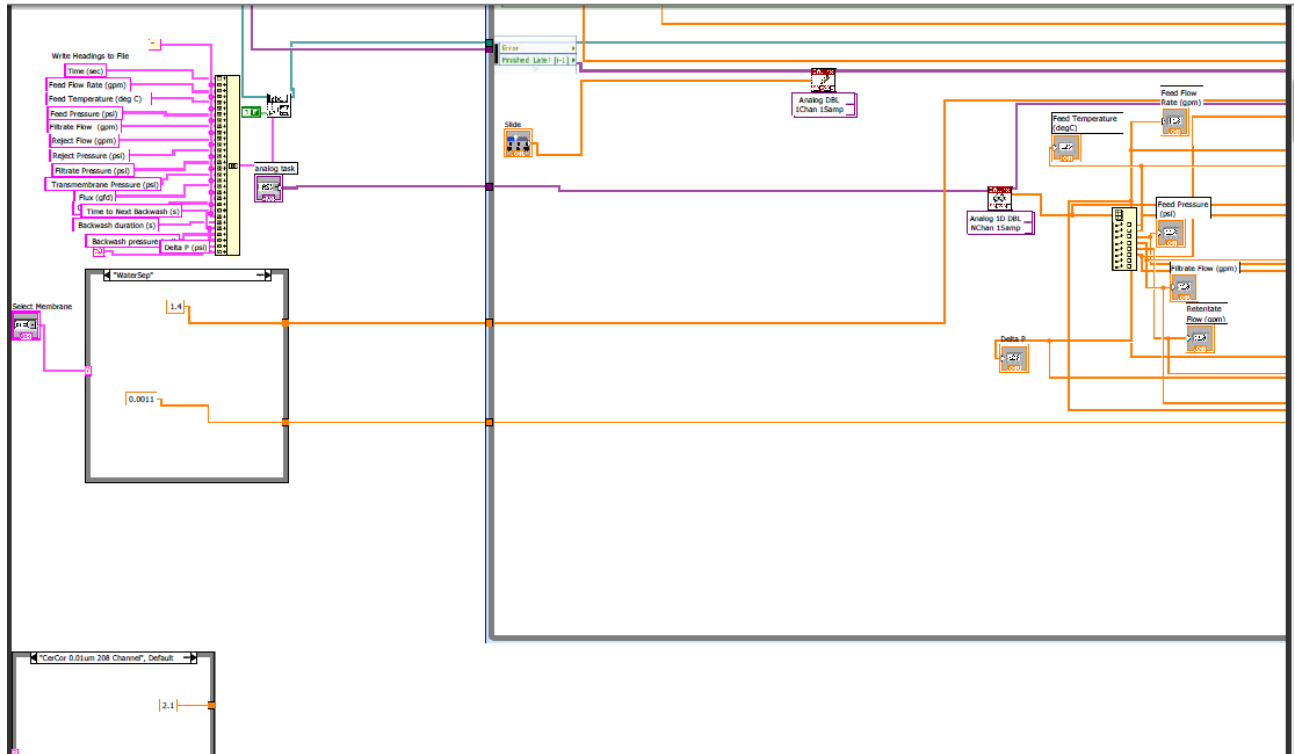


Figure A.4. LabVIEW™ wiring diagram showing the data file definitions and parsing the array to display instrument readings.

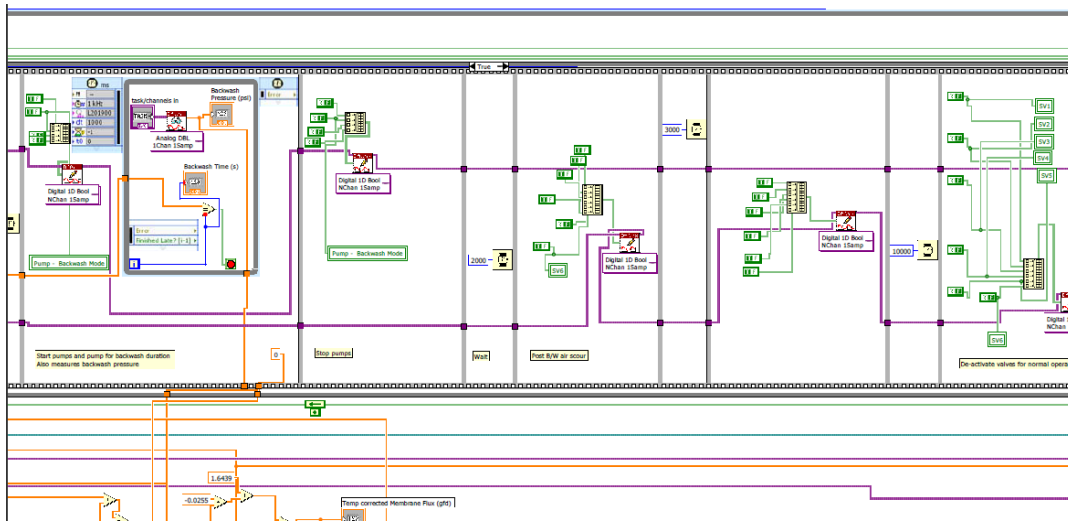


Figure A.5. LabVIEW™ wiring diagram showing backwash sequence.

3. Generic operating procedure

- 1) Start LabVIEW program
- 2) Make up desired feed water or fill feed water tank with desired source water
- 3) Set backwash frequency and duration to desired values
- 4) Ensure that reject line is going to drain and filtrate line is filling the white tank on the skid (so there is water on-hand for backwashes and cleaning).
- 5) Start LabVIEW program
 - a. Chose data file name and location
 - b. Name data file
- 6) Begin experiment
- 7) Slowly increase pump speed, ensure that filtrate is being generated and is filling the white tank on the skid
- 8) Slowly increase pump speed and close the backpressure valve until the desired transmembrane pressure is reached
- 9) Set speed of filtrate pump until desired flux is achieved.
- 10) After the experiment is complete open the backpressure valve and slow the pump speed.
- 11) Stop the LabVIEW™ program

APPENDIX B

Hydrodynamic Conditions for Modules

The following data represent the operating conditions used for the commercially available and hypothetical alumina and PES membranes in the cost model simulations, tables B.1–B.6.

Table B.1 Flux, TMP, and cross-flow velocity for alumina membranes at Pe = 5.5

Flux (L m ⁻² h ⁻¹)	TMP (kPa)	CFV (m/s)		
		Alumina – d = 2 mm, L = 86.4 cm	Alumina – d = 5 mm, L = 86.4 cm	Alumina (hypothetical) – d = 0.9mm, L = 86.4 cm
25	22.1	0.03	0.08	0.01
50	44.2	0.26	0.57	0.10
75	66.4	0.86	2.2	0.39
100	88.5	2.1	5.1	0.92
125	110	4.0	10	1.8
150	132	6.9	17	3.1
175	155	11	27	4.9
200	178	16	41	7.4
225	201	23	58	10
250	224	32	80	14

Table B.2 Flux, TMP, and cross-flow velocity for alumina membranes at Pe = 9.1

Flux (L m ⁻² h ⁻¹)	TMP (kPa)	CFV (m/s)		
		Alumina – d = 2 mm, L = 86.4 cm	Alumina – d = 5 mm, L = 86.4 cm	Alumina (hypothetical) – d = 0.9mm, L = 86.4 cm
25	22.1	0.007	0.018	0.0032
50	44.2	0.056	0.14	0.025
75	66.4	0.19	0.48	0.086
100	88.5	0.45	1.1	0.20
125	110	0.88	2.2	0.40
150	132	1.5	3.8	0.69
175	155	2.4	6.1	1.1
200	178	3.6	9.0	1.6
225	201	5.1	13	2.3
250	224	7.1	18	3.2

Table B.3 Flux, TMP, and cross-flow velocity for alumina membranes at Pe = 11.4

Flux (L m ⁻² h ⁻¹)	TMP (kPa)	CFV (m/s)		
		Alumina – d = 2 mm, L = 86.4 cm	Alumina – d = 5 mm, L = 86.4 cm	Alumina (hypothetical) – d = 0.9mm, L = 86.4 cm
25	22.1	0.0036	0.0090	0.0016
50	44.2	0.029	0.072	0.013
75	66.4	0.097	0.24	0.044
100	88.5	0.23	0.57	0.10
125	110	0.45	1.1	0.20
150	132	0.78	1.9	0.35
175	155	1.2	3.1	0.55
200	178	1.8	4.6	0.83
225	201	2.6	6.5	1.2
250	224	3.6	9.0	1.6

Table B.4 Flux, TMP, and cross-flow velocity for PES membranes at Pe = 5.5

Flux (L m ⁻² h ⁻¹)	TMP (kPa)	CFV (m/s)		
		PES – d = 0.9 mm, L = 147 cm	PES – d = 1.5 mm, L = 147 cm	PES (hypothetical) – d = 0.9mm, L = 86.4 cm
25	22.9	0.02	0.04	0.01
50	45.9	0.20	0.33	0.10
75	68.8	0.67	1.1	0.39
100	91.7	1.6	2.6	0.92
125	115	3.1	5.2	1.8
150	138	5.3	8.9	3.1
175	161	8.5	14	4.9
200	183	13	21	7.4
225	206	18	30	10
250	229	25	41	14

Table B.5 Flux, TMP, and cross-flow velocity for PES membranes at Pe = 9.1

Flux (L m ⁻² h ⁻¹)	TMP (kPa)	CFV (m/s)		
		PES – d = 0.9 mm, L = 147 cm	PES – d = 1.5 mm, L = 147 cm	PES (hypothetical) – d = 0.9mm, L = 86.4 cm
25	22.9	0.01	0.01	0.0032
50	45.9	0.04	0.07	0.025
75	68.8	0.15	0.25	0.086
100	91.7	0.35	0.58	0.20
125	115	0.68	1.1	0.40
150	138	1.2	2.0	0.69
175	161	1.9	3.1	1.1
200	183	2.8	4.7	1.6
225	206	4.0	6.6	2.3
250	229	5.5	9.1	3.2

Table B.6 Flux, TMP, and cross-flow velocity for PES membranes at Pe = 11.4

Flux (L m ⁻² h ⁻¹)	TMP (kPa)	CFV (m/s)		
		PES – d = 0.9 mm, L = 147 cm	PES – d = 1.5 mm, L = 147 cm	PES (hypothetical) – d = 0.9mm, L = 86.4 cm
25	22.9	0.01	0.0046	0.0016
50	45.9	0.04	0.037	0.013
75	68.8	0.15	0.13	0.044
100	91.7	0.35	0.30	0.10
125	115	0.68	0.58	0.20
150	138	1.2	1.0	0.35
175	161	1.9	1.6	0.55
200	183	2.8	2.4	0.83
225	206	4.0	3.4	1.2
250	229	5.5	4.6	1.6

APPENDIX C

Inputs and Outputs

Table C.1 Alumina - d = 2 mm, Pe = 5.5

Parameters		
Design plant flow rate (product delivered)	L/day	18,925,000
Plant lifespan	years	40
Annual interest rate	%/year	0.04
Integrity test frequency	times per day	1
Integrity test duration	min	20
Channel diameter	m	0.0020
Channel length	m	0.8640
Number of channels per module		1,971.0
Area per membrane module	m ²	10.7
Membrane module cost	\$/m ²	500.00
Modules per vessel		1
Cost per vessel	\$	2,000
Pump cost index ratio (I)		3.32
Pump material adjustment factor (f1)		1.5
Pump suction pressure range adjustment factor (f2)		1
Factor to account for labor costs (L)		1.4
Membrane Lifespan	years	20
Pump Efficiency		0.8
Electricity cost	\$/kW-hr	0.1
Personnel salary	\$/person/year	80,000
Time required for valve movement and air scour	min	0.5
Offline time - routine maintenance	min/day	18
Number personnel		2.5
Cleaning duration	min	18
Backwash duration	min	0.75
Backwash pressure	kPa	206.8419978
Cleaning frequency	times per y	2
Citric acid soln cost	\$/L	0.17
NaOH + NaOCl cost	\$/L	0.07
Citric acid per cleaning	L/m ²	2.2
NaOH+NaOCl per cleaning	L/m ²	5
Cleaning cost	\$/m ² /yr	1.4
Cleaning skid	\$	25,000
Membrane friction constant		23.5

Variables

Operating Conditions

Design flux rate	L/m ² /hr	50
Channel cross-flow velocity	m/s	0.26
Backwash frequency	min	60
Average TMP	kPa	22.1

Sets of replacement membranes		1.0
Pressure drop across module	kpa	2.5
Re-circulated volume (due to cross-flow velocity)	L/day	224,384,237
Backwash flux	L/m ² /hr	231
Number backwash per day		24
Total time per backwash (including valve movement)	min	1.25
Volume consumed by backwash	L/day	1,216,621
Offline time - backwash	min/day	30
Offline time - integrity test	min/day	20
Offline time - cleaning	min	0.055
Total offline line	min/day	68
Percent of time offline		0.047
Actual plant feed flow rate (to account for offline and BW)	L/day	21,140,739
Membrane area	m ²	17,530
Number membranes		1,638
Number vessels	vessels	1,638
Total membrane cost	\$	8,765,009
Vessel cost	\$	3,276,639
Pipes and valves	\$	359,054
Instruments and controls	\$	913,933
Tanks and frames	\$	540,888
Miscellaneous	\$	2,063,744
Feed pump	\$	1,363,652
Re-circulated pump		1,513,755
Total capital cost	\$	18,821,674
Amortized capital cost	\$/yr	950,937
Amortized cost of replacement membranes	\$/year	442,839
Energy usage - feed delivery	kWh/d	146
Energy usage - recirculation	kWh/d	2,031
Energy cost for pumping	\$/year	79,449
Annual maintenance cost	\$/year	150,850
Cleaning cost	\$/year	24,621
Total personnel cost	\$/year	200,000
Total O&M cost	\$/year	897,758

Output summary

Total annual cost	\$	1,848,695
Total production cost (\$/m ³)	\$/m ³	0.268
Amortized capital cost per volume produced (\$/m ³)	\$/m ³	0.138
O&M cost (\$/m ³)	\$/m ³	0.130
Total power requirement	kWh/d	2177
Membrane capital		\$8,765,009.24
Non-membrane capital		\$10,056,664.81
Amortized cost of replacement membranes		\$442,838.85

Table C.2 Alumina, d = 5 mm, Pe = 5.5

Parameters		
Design plant flow rate (product delivered)	L/day	18,925,000
Plant lifespan	years	40
Annual interest rate	%/year	0.04
Integrity test frequency	times per day	1
Integrity test duration	min	20
Channel diameter	m	0.0050
Channel length	m	0.8640
Number of channels per module		368.4
Area per membrane module	m ²	5.0
Membrane module cost	\$/m ²	500.00
Modules per vessel		1
Cost per vessel	\$	2,000
Pump cost index ratio (I)		3.32
Pump material adjustment factor (f1)		1.5
Pump suction pressure range adjustment factor (f2)		1
Factor to account for labor costs (L)		1.4
Membrane Lifespan	years	20
Pump Efficiency		0.8
Electricity cost	\$/kW-hr	0.1
Personnel salary	\$/person/year	80,000
Time required for valve movement and air scour	min	0.5
Offline time - routine maintenance	min/day	10
Number personnel		2.5
Cleaning duration	min	18
Backwash duration	min	0.75
Backwash pressure	kPa	206.8419978
Cleaning frequency	times per y	2
Citric acid solution cost	\$/L	0.17
NaOH + NaOCl cost	\$/L	0.07
Citric acid per cleaning	L/m ²	2.2
NaOH+NaOCl per cleaning	L/m ²	5
Cleaning cost	\$/m ² /yr	1.4
Cleaning skid	\$	25,000
Membrane friction constant		23.5
Variables		
Operating Conditions		
Design flux rate	L/m ² /hr	50
Channel cross-flow velocity	m/s	0.57
Backwash frequency	min	60
Average TMP	kPa	44.2
Sets of replacement membranes		1.0
Pressure drop across module	kpa	0.9
Re-circulated volume (due to cross-flow velocity)	L/day	1,231,489,849
Backwash flux	L/m ² /hr	231.3
Number backwash per day		24

Total time per backwash (including valve movement)	min	1.25
Volume consumed by backwash	L/day	1,210,167
Offline time - backwash	min/day	30
Offline time - integrity test	min/day	20
Offline time - cleaning	min	0.054794521
Total offline line	min/day	60
Percent of time offline		0.0417
Actual plant feed flow rate (to account for offline and BW)	L/day	21,011,444
Membrane area	m ²	17,437
Membrane area solver		
Number membranes		3,487.40
Number vessels	vessels	3,487.40
Total membrane cost	\$	\$8,718,512.21
Vessel cost	\$	\$6,974,809.76
Pipes and valves	\$	\$358,252.78
Instruments and controls	\$	\$910,730.46
Tanks and frames	\$	\$539,364.98
Miscellaneous	\$	\$2,057,496.41
Feed pump	\$	\$1,782,650.99
Re-circulated pump		\$1,904,336.99
Total Capital Cost	\$	\$23,271,154.58
Annualized capital cost	\$/yr	\$1,175,739.93
Annualized cost of replacement membranes	\$/year	\$440,489.66
Energy usage - feed delivery	kWh/d	305.95
Energy usage - recirculation	kWh/d	3,958.79
Energy cost for pumping	\$/year	\$155,662.93
Annual maintenance cost	\$/year	\$ 218,289.64
Cleaning cost	\$/year	\$24,490.15
Total personnel cost	\$/year	200,000.00
Total O&M Cost	\$/year	\$1,038,932.37
Output summary		
Total annual cost	\$	2,214,672
Total production cost (\$/m ³)	\$/m ³	0.321
Amortized capital cost per volume produced (\$/m ³)	\$/m ³	0.170
O&M cost (\$/m ³)	\$/m ³	0.150
Membrane area	m ²	17437
Power requirement	kWh/d	4265
Membrane capital		\$8,718,512.21
Non-membrane capital		\$14,552,642.37
Amortized cost of replacement membranes		\$440,489.66

Table C.3 Alumina, hypothetical module, Pe = 5.5

Parameters		
Design plant flow rate (product delivered)	L/day	18,925,000
Plant lifespan	years	40
Annual interest rate	%/year	0.04
Integrity test frequency	times per day	1
Integrity test duration	min	20
Channel diameter	m	0.0009
Channel length	m	0.8640
Number of channels per module		4,380.0
Area per membrane module	m ²	10.7
Membrane module cost	\$/m ²	500.00
Modules per vessel		1
Cost per vessel	\$	2,000
Pump cost index ratio (I)		3.32
Pump material adjustment factor (f1)		1.5
Pump suction pressure range adjustment factor (f2)		1
Factor to account for labor costs (L)		1.4
Membrane Lifespan	years	20
Pump Efficiency		0.8
Electricity cost	\$/kW-hr	0.1
Personnel salary	\$/person/year	80,000
Time required for valve movement and air scour	min	0.5
Offline time - routine maintenance	min/day	10
Number personnel		2.5
Cleaning duration	min	18
Backwash duration	min	0.75
Backwash pressure	kPa	206.8419978
Cleaning frequency	time per y	2
Citric acid soln cost	\$/L	0.17
NaOH + NaOCl cost	\$/L	0.07
Citric acid per cleaning	L/m ²	2.2
NaOH+NaOCl per cleaning	L/m ²	5
Cleaning cost	\$/m ² /yr	1.4
Cleaning skid	\$	25,000
Membrane friction constant		23.5

Variables***Operating Conditions***

Design flux rate	L/m ² /hr	75
Channel cross-flow velocity	m/s	0.39
Backwash frequency	min	60
Average TMP	kPa	66.4
Sets of replacement membranes		1.0
Pressure drop across module	kpa	18.6
Re-circulated volume (due to cross-flow velocity)	L/day	99,448,586
Backwash flux	L/m ² /hr	231

Number backwash per day		24
Total time per backwash (including valve movement)	min	1.25
Volume consumed by backwash	L/day	790,601
Offline time - backwash	min/day	30
Offline time - integrity test	min/day	20
Offline time - cleaning	min	0.055
Total offline line	min/day	60
Fraction of time offline		0.042
Actual plant feed flow rate (to account for offline and BW)	L/day	20,573,618
Membrane area	m ²	11,392
# membranes		1,064.6
Number vessels	vessels	1,064.6
Total membrane cost	\$	5,695,795.3
Vessel cost	\$	2,129,269.3
Pipes and valves	\$	299,596.4
Instruments and controls	\$	687,644.2
Tanks and frames	\$	430,419.7
Miscellaneous	\$	1,614,183.6
Feed pump	\$	2,072,194.7
Re-circulated pump		2,510,471.3
Total Capital Cost	\$	15,464,574.3
Annualized capital cost	\$/yr	781,324.3
Annualized cost of replacement membranes	\$/year	287,771.5
Energy usage - feed delivery	kWh/d	390.8
Energy usage - recirculation	kWh/d	6,775.9
Energy cost for pumping	\$/year	261,586.7
Annual maintenance cost	\$/year	146,531.7
Cleaning cost	\$/year	15,999.4
Total personnel cost	\$/year	200,000.0
Total O&M Cost	\$/year	911,889.2
Output summary		
Total annual cost	\$	1,693,213
Total production cost (\$/m ³)	\$/m ³	0.245
Amortized capital cost per volume produced (\$/m ³)	\$/m ³	0.113
O&M cost (\$/m ³)	\$/m ³	0.132
Total power requirement	kWh/d	7167
Membrane capital		\$5,695,795.28
Non-membrane capital		\$9,768,779.05
Amortized cost of replacement membranes		\$287,771.45

Table C. 4 PES, d = 0.9 mm, Pe = 5.5

Parameters		
Design plant flow rate (product delivered)	L/day	18,925,000
Plant lifespan	years	40
Annual interest rate	%/year	0.04
Integrity test frequency	times per day	1
Integrity test duration	min	20
Channel diameter	m	0.0009
Channel length	m	1.4860
Number of channels per module		14,280.4
Area per membrane module	m ²	60.0
Membrane module cost	\$/m ²	50.00
Modules per vessel		1
Cost per vessel	\$	0
Pump cost index ratio (I)		3.32
Pump material adjustment factor (f1)		1.5
Pump suction pressure range adjustment factor (f2)		1
Factor to account for labor costs (L)		1.4
Membrane Lifespan	years	5
Pump Efficiency		0.8
Electricity cost	\$/kW-hr	0.1
Personnel salary	\$/person/year	80,000
Time required for valve movement and air scour	min	0.5
Offline time - routine maintenance	min/day	10
Number personnel		2.5
cleaning duration	min	15
Backwash duration	min	0.75
Backwash pressure	kPa	206.8419978
Cleaning frequency	times per y	2
Citric acid soln cost	\$/L	0.17
NaOH + NaOCl cost	\$/L	0.07
Citric acid per cleaning	L/m ²	1.3
NaOH+NaOCl per cleaning	L/m ²	1.6
Cleaning cost	\$/m ² /y	0.65
Cleaning skid	\$	25,000
Total personnel cost	\$/year	200,000
Membrane friction constant		8.9

Variables**Operating Conditions**

Design flux rate	L/m ² /hr	50
Channel cross-flow velocity	m/s	0.20
Backwash frequency	min	60
Average TMP	kPa	45.9
Sets of replacement membranes		7.0
Pressure drop across module	kpa	6.3
Re-circulated volume (due to cross-flow velocity)	L/day	46,229,190
Backwash flux	L/m ² /hr	231.3

Number backwash per day		24
Total time per backwash (including valve movement)	min	1.25
Volume consumed by backwash	L/day	1,226,258
Offline time - backwash	min/day	30
Offline time - integrity test	min/day	20
Offline time - cleaning	min	20
Total offline line	min/day	80
Percent of time offline		0.0556
Actual plant feed flow rate (to account for offline and BW)	L/day	21,336,626
Membrane area	m ²	17,669
Number membranes		294.48
Number vessels	vessels	294.48
Total membrane cost	\$	\$883,443.63
Vessel cost	\$	\$ -
Pipes and valves	\$	\$ 360,245.77
Instruments and controls	\$	\$ 918,704.68
Tanks and frames	\$	\$ 543,154.11
Miscellaneous	\$	\$2,073,045.67
Feed pump	\$	\$1,819,951.57
Re-circulated pump		\$1,310,951.77
Total capital cost	\$	\$7,934,497.20
Annualized capital cost	\$/yr	\$400,878.48
Annualized cost of replacement membranes	\$/year	\$312,442.58
Energy usage - feed delivery	kWh/d	299.29
Energy usage - recirculation	kWh/d	1,042.29
Energy cost for pumping	\$/year	\$48,967.83
Annual maintenance cost	\$/year	\$105,765.80
Cleaning cost	\$/year	\$11,502.27
Total O&M Cost	\$/year	\$ 678,678.50

Output summary

Total annual cost	\$	1,079,557
Total production cost (\$/m ³)	\$/m ³	0.156
Amortized capital cost per volume produced (\$/m ³)	\$/m ³	0.058
O&M cost (\$/m ³)	\$/m ³	0.098
Membrane area	m ²	17669
Power requirement	kWh/d	1342

Table C.5 PES d = 1.5 mm, Pe = 5.5

Parameters		
Design plant flow rate (product delivered)	L/day	18,925,000
Plant lifespan	years	40
Annual interest rate	%/year	0.04
Integrity test frequency	times per day	1
Integrity test duration	min	20
Channel diameter	m	0.0015
Channel length	m	1.4860
Number of channels per module		5,712.2
Area per membrane module	m ²	40.0
Membrane module cost	\$/m ²	50.00
Modules per vessel		1
Cost per vessel	\$	0
Pump cost index ratio (I)		3.32
Pump material adjustment factor (f1)		1.5
Pump suction pressure range adjustment factor (f2)		1
Factor to account for labor costs (L)		1.4
Membrane Lifespan	years	5
Pump Efficiency		0.8
Electricity cost	\$/kW-hr	0.1
Personnel salary	\$/person/year	80,000
Time required for valve movement and air scour	min	0.5
Offline time - routine maintenance	min/day	10
Number personnel		2.5
Cleaning duration	min	15
Backwash duration	min	0.75
Backwash pressure	kPa	206.8419978
cleaning frequency	times per y	2
Citric acid soln cost	\$/L	0.17
NaOH + NaOCl cost	\$/L	0.07
Citric acid per cleaning	L/m ²	1.3
NaOH+NaOCl per cleaning	L/m ²	1.6
Cleaning cost	\$/m ² /y	0.65
Cleaning skid	\$	25,000
Total personnel cost	\$/year	200,000.00
Membrane friction constant		8.9
Variables		
Operating Conditions		
Design flux rate	L/m ² /hr	50
Channel cross-flow velocity	m/s	0.33
Backwash frequency	min	60
Average TMP	kPa	45.9
Sets of replacement membranes		7.0
Pressure drop across module	kpa	3.7
Re-circulated volume (due to cross-flow velocity)	L/day	125,081,901
Backwash flux	L/m ² /hr	231.3
Number backwash per day		24

Total time per backwash (including valve movement)	min	1.25
Volume consumed by backwash	L/day	1,210,167
Offline time - backwash	min/day	30
Offline time - integrity test	min/day	20
Offline time - cleaning	min	0.054794521
Total offline line	min/day	60
Percent of time offline		0.0417
Actual plant feed flow rate (to account for offline and BW)	L/day	21,011,444
Membrane area	m ²	17,437
Membrane area solver		
Number membranes		435.93
Number vessels	vessels	435.93
Total membrane cost	\$	\$871,851.22
Vessel cost	\$	\$ -
Pipes and valves	\$	\$358,252.78
Instruments and controls	\$	\$910,730.46
Tanks and frames	\$	\$539,364.98
Miscellaneous	\$	\$2,057,496.41
Feed pump	\$	\$1,809,083.39
Re-circulated pump		\$1,443,649.35
Total Capital Cost	\$	\$8,015,428.59
Annualized capital cost	\$/yr	\$ 404,967.42
Annualized cost of replacement membranes	\$/year	\$308,342.76
Energy usage - feed delivery	kWh/d	307.97
Energy usage - recirculation	kWh/d	1,694.56
Energy cost for pumping	\$/year	\$73,092.35
Annual maintenance cost	\$/year	\$107,153.66
Cleaning cost	\$/year	\$11,351.34
Total O&M Cost	\$/year	\$699,940.11
Output summary		
Total annual cost	\$	1,104,908
Total production cost (\$/m ³)	\$/m ³	0.160
Amortized capital cost per volume produced (\$/m ³)	\$/m ³	0.059
O&M cost (\$/m ³)	\$/m ³	0.101
Membrane area	m ²	17437
Power requirement	kWh/d	2003

Table C.6 PES – hypothetical module, Pe = 5.5

Parameters		
Design plant flow rate (product delivered)	L/day	18,925,000
Plant lifespan	years	40
Annual interest rate	%/year	0.04
Integrity test frequency	times per day	1
Integrity test duration	min	20
Channel diameter	m	0.0009
Channel length	m	0.8640
Number of channels per module		4,380.0
Area per membrane module	m ²	10.7
Membrane module cost	\$/m ²	50.00
Modules per vessel		1
Cost per vessel	\$	0
Pump cost index ratio (I)		3.32
Pump material adjustment factor (f1)		1.5
Pump suction pressure range adjustment factor (f2)		1
Factor to account for labor costs (L)		1.4
Membrane Lifespan	years	5
Pump Efficiency		0.8
Electricity cost	\$/kW-hr	0.1
Personnel salary	\$/person/year	80,000
Time required for valve movement and air scour	min	0.5
Offline time - routine maintenance	min/day	10
Number personnel		2.5
Cleaning duration	min	15
Backwash duration	min	0.75
Backwash pressure	kPa	206.8419978
Cleaning frequency	times per y	2
Citric acid soln cost	\$/L	0.17
NaOH + NaOCl cost	\$/L	0.07
Citric acid per cleaning	L/m ²	1.3
NaOH+NaOCl per cleaning	L/m ²	1.6
Cleaning cost	\$/m ² /y	0.65
Cleaning skid	\$	25,000
Total personnel cost	\$/year	200,000.00
Membrane friction constant		8.9
Variables		
Operating Conditions		
Design flux rate	L/m ² /hr	75
Channel cross-flow velocity	m/s	0.39
Backwash frequency	min	60
Average TMP	kPa	68.8
Sets of replacement membranes		7.0
Pressure drop across module	kpa	7.1
Re-circulated volume (due to cross-flow velocity)	L/day	99,961,207
Backwash flux	L/m ² /hr	231.3

Number backwash per day		24
Total time per backwash (including valve movement)	min	1.25
Volume consumed by backwash	L/day	790,601
Offline time - backwash	min/day	30
Offline time - integrity test	min/day	20
Offline time - cleaning	min	0.055
Total offline line	min/day	60
Percent of time offline		0.0417
Actual plant feed flow rate (to account for offline and BW)	L/day	20,573,618
Membrane area	m ²	11,392
Number membranes		1,064.63
Number vessels	vessels	1064.63
Total membrane cost	\$	\$ 569,579.53
Vessel cost	\$	\$ -
Pipes and valves	\$	\$299,596.41
Instruments and controls	\$	\$687,644.19
Tanks and frames	\$	\$ 430,419.66
Miscellaneous	\$	\$1,614,183.56
Feed pump	\$	\$2,101,089.22
Re-circulated pump		\$1,725,415.07
Total capital cost	\$	\$7,452,927.64
Annualized capital cost	\$/yr	\$376,547.91
Annualized cost of replacement membranes	\$/year	\$201,440.02
Energy usage - feed delivery	kWh/d	446.73
Energy usage - recirculation	kWh/d	2,592.72
Energy cost for pumping	\$/year	\$110,940.01
Annual maintenance cost	\$/year	\$103,250.22
Cleaning cost	\$/year	\$7,415.82
Total O&M Cost	\$/year	\$623,046.07
Output summary		
Total annual cost	\$	999,594
Total production cost (\$/m ³)	\$/m ³	0.145
Amortized capital cost per volume produced (\$/m ³)	\$/m ³	0.055
O&M cost (\$/m ³)	\$/m ³	0.090
Membrane area	m ²	11,392
Power requirement	kWh/d	3,039